ENTANGLEMENT AND THE QUANTUM-CLASSICAL TRANSITION

by

Sol H. Jacobsen, B.Sc. Hons (York, UK)

Submitted in fulfilment of the requirements
for the Degree of Doctor of Philosophy

Department of Physics
University of Tasmania
November, 2010

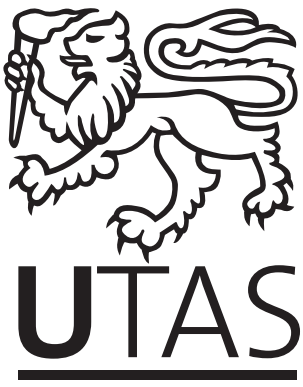

I declare that this thesis contains no material which has been accepted for a degree or diploma by the University or any other institution, except by way of background information and duly acknowledged in the thesis, and that, to the best of my knowledge and belief, this thesis contains no material previously published or written by another person, except where due acknowledgement is made in the text of the thesis.

Signed: _____
Sol H. Jacobsen

Date: _____

ABSTRACT

The ubiquitous theory of quantum mechanics has sparked many controversial debates about possible interpretations and its place in fundamental physical theory. Perhaps most sustained of all the questions is the quest for a complete explanation of the process behind the reduction from quantum to classical phenomena. This thesis shall examine this question through detailed investigation of specific models. The models include a careful exposition of quantum entanglement through the original EPR thought experiment for continuous variables and its mathematical transcription. The transcription is compared with existing methods from quantum optics for achieving experimentally verifiable Bell-type inequality violations, which are commonly interpreted as violations of locality. In further development of this famous paradox, the mathematical model is extended to tripartite continuous variable states, and detailed measures of their violation of locality are presented.

Having carefully examined quantum phenomena by the EPR-paradox and its extension to tripartite cases, the investigation proceeds by considering the effect on quantum systems by an environment. This involves a re-examination of some well-known quantum system-environment models: the spin-$\frac{1}{2}$ Spin-Boson and Kondo models, in which a two-level quantum system interacts with a bath of bosons or fermions respectively. The technicalities of the interactions are exposed in intricate detail, with a careful description of the constructive bosonisation and transformation methods involved. The thorough analysis leads to a new observation about the elliptic, or fully anisotropic, Kondo model. Importantly, the re-examination of the detailed structure of fermion-gas impurity models and their connection to quantum dissipative systems enables a comprehensive extension of the family of models to include in particular a new three-level dissipative system. To underline the importance of this model, it is shown that the model is exactly solvable by admitting a reparametrisation of the scattering matrix in terms of R-matrices which obey the Yang-Baxter equation.

The examination of the interaction between the quantum and the classical concludes with an investigation of entanglement criteria in the system-environment models discussed. A variational Ansatz for the ground state is used to demonstrate the numerical calculation of entropy expressions for the three-level systems, while the Feynman-Hellmann Theorem is used to give in-principle exact results for the entropy corresponding to the specific three-level model Hamiltonian introduced in this thesis. Throughout we provide several suggestions for further work, procedures for experimental verification and practical application.

ACKNOWLEDGEMENTS

I am indebted to so many whose encouragement, support and enthusiasm for this topic have helped the development of this thesis, and here I will give a special mention to a few. My most heartfelt thanks go to Peter Jarvis for agreeing to take on my proposed project and help mould it into something exact, explicit and explicative with his expert mentoring and support – not only a great mathematician and supervisor, but also now a wonderful colleague and friend. I owe much to my partner Peter While for his careful proofreading and demands for clarity, and for his endless encouragement. I thank my parents Hege and Yngve for nurturing an inquisitive spirit, and for their continuing inspirational independence. I thank Phil, for being there throughout. The small theory group at UTAS, comprising, Robert Delbourgo and Peter Jarvis, and, at various times, Jeremy Sumner, Luke Yates, Graham Legg, Isamu Imahori and Stuart Morgan, has provided many stimulating discussions. The whole department has at all times made me feel welcome and included, with special thanks to Simon Wotherspoon for his friendship. I am also indebted to my past tutors and lecturers for encouraging me into this field, starting with William MacKenzie's enthusiasm at Lochaber High School. Special thanks go to Richard Keesing, who helped make it possible for me to pursue my own investigations, and to Tom Stoneham, David Efird and Barry Lee for showing me the importance of good philosophy in science.

The many dedicated and fascinated students at Laxmipur secondary school in Tokha, Nepal, helped to inspire me to pursue further education, and I am grateful and humbled to be fortunate enough to engage in such a fulfilling investigation. For their generous hospitality and helpful discussions, I thank all of the Mathematical Physics group at the University of Queensland, in particular Tony Bracken, John Links and Ross McKenzie. My thanks go also to the editors and referees of the papers that have been published on some of the work herein, for their many useful and refining comments. I am grateful to Hans Bachor for the invitation to present and discuss my work with the group at the ARC Centre of Excellence in Quantum-Atom Optics in Canberra. Their interest and enthusiasm for some of the practical applications and implications of this work has been tremendously encouraging. None of this would have been possible without the confidence shown in me by the Commonwealth of Australia, whose generous Endeavour Europe Award helped to fund the start of this project, and the University of Tasmania and School of Mathematics and Physics' own generous contributions towards its completion. I am deeply touched by the confidence and interest you have all shown in this project.

TABLE OF CONTENTS

LIST OF FIGURES

Chapter 1

Introduction

Quantum entanglement is a phenomenon that has fascinated and perplexed all who have considered it almost since the inception of quantum mechanics itself. Physicists, mathematicians and philosophers have argued for nearly a century about its implications and applications, and despite enduring interest in the subject there is no completely satisfactory account of its place in current theory. For many theoretical physicists who investigate fundamental physical laws and the interpretation of quantum mechanics, there is an uneasy tension caused by the paradox made evident by the Einstein-Podolsky-Rosen thought experiment and its related verified tests. The paradox highlights inconsistencies in our description of reality, and hinges on the analysis of quantum entanglement and the quantum to classical transition. Speculations about this transition have resulted in diverse beliefs about reality, including the well-known but metaphysically crowded many-worlds interpretation [51, 52], and conjectures about mechanisms that might enforce a directionality of time, which is not currently required by accepted fundamental laws of physics (see for example [69, 94, 97, 64, 139, 75, 46, 93, 76] and references therein for a philosophical introduction).

This thesis is a project in theoretical physics devoted to the careful development of individual quantum-mechanical features and the interaction between simple quantum systems coupled to a classical environment. Although the majority of the analysis pertains directly to the explanation of the technicalities of each system, we shall keep in mind the more general interpretational context. The details provided herein may therefore be of some use to those

who search for the advancement of fundamental physical theory. Although an entirely theoretical investigation, we acknowledge another essential aspect of scientific development by making constant connections to experimentally verifiable outcomes.

Each chapter of this thesis will deal with a different aspect of the relationship between the quantum and the classical, and a comprehensive introduction to the specific models used for each chapter is reserved for their relevant sections. In this chapter we will introduce the general concepts and background to the investigations, providing motivation for the specific examinations. We begin by defining quantum entanglement in Section 1.1 and reviewing its historical origins and some philosophical implications in Section 1.2. The effect of classical systems on quantum phenomena is introduced in Section 1.3, before the specific system-environment models that we will use later are outlined in Section 1.4. Entropic criteria for entanglement are considered in Section 1.5 before Section 1.6 closes this general introduction with an overview of the structure of the thesis.

1.1 Entanglement

The term 'entangled state' was coined by Erwin Schrödinger in 1935 [112, 113, 114] and is a translation from the German "verschränkter Zustand". It is used to describe any composite quantum state $|\psi\rangle_{AB}$ that is *not separable*, where the composite state can be described by this wave function only, even if the subsystems of the compound system become spatially separated. By composite system $|\psi\rangle_{AB}$ we mean the tensor product of the wavefunctions representing each subsystem A and B ($|\psi\rangle_A$ and $|\phi\rangle_B$ respectively). If the bases of these subsystem wavefunctions are taken to be $\{|i\rangle_A\}$ and $\{|j\rangle_B\}$, in the respective Hilbert spaces H_A and H_B, the subsystem wavefunctions can be written as

$$|\psi\rangle_A = \sum_i a_i |i\rangle_A, \quad |\phi\rangle_B = \sum_j b_j |j\rangle_B. \tag{1.1}$$

In the tensor product space, the general composite state $|\psi\rangle_{AB}$ which can represent either a separable or an entangled composite system is thus:

$$|\psi\rangle_{AB} = \sum_{i,j} c_{ij} |i\rangle_A \otimes |j\rangle_B. \tag{1.2}$$

The separability condition is a condition on the coefficients c_{ij}: the state is separable if $c_{ij} = a_i b_j$, but if $c_{ij} \neq a_i b_j$ then the state is not separable. This is an entirely quantum description with no classical analogue, which can lead to conventionally unintuitive circumstances. Entangled systems may be created by any process that generates inextricably linked properties, and typically occurs as a result of natural or induced collisions of particles resulting in entangled or 'linked' product particles.

A well-known example of an entangled state is the 'Bell singlet state':

$$|\psi\rangle_{AB} = \frac{1}{\sqrt{2}} \left(|0\rangle_A \otimes |1\rangle_B - |1\rangle_A \otimes |0\rangle_B \right). \tag{1.3}$$

This is one of a family of four maximally entangled Bell states using two subsystems (A and B) of eigenbasis $\{|0\rangle, |1\rangle\}$. States taking this eigenbasis are called 'qubits', in analogy to the classical computing 'bit' which takes values 0 or 1. Qubits can take the values 0 or 1, or a *superposition* of the two, as is the case for the subsystems A and B in the Bell states (e.g. (1.3)). One might hypothesise this state of superposition to mean that the qubit somehow has *both* these values at the same time (the famous Schrödinger's Cat thought experiment [112, 124] is an extrapolation of such an interpretation to macroscopic components). An alternative familiar presentation of the Bell singlet (1.3) in which the superposition of states is arguably more clear is

$$|\psi\rangle_{AB} = \frac{1}{\sqrt{2}} \left(|-\rangle \otimes |+\rangle - |+\rangle \otimes |-\rangle \right), \tag{1.4}$$

where the qubits in question consist of the following combination of basis vectors:

$$|+\rangle = \frac{1}{\sqrt{2}}(|0\rangle + |1\rangle), \quad |-\rangle = \frac{1}{\sqrt{2}}(|0\rangle - |1\rangle).$$

It is important to note that it is in general difficult to ascertain whether a state is entangled or not. In some instances it is possible to perform a basis transformation to re-express a state that initially appeared entangled into a

form that is separable. This is an entire field unto itself, and one that we shall not consider further in this thesis, restricting our investigations to states that have been confirmed to be entangled.

It has recently been reported that entanglement may exist for even a single particle [47]. The authors suggest that the philosophical implications may be to strengthen the assertion that 'particle' is a concept that should instead be described as "an excitation of a given mode of the field representing the particle" [130]. The proposition is that the nonlocality exhibited by the single particle can be described as a superposition of the single-particle wavefunction and the vacuum, in what Greenberger, Horne and Zeilinger termed 'partlycles' [65]. It has also been conjectured that this observation suggests that the concepts of entanglement and decoherence (the term often given to the reduction of quantum to classical phenomena, which we shall discuss further in Section 1.3) are in essence the same 'mystery' [47]. This is one of many philosophical stipulations which add to the growing need for re-examination and re-evaluation of current concepts and theory regarding the quantum-classical transition, and in what follows we shall re-visit the historical origins of the philosophical problems highlighted by entanglement, before examining some specific models that inform the discussion.

1.2 EPR and philosophical implications

The advent of quantum theory provided the solution to a multitude of long-standing problems in physics, such as the ultraviolet catastrophe of black body radiation, the photoelectric effect and the structure and behaviour of subatomic particles. Having satisfactorily resolved these phenomena, it seemed implausible to most that such a theory could be inaccurate. Amongst some of the developers of quantum theory there was, however, speculation that the theory was still incomplete, as some predictions appeared highly counter-intuitive. At the root of the discontent was the principle of superposition, demonstrated in (1.3), which is at the foundation of the Copenhagen interpretation of quantum mechanics developed by Niels Bohr and Werner Heisenberg (and subsequently many others). The Copenhagen interpretation stipulates that a compound state will 'collapse' into precise single values for a subsystem

only when a measurement is made. Erwin Schrödinger and Albert Einstein in particular were unsatisfied with such a hypothesis, and designed a number of thought experiments to highlight this fact.

In 1935, Einstein, Podolsky and Rosen (EPR) posited [49] that either quantum mechanics must be incomplete, with room for a hidden variable theory, or spatiotemporal locality must be violated when a measurement of an entangled pair of particles is performed. Spatiotemporal locality requires that physical processes occurring at one point in spacetime should have no immediate effect on elements of reality at another point. Consequently, to demonstrate locality violation the measurement must be performed after the particles have been separated such that no classical communication channels are open when the wavefunction collapses. EPR concluded that quantum mechanics must be incomplete by considering a thought experiment that is now known as the EPR paradox. The thought experiment was designed to expose what they believed to be the absurd conclusions of quantum theory.

The experiment is deceptively simple in its construction: create an entangled system of two particles; Alice and Bob (A and B) each take one part of the system to opposite sides of the Earth; Alice measures her subsystem, and knows instantly what the outcome of the measurement on Bob's particle would be, if he performed it in the same basis as she did. Despite the simple construction, there has been long-standing philosophical debate about the implications of EPR's underlying assumptions. However, for the purposes of the present investigation we can obtain significant insight into the physical paradox without delving into the more metaphysical debates of ontology, which contend what may legitimately be given the term "real". In essence, the paradox relies on two important physical principles that were by this time well established, corroborated and considered irrefutable:

1) Heisenberg's uncertainty principle [70]: values of observables with non-commuting operators cannot be measured precisely at the same time. For the example of the non-commuting operators of position and momentum, the consequence for their corresponding observables x and p is famously written as the non-zero product of differences $\Delta x \Delta p \approx \hbar$.

2) A consequence of Einstein's own special theory of relativity [48]: nothing can travel faster than the speed of light.

To get a clear understanding of the paradox and violation of spatiotemporal locality, consider the following:

- Alice measures the spin of her particle (one subsystem of the entangled pair) in the x-direction, and can therefore know precisely the value of this physical quantity at Bob's location even *before* he measures it. EPR defined any element that can be known precisely before measurement as an element of physical reality.

- We know from the uncertainty principle that Alice cannot know definite values of the spin along the $x-$ and $z-$directions simultaneously.

- Alice's decision on which measurement to carry out on her particle (spin in x- or z-direction) thus has an *immediate effect* on elements of physical reality at Bob's location, violating the principle of locality.

- This results in the apparently absurd conclusion that Alice's *choice* at one point affects *reality* at another, instantaneously. According to EPR, the only alternative is that the particle must have been programmed with the outcome of all measurements, in *any* direction, prior to measurement. This pre-programming amounts to the particles storing hidden variables – 'hidden' because we know we cannot access this information due to the uncertainty principle.

Although it was the spark that prompted what is arguably the most hotly debated topic in fundamental quantum mechanics, at the time of its publication the EPR thought experiment appeared much less astounding to many than it perhaps seems today. Niels Bohr penned a rapid reply to EPR [30, 29], stating that the EPR experiment contained 'an ambiguity', in that their description of reality did not appropriately deal with quantum phenomena. Bohr's reply was, by many at the time, considered to be a 'conclusive' rebuttal, although it can be argued that he simply failed to accept the problem (see for example Werner's brief historical survey [138]). While this subdued the nonlocality question for a short period, the EPR thought experiment nevertheless dis-

mantled the usual interpretation of a measurement process as a physical disturbance of a measured system – that measuring position by scattering with a photon in turn causes the uncertainty in the position – since it highlights that complete knowledge of a spatially separated subsystem can be determined without direct observation of that subsystem.

It was not until 1965 that the first experimental tests of the EPR paradox were conducted by John Bell [23]. Bell recorded a series of outcomes of measurements on entangled systems, and arrived at the astounding conclusion that hidden variables are not compatible with quantum mechanical probability outcomes. In fact he demonstrated that it was possible to construct an inequality, the violation of which must involve states that are not describable by hidden variable theory. Bell's conclusions were strongly supported by a series of experiments by Alain Aspect and co-workers in the 1980s [13, 12]. We shall examine such inequalities and their violation in detail in Chapter 2. Bell's inequality, also called Bell's theorem, was later complemented by the Kochen Specker theorem [86], which showed that there is a contradiction between two assumptions of hidden variable theory: that all observables have definite values at a given time, and that their values are intrinsic and independent of the measuring device.

Despite raising fundamental questions about the nature of quantum theory and the theory of measurement, the paradox still does not always trouble many pragmatic experimentalists. It can be argued that we can violate locality without violating causality since Alice can in no way influence the outcome of her measurement, and has no means of *transmitting information* to Bob faster than the speed of light. For many pragmatists, this is the only matter of importance, as we can only ever be observers, and quantum mechanics describes accurately the results of all directly measurable outcomes. Thus, although there appears to be a paradox, unless it results in problems for measurement, why should a paradox matter? My own answer in this thesis is that a paradox does nevertheless point to inconsistencies which may, on examination, reveal new ways of not only progressing fundamental theory but also advancing experimental tests for new technological uses.

1.3 Decoherence and the impact of the classical on the quantum

So far we have discussed quantum entanglement and some of the questions it raises about our understanding of fundamental physics. Some detailed examples and further discussion on this will be presented in Chapter 2. There we shall demonstrate some applications most directly reliant on these quantum features, and consider the interplay between quantum mechanics and its implications for macroscopic measurements. Those discussions therefore concern the effect of quantum phenomena on classical outcomes. For a more detailed investigation into the quantum-classical transition we must also investigate the effect of the classical on the quantum. The precise relationship between the quantum and the classical physical theories is not established, and is the subject of continued debate. By investigating some of the simpler examples where the effects of their relationship can be demonstrated most clearly, we hope with this thesis to bring some interesting new information to inform the debate.

Quantum entanglement between two specific subsystems as discussed in Section 1.1 does not persist indefinitely, but is suppressed extremely quickly, as we know well from our every day, predominantly classical, experiences. This rapid suppression of quantum features is referred to as "decoherence" in the literature (see e.g. [155, 63, 81, 110]) and corresponds to a rapid diagonalisation of the system Hamiltonian. Despite becoming a widely used term, the precise reason and mechanism for the suppression remains largely unexplained (although there have been some tentative suggestions – see for example [155, 63] and references therein). There has been much discussion and controversial debate on the subject of decoherence, which we shall not review here, but will note a few main points relevant to our particular investigation.

There have been some proposals for quantitative measures for the timescales of decoherence [80, 154, 84] confirming the rapid nature of the effect. Joos and Zeh [80] calculated a decoherence time of 10^{-23} seconds for a superposition of two states with a difference of $1cm$ between their centres at low environmental temperature. Roger Penrose [105, 106] and others have argued that decoherence is intricately related to brain processes and consciousness. It may be

informative to note that temperature dependent decoherence measures (scaling as $\sqrt{T}$) have been compared with timescales for neuron firing excitation in the brain [120], where it was found that neuron firing is significantly slower than decoherence timescales, seemingly refuting Penrose's suggestions.

There are many who, in a similar manner to Penrose, would like to appeal to the unexplained facets of quantum theory to explain persistent philosophical problems, such as consciousness, and the apparent directionality of time. Because decoherence is still somewhat open to interpretation there has sometimes been a tendency in the literature to refer to decoherence as a "measurement" of the system by the environment, with the assumption that measurement causes and explains the suppression of the quantum features. The concept of measurement carries no intrinsic explicative powers or imperatives on the time directionality of fundamental laws, and so the transfer of explanation from decoherence to measurement is not a useful one, leaving us instead with the famous problem of measurement. It is clear that for further insight we must continue to examine the quantum-classical transition explicitly, a longstanding pursuit that we aim to contribute to here.

Caldeira and Leggett [34] suggested that suppression of quantum features is linked to dissipation of energy with an analogue of the standard friction coefficient, and for much of the early development of the theory of decoherence it was considered synonymous with dissipation and friction. However, it is pointed out in [84] that decoherence can occur at a much faster rate than dissipation, and it is argued that the two are distinct. This is now a widely held belief (although it is by no means universally adopted) but the exact relationship between the two descriptions is not fully formalised. In Chapters 3 and 4 of this thesis we will develop some quantum system-environment models and provide explicit details of their interaction. Specifically, we will examine the well-known Spin-Boson [95, 96, 136] and Kondo [87] models, and provide a comprehensive extension of these systems to new three-level dissipative systems. Chapter 4 will investigate criteria for entanglement in these models via entropy measures.

1.4 Quantum system-environment models

Spin-Boson and Kondo models are simplified system-environment models in which a spin-$\frac{1}{2}$ impurity interacts with an environment – or bath – of bosons or fermions respectively. The Kondo model is one of a class of models designed to investigate the theory of magnetism, as originally proposed by Werner Heisenberg in 1928 [71]. More specifically, the Kondo model was originally devised to describe conduction electron resistivity in dilute magnetic alloys, and continues to be of great importance in the development of that field. The Spin-Boson model has, on the other hand, been used primarily to investigate the quantum-classical link for some time [95, 96, 34]. The Spin-Boson (SB) model has been shown to be equivalent to the standard anisotropic Kondo model, which we outline in Subsection 3.3.1. This equivalence is of quintessential importance to our investigation, as it permits an extension of the link between fermion-gas impurity models and quantum dissipative systems. The link will also aid the investigation of the interaction in system-environment models more generally by facilitating interpretation of individual contributions to the coupling terms that emerge in the joint system-bath Hamiltonian.

In isolation, a quantum two-level system such as the spin-$\frac{1}{2}$ impurity in the SB model can be considered as a two-level double potential well, with the two wells corresponding to the two possible spin states $\pm\frac{1}{2}$ of the impurity. In this case the wavefunction describing the system would be a superposition showing the impurity as being in the two wells at the same time. When this system is coupled to an (in principle infinite) environment or bath the interactions between a quantum impurity and its environment results in a sharing of information between them, meaning the joint system is generally regarded as an "open", or dissipative system. When any experimental measurement is made of this joint system, one would observe a localisation of the state of the system to a single well and the destruction of the superposition description of the quantum state. Mathematically, this corresponds to a rapid diagonalisation of the interaction Hamiltonian (decoherence), which removes the possibility of tunnelling between the two wells. Any measurement on the system would subsequently reveal a quantum system localised to one of the two wells.

In this thesis we will concentrate on the suppression of quantum features which

is demonstrated in specific system-environment models. In order to gain further insight into the relationship between the components of these models, the careful examination will require several mathematical tools, which will be discussed in detail in Section 3.2. In particular, we shall use constructive bosonisation [67, 132], which permits a formal identification between fermionic and bosonic operators. The careful re-examination of the structure of fermion-gas impurity models enables the construction of a new exactly solvable three-level dissipative model in Section 3.4, with several potential applications in condensed matter physics.

The specific system-environment models that are examined herein are of particular interest since they have been shown to be exactly solvable [145, 21, 17]. This means we can investigate the asymptotic limits of the models and evaluate physical parameters with precision. Systems that are exactly solvable are extremely valuable for this reason, and there are a number of established tests that check whether any particular system conforms to the requirement. Once we have constructed the new system-environment model in Section 3.4, we show in Subsection 3.4.1 that this model remains exactly solvable by demonstrating that the scattering matrix associated with the interaction in the model corresponds to a standard trigonometric R-matrix.

1.5 Entanglement criteria

After the structures of the system-environment models have been discussed and the details of the couplings between the quantum system and the bath have been analysed in Chapter 3, we take the further step of calculating the criteria for entanglement in the models in Chapter 4. Investigating entanglement in many-body systems is a relatively young venture, and an overview of recent developments can be found in [5]. Initial investigations into entanglement in spin chains began around 2001, when O'Connor and Wootters [100] reported on maximizing pairwise entanglement in isotropic Heisenberg rings. Impurities were not introduced into these systems until 2003 when Osenda et al [102] reported that the impurity could in some sense be used to tune the level of entanglement. Vedral [130] studied entanglement effects in the Fermi gas (and in bosonic systems), stating that bipartite entanglement disappears beyond

distances of the inverse Fermi wavenumber.

Some initial investigations into entanglement in Spin-Boson and Kondo models have also been proposed. Costi and McKenzie [45] provide a quantitative description of entanglement for the ground state of the Spin-Boson model via the anisotropic Kondo model, using numerical renormalisation group treatment. Kopp and Le Hur [88] present a similar analysis for the interacting resonant level model, which is equivalent to the anisotropic Kondo model in the long time approximation [127]. (A *refermionisation* [132] of the Spin-Boson Hamiltonian gives the interacting resonant level Hamiltonian.) Extensions of the standard Kondo model to a two-impurity Kondo model have also been considered [41]. Some discussion exists on electron-electron entanglement in the standard two-level Kondo model [101], but entanglement between the components of the bath will not be considered in this work as we are interested primarily in the effect of and on the impurity (and it is indicated in [101] that the impurity has little effect on the entanglement between the conduction electrons themselves).

A *measure* of entanglement is any function of a quantum state that is zero for separable states and non-negative and real for other states, provided that the value of the function cannot increase under local operations and classical communication. This has resulted in several proposals for measures of entanglement (see for example [5] and references therein), but we shall focus in this thesis on the use of entropy – specifically the quantum Rényi [74, 135, 121] and related von Neumann [133] entropies – as a *criterion* for entanglement. This will be discussed in more detail in Chapter 4, but note here that entropy measures are a relative measure between the fully mixed and the pure states. The fully mixed bipartite state has a von Neumann entropy measure of one, and pure states have zero entropy. The use of zero entropy for pure states indicates that no further information is necessary in order to predict the outcome of measurement. It is argued in [116] that this fails to take account of the inherent uncertainties of measurement, and that rather than a pure state with zero entropy there should instead be a 'minimum uncertainty pure state'. Because we are concerned in this thesis with an entanglement criterion and not a measure, using an established inequality criterion that has been shown to hold for all separable states, it will be sufficient for this thesis to follow

convention regarding the entropy of pure states.

The entanglement criteria calculations that we present in Chapter 4 will focus on the extension of two methods that have been used previously by other authors to investigate entanglement in the spin-$\frac{1}{2}$ two-level case. In particular, we will use a variational Ansatz to suggest a possible ground state for the three-level model in Section 4.2, and find the reduced density matrices of the relevant subsystem following the method in [101]. We shall also provide an in-principle exact density matrix for the three-level model in Section 4.3 using the Feynman-Helmann Theorem, along with the corresponding entropy measures. Full details of the methods will be reserved for discussion in Chapter 4.

Using entropy as an entanglement criterion bridges the gap between theoreticians and experimentalists. The use of entropy will also make the results more directly relevant to those philosophers of science who wish to make links between the laws of thermodynamics and time. Although we shall make no direct conclusions about this matter here, the detailed experiments described herein will be informative to the discussion, especially with further work into entanglement measures. It is the author's view, however, that empirically derived laws about dynamics, such as the second law of thermodynamics, should not be used to argue for more fundamental relations. Nevertheless, there are several other reasons why investigations using entropy as a criterion and measure of entanglement can be most informative. Certainly empirical evidence is useful in indicating areas of interest, and provides an essential framework for theoretical development. One might well expect that this empirical data would be informative to the foundations of quantum mechanics, and provide information that might eventually lead to a more unified theory. Indeed, there are already such speculations in the literature. For example, we have already mentioned Dunningham and Vedral [47], who assert that entanglement and superposition are the same mystery, and Karyn Le Hur [92] argues that, using entanglement entropy, one can *'make a unification between entanglement of the spin with its environment, decoherence, and quantum phase transitions'*. In a cosmological, 'quantum gravity' context, it has also been argued that decoherence and entropy are different manifestations of the same phenomenon [82] (also [76]).

1.6 Overview of thesis structure

This thesis will present the detailed investigation of specific models involving quantum entanglement that may aid the interpretation of the quantum-classical transition. Each theoretical model is explained, contextualised and thoroughly extended, and several connections to experimental applications are suggested throughout. The general outline of the thesis is as follows. Chapter 2 will examine the EPR paradox in more detail through the Bell inequalities that have mediated experimental testing of the entanglement phenomenon. The rigorous first-principles transcription of the paradox is compared in Section 2.2 with states from experimental quantum optics that have already been shown to exhibit entanglement. In the bipartite case, it is demonstrated that the two descriptions approach equivalence in Subsection 2.2.1. The methods are comprehensively extended to tripartite states in Section 2.3, and some significant differences with current experiments are highlighted.

Chapter 3 introduces the idea of interaction between a quantum system and its environment. We give a thorough introduction to the Spin-Boson and Kondo system-environment models, and expose the intricacies of the methods used in relating a fermion-gas impurity model to a dissipative system in Section 3.2. With this as a basis we introduce the larger class of Kondo models in Section 3.3, and discuss the established equivalence between the Spin-Boson and standard anisotropic Kondo model in Subsection 3.3.1. We extend the analysis in Subsection 3.3.2 to reveal a new structure for the well-studied elliptic, or fully anisotropic Kondo model. Furthermore, we apply the analysis to another member of the family of fermion-gas impurity models, the anisotropic Coqblin-Schrieffer (ACS) model for three-component fermions, in Section 3.4. The ACS model is shown to relate to three-level dissipative systems, and moreover it is shown to be exactly solvable in Subsection 3.4.1.

Chapter 4 extends the analysis of the dissipative systems discussed in Chapter 3 by calculating entanglement criteria for the new ACS model. A numerically accessible variational method is used in Section 4.2, following a similar analysis of the corresponding two-level system. Placing emphasis on the exactly solvable nature of the ACS model, we also demonstrate how to calculate exact values of the density matrix and the related entropy measures using the

Feynman-Hellmann method in Section 4.3. We conclude the thesis in Chapter 5 with a summary of the main results and their development, and provide an overview of their place in a more general theory. In addition, some interpretative suggestions are given, and some open questions discussed. At the end of the thesis we provide some appendices with further details of selected calculations from each chapter. For ease of reference, an index of main terms and concepts is given after the bibliography.

Chapter 2

Quantum Entanglement and regularized EPR-type states

This chapter discusses in detail a direct mathematical transcription of the EPR paradox, and the results are compared with current experimental approaches to the EPR limit from quantum optics. The established EPR transcription for bipartite continuous variables is introduced and extended by regularisation in Section 2.2. The role of these states in Bell-type inequalities for local realistic theories are investigated using a Wigner function representation. A comprehensive development of the methods to tripartite states is performed in Section 2.3, and we conclude with an extensive discussion of the implications and importance of this work in Section 2.4. The material of this chapter has been published in a condensed form in Journal of Physics A [77].

2.1 Introduction – testing the EPR paradox

In Chapter 1 we discussed the origins of entanglement as described by the EPR thought experiment. The first experimentally testable form of the EPR paradox was pioneered by David Bohm (1951) [28], in terms of discrete spin-$\frac{1}{2}$ particles. This was a departure from the original EPR thought experiment which had been phrased in terms of the continuous variables of position and momentum. In the discrete case of electrons with spin up or down, their matrix representations are in finite dimensional space, and measurements of an observable in this case will give a discrete distribution of real values. Until

recently, the infinite-dimensional spaces necessary for dealing with continuous variables were too much of a technical difficulty for further development and practical implementation. For continuous variables, the N canonical bosonic modes are represented by H= $\otimes_{k=1}^{N} H_k$, with H_k as the infinite dimensional Fock spaces associated with the single modes. Due to the complexities associated with continuous variables, we were restricted to considering discretised quantum phenomena until very recently – indeed this continues to be the standard fare of most undergraduate quantum mechanics courses, involving such things as the determination of an electron's energy in an atom, for example.

The discretised form of the EPR paradox thus uses the standard notation for entangled pairs of spin-$\frac{1}{2}$ particles (electrons in this case), with each quantum state represented by a vector in a two-dimensional Hilbert Space. The Hilbert Space for the pair is the tensor product of their respective Hilbert Spaces. The spin singlet state is akin to (1.3):

$$|\psi\rangle \;=\; \frac{1}{\sqrt{2}}\left(|+z\rangle \otimes |-z\rangle - |-z\rangle \otimes |+z\rangle\right),$$

where here $|\pm z\rangle$ denote eigenstates of the spin operator S_z corresponding to the spin in the z-direction. The spin operators S_x, S_y, S_z can be represented using standard Pauli matrices $\sigma_x, \sigma_y, \sigma_z$ respectively by $S_{x,y,z} = \frac{1}{2}\sigma_{x,y,z}\hbar$, where the Pauli matrices are:

$$\sigma_x = \begin{bmatrix} 0 & 1 \\ 1 & 0 \end{bmatrix}, \sigma_y = \begin{bmatrix} 0 & -i \\ i & 0 \end{bmatrix}, \sigma_z = \begin{bmatrix} 1 & 0 \\ 0 & -1 \end{bmatrix}. \tag{2.1}$$

When we make a measurement on $|\psi\rangle$ in the z-direction, the state of the system 'collapses' into an eigenvector of S_z, according to the Copenhagen interpretation of quantum mechanics. The entanglement correlation thus dictates that, for the singlet state above[1], if Alice measures her subsystem to have the eigenvalue $+z$, then Bob must have the corresponding eigenvalue of $-z$. It is easy to show that the spin operators S_x, S_y, S_z do not commute, such that they cannot have definite values simultaneously.

Bohm's discretised translation of the EPR paradox was taken up by John Bell in 1965 [23], who used the transcription to test the paradox experimentally,

[1]The other three states in the family of maximally entangled Bell states dictate other correlations but describe the same feature.

with some startling results. Bell showed that hidden variables were not permitted in the EPR case if we preserve both the assumptions of standard theory (such as locality) and the probabilities predicted by quantum mechanics. Bell demonstrated this by constructing an inequality from a combination of the probabilities of outcomes of measurements by Alice and Bob. This inequality must be less than or equal to 2 if we allow hidden variables and locality (see (2.2) below), and we shall call this the classical bound. The equivalent inequality with quantum mechanical predictions show that an upper bound of $2\sqrt{2}$ is possible (see (2.3) below), called the Cirel'son bound. To date, all experimental evidence has supported the quantum mechanical prediction, and there were a series of famous experiments by Alain Aspect and his co-workers in the 1980s which lent overwhelming support to the violation of Bell's inequalities by certain classes of correlations [13, 12].

The Bell inequality has now been superseded by generalised versions, originally introduced in 1969 by Clauser, Horne, Shimony and Holt, and consequently dubbed the CHSH inequalities [42]. These can appear in many different guises, but essentially demonstrate the same feature. Here we outline the main steps to give an understanding of the emergence of the classical bound as differing from the quantum mechanical.

As before, Alice (A) receives one part of the system and Bob (B) receives the other. They can independently choose a direction in which to measure the spin of their component (say A measures in the direction of unit vector a and B in the direction b), and in each instance there are two possible outcomes of measurement, denoted by $A(a,\lambda) = \pm 1; B(b,\lambda) = \pm 1$. Here we also assume a hidden variable λ to be present and shared between each subsystem to be measured. With $\rho(\lambda)$ as the probability measure of λ, and the integral of $\rho(\lambda)$ being equal to one, the average from a joint series of measurements can be found from:

$$P(a,b) = \int \rho(\lambda) A(a,\lambda) B(b,\lambda) d\lambda.$$

Due to the joint history of the particles, if their spins are measured along the same axis one would get $A(a,\lambda) = -B(a,\lambda)$ (or other correlations depending on which singlet state is used), in which case $P(a,b)$ would be (-1). Note also that $1/A(a,\lambda) = A(a,\lambda)$. Bob is not constrained to measure along b, but could instead choose to measure along b' (and indeed A could measure along

a'). From these considerations it is straightforward to show the emergence of the classical bound in the form of Bell's inequality by considering the following combination of the possible measurements:

$$|P(a,b) - P(a,b')| \leq 1 + P(b,b').$$

In realizable measurements [42] it is necessary to make the additional assumption that the probability of the joint detection of any pair held by A and B is independent of their direction of measurement. In the most frequently used formulation of the inequality the probabilities of measurements are thus expressed in terms of the rate of coincidence detection – that is, given in terms of conditional probabilities [24, 42] – giving combinations of correlations:

$$|C(A(a)B(b)) + C(A(a)B(b')) + C(A(a')B(b)) - C(A(a')B(b'))| \leq 2. \quad (2.2)$$

This is the common form of the CHSH inequality [42] showing a classical bound of 2 on the right hand side. To get an intuitive understanding of this bounding value, a useful transcription of the inequality (2.2) is:

$$\int \{(A(a,\lambda)\,(B(b,\lambda)+B(b',\lambda))+A(a',\lambda)\,(B(b,\lambda)-B(b',\lambda)))\}\,\rho(\lambda)d\lambda \leq 2.$$

Since the possible measurement outcomes for B are ± 1, then one of either $(B + B)$ or $(B - B)$ in the above must be zero, with the other having a maximum value of 2. The prefactor A can have a maximum value of $+1$, and it is clear that the inequality holds.

By contrast to (2.2), the quantum mechanical prediction of measurement outcomes results in the Cirel'son bound $2\sqrt{2}$ on the right hand side. This is best seen by considering the conventional construction whereby Alice can choose to make measurements in the x- or z-direction, denoted by $A(x)$ and $A(z)$, while Bob can measure along his x'- or z'-directions ($B(x')$ and $B(z')$), where his coordinate system is rotated by 45 degrees with respect to Alice's. Alice's measurement outcomes $A(x)$ and $A(z)$ are then given by the spin operators $S_x \otimes I$ and $S_z \otimes I$ respectively, where I is the identity, while Bob's $B(x')$ and $B(z')$ are given by $(-\frac{1}{\sqrt{2}} I \otimes (S_z + S_x))$ and $(\frac{1}{\sqrt{2}} I \otimes (S_z + S_x))$ respectively. It is then straightforward to find the Cirel'son bound for the corresponding combination of expectation values of joint measurement outcomes using the

singlet state of (1.4) to give:

$$\begin{aligned} & \langle A(x)B(x')\rangle + \langle A(x)B(z')\rangle + \langle A(z)B(x')\rangle - \langle A(z)B(z')\rangle \\ = \quad & \frac{1}{\sqrt{2}} + \frac{1}{\sqrt{2}} + \frac{1}{\sqrt{2}} - \left(-\frac{1}{\sqrt{2}}\right) = 2\sqrt{2}. \end{aligned} \tag{2.3}$$

Note that it is well documented that violation of Bell inequalities is not a necessary condition for entanglement [62, 131], and as such may not be a good measure of entanglement in general. Gisin [62], for example, showed that some (entangled) states satisfying the Bell inequality initially could be manipulated using local filtering to later produce violations. However, this condition is not symmetrical, and all states violating the inequalities must be entangled. Thus if we determine that the inequality is violated we know that we have an entangled state and can produce a relative violation measure.

In the following sections we will make use of a specific transcription of the CHSH inequalities to indicate the presence of entanglement in new bipartite and tripartite continuous variable states. These states and measures of their entanglement will then be compared with results that are well-established in quantum optics. We highlight some interesting similarities and important differences of these states, and provide an extensive discussion section to indicate further work and useful applications of the study.

2.2 Bipartite entangled states and quantum optics

In Section 2.1 we discussed some of the early background into experimental testing of the EPR paradox by making use of its discretised transcription. It is only recently that experimental testing of the paradox in its original continuous variable form has been possible, but the importance and value of continuous variable states has become increasingly apparent. The advent of probing the nature of CV states has allowed for the investigation of quantum computation, teleportation and communication in an entirely new framework. Experiments using entanglement to probe the EPR limit of maximal inequality (locality) violation have required the development of a range of new tools [14]. Herein we will concentrate on one significant contribution – the so-called NOPA state

that is now commonplace in quantum optics [108, 103, 104, 15, 16]:

$$|NOPA\rangle \;=\; e^{r\left(a^\dagger b^\dagger - ab\right)}|00\rangle. \tag{2.4}$$

NOPA states are produced by Nondegenerate Optical Parametric Amplification, and approach maximal inequality violation in the limit of strong squeezing ($r \to \infty$), which we shall discuss further below. The creation and annihilation operators $a^\dagger, a, b^\dagger, b$ satisfy the standard bosonic commutation relations $[a, a^\dagger] = 1$ and $[b, b^\dagger] = 1$, where $a, a^\dagger$ act on the first space and $b, b^\dagger$ act on the second space as indicated by the two-mode vacuum state $|00\rangle \equiv |0, 0\rangle$. Creation and annihilation operators are discussed in more detail in Subsection 3.2.1, but we note here that bosonic annihilation operators annihilate the ground state (in this case the vacuum), meaning that $a|0\rangle = 0$, for example. The NOPA state has already been shown to be a genuinely entangled state that produces violations of the CV transcription of the CHSH inequality [15, 104, 90].

The NOPA state was designed to approach the ideal EPR state with strong squeezing, with particular Wigner function behaviour (see later sections) and was not explicitly derived from the EPR first principles. For a first principles investigation we must re-visit the original case considered by EPR in [49]. This discusses the simultaneous diagonalisation of the two commuting variables of difference in position $(X_1 - X_2)$ and total momentum $(P_1 + P_2)$, where $X_j,\ P_j,\ j = 1, 2$ are a standard pair of canonically conjugate variables with $[X_j, P_k] = i\delta_{jk}$ (note we have set $\hbar = 1$). Fan and Klauder [54] prove that an explicit form for the common eigenvectors of the relative position and total momentum for two EPR particles can be found:

$$(X_1 - X_2)\,|\eta\rangle = \sqrt{2}\eta_1|\eta\rangle, \quad (P_1 + P_2)\,|\eta\rangle = \sqrt{2}\eta_2|\eta\rangle, \tag{2.5}$$

where the common eigenvector $|\eta\rangle$ is expressible as

$$|\eta\rangle = e^{-\frac{1}{2}|\eta|^2 + \eta a^\dagger - \eta^* b^\dagger + a^\dagger b^\dagger}|00\rangle. \tag{2.6}$$

This makes (2.6) an ideal mathematical transcription of the EPR proposal from first principles. Here $\eta = \eta_1 + i\eta_2$ is an arbitrary complex number and

the coordinate and momentum operators are definable as:

$$\begin{aligned} X_1 &= \frac{1}{\sqrt{2}}\left(a+a^\dagger\right), \quad X_2 = \frac{1}{\sqrt{2}}\left(b+b^\dagger\right), \\ P_1 &= \frac{1}{i\sqrt{2}}\left(a-a^\dagger\right), \quad P_2 = \frac{1}{i\sqrt{2}}\left(b-b^\dagger\right). \end{aligned} \tag{2.7}$$

As a genuine representation of ideal generalised EPR states, with appropriate orthonormality and completeness, $|\eta\rangle$ is singular. Consequently, it is not possible to use this state to calculate expectation values directly, for use in Bell-type inequalities testing the EPR paradox. In order for the mathematical transcription to be useful experimentally, we shall instead consider a regularised state which approaches the singular state for a particular value of the regularisation parameter[2]. In [77] we introduced the following regularised version of Fan and Klauder's first-principles EPR transcription (2.6):

$$|\eta\rangle_s := N_2\, e^{-\frac{1}{2s^2}|\eta|^2+\frac{1}{s}\eta a^\dagger-\frac{1}{s}\eta^* b^\dagger+\frac{1}{s^2}a^\dagger b^\dagger}|00\rangle, \tag{2.8}$$

with normalisation[3]

$$|N_2| = \left|\frac{(s^4-1)^{1/2}}{s^2}\exp\left(-\frac{1}{2}|\eta|^2\frac{(s^2-1)}{s^2(s^2+1)}\right)\right|, \tag{2.9}$$

tending to the EPR ideal (2.6) in the regularisation limit $s \to 1$ (see Appendix A.1 for details). The state (2.8) contains a natural regularisation as it is the simplest generalisation of (2.6) that introduces one regularisation parameter for each mode $a^\dagger, b^\dagger$, which we have chosen to be equal $(1/s)$.

Note here that we shall at times use an alternative, more explicit notation for the state (2.8) – especially in the extension of the notation to tripartite states in Section 2.3. The alternative notation indicates the individual components of $|\eta\rangle_s$ corresponding to the respective modes, with $|\eta\rangle_s \equiv |\eta, \eta'\rangle_s$. Here it is clear that η is associated with the first mode and η' with the second mode, and we recover (2.8) when $\eta' = -\eta^*$.

The NOPA states (2.4) do, as mentioned above, tend towards maximal Bell-type inequality violation in the limit of strong squeezing. The inequalities

[2]This is as opposed to what is often referred to as 'regularising' in experimental quantum optics, which means 'to make the state more regular'.

[3]Note misprint in the paper [77], which quoted $|N_2^2|$ instead of $|N_2|$, and chose the $\eta = 0$ limit.

used are a generalised N-mode transcription of the continuous variable CHSH inequalities (see for example [98, 40]), and we shall introduce these in the following subsection. Having proposed a regularisation to the established first-principles transcription of the EPR paradox, we are now in a position to compare other aspects of the NOPA state and this more direct transcription. The methods of comparison will then be extended to tripartite states in Section 2.3.

2.2.1 Bipartite CHSH inequalities, Wigner functions and comparisons

The Wigner function [143, 73], was an attempt to provide the Schrödinger wavefunction with a probability in phase space. The time-independent function for one pair of conjugate x and p variables is[4]:

$$W(x,p) = \frac{1}{\pi\hbar}\int_{-\infty}^{\infty} dy \psi^*(x+y)\psi(x-y)e^{2ipy/\hbar}. \tag{2.10}$$

Alternatively, it has been shown that a useful expression of the Wigner function is in the form of quantum expectation values [99, 109]. For N modes, the Wigner function for a state $|\psi\rangle$ may be expressed as the expectation value of the displaced parity operator, where the parity operator itself performs reflections about phase-space points $\alpha_j = \frac{1}{\sqrt{2}}(x_j + ip_j)$, with $j = 1, 2, \ldots, N$ denoting the mode:

$$W(\alpha_1,\alpha_2,...,\alpha_N) = \left(\tfrac{2}{\pi}\right)^N \langle \hat{\Pi}(\alpha_1,\alpha_2,...,\alpha_N)\rangle = \left(\tfrac{2}{\pi}\right)^N \Pi(\alpha_1,\alpha_2,...,\alpha_N). \tag{2.11}$$

The displaced parity operator is:

$$\hat{\Pi}(\alpha_1,\alpha_2,...,\alpha_N) \;=\; \otimes_{\boldsymbol{j=1}}^{\boldsymbol{N}} D_j(\alpha_j)(-1)^{n_j} D_j^\dagger(\alpha_j), \tag{2.12}$$

where n_j are the number operators for each mode j, and the corresponding Glauber displacement operators $D_j(\alpha_j)$ are:

$$D_j(\alpha_j) = e^{\alpha_j a_j^\dagger - \alpha_j^* a_j}. \tag{2.13}$$

[4]The generalised expression of (2.10) to include mixed states replaces $\psi^*(x+y)\psi(x-y)$ with the density matrix description $\rho(x+y, x-y)$.

CHSH inequalities for bipartite systems can be written in terms of the bipartite Bell operator B_2, which consists of the following combination of expectation values [15, 129]:

$$B_2 = \Pi(0,0) + \Pi(0,\beta) + \Pi(\alpha,0) - \Pi(\alpha,\beta), \tag{2.14}$$

$$\text{where } |B_2| \leq 2. \tag{2.15}$$

$\Pi(\alpha,\beta)$ is the expectation value of the displaced parity operator (2.12) and α,β denote phase space points relating to the modes 1 and 2 respectively. This transcription means that the Bell operator (2.14) can be expressed in terms of Wigner functions (2.11). Originally, Bell argued that because the Wigner function for the original EPR state was positive everywhere it would permit a hidden variable theory and as such would not exhibit nonlocality. However, Banaszek and Wodkiewicz [15] demonstrated that the Wigner function of the two-mode squeezed vacuum NOPA states (2.4) is positive definite while the states exhibit non-local character.

For the regularised bipartite $|\eta\rangle_s$ state (2.8), the corresponding Wigner function therefore becomes:

$$W(\alpha,\beta) = (\tfrac{2}{\pi})^2{}_s\langle\eta,\eta'|e^{\alpha a^\dagger - \alpha^* a}e^{\beta b^\dagger - \beta^* b}(-1)^{n_a+n_b}e^{\alpha^* a - \alpha a^\dagger}e^{\beta^* b - \beta b^\dagger}|\eta,\eta'\rangle_s \tag{2.16}$$

Explicit details of the evaluation process for these Wigner functions will be reserved for the more complex tripartite extension in the next section. In general, we evaluate matrix elements of the form (2.16) by first commuting mode operators with the parity operator and rearranging using Baker-Campbell-Hausdorff (BCH) identities

$$\begin{aligned} e^A e^B &= e^{A+B+\frac{1}{2}[A,B]+\frac{1}{12}[A,[A,B]]-\frac{1}{12}[B,[A,B]]-\frac{1}{48}\cdots} \\ &\equiv e^A e^B e^{-A} e^A \\ &= e^{e^A B e^{-A}} e^A \\ &= e^{B+[A,B]+\frac{1}{2}[A,[A,B]]+\frac{1}{3!}[A,[A,[A,B]]]+\cdots} e^A, \end{aligned} \tag{2.17}$$

before casting the operators into anti-normal ordered form[5]. In this case, the

[5]Normal ordering will be discussed in Subsection 3.2.1, and here anti-normal ordered is understood to mean the arrangement of creation operators to the right of the annihilation operators.

bipartite Wigner function (2.16) becomes:

$$W(\alpha,\beta) = (\tfrac{2}{\pi})^2 {}_s\langle \eta,\eta'| \underbrace{e^{2|\alpha|^2} e^{2|\beta|^2} e^{-2\alpha^* a} e^{-2\beta^* b} e^{2\alpha a^\dagger} e^{2\beta b^\dagger}}_{F(\alpha,\beta)} (-1)^{n_a+n_b} |\eta,\eta'\rangle_s.$$

Substituting in (2.8) and remembering that in this case $\eta' = -\eta^*$, the parity operator causes a change in sign for each mode to give[6]

$$\begin{aligned} W(\alpha,\beta) &= (\tfrac{2}{\pi})^2 \langle 00| \exp\left(-\tfrac{1}{4s^2}|\eta|^2 - \tfrac{1}{4s^2}|\eta'|^2 + \tfrac{1}{s}\eta^* a + \tfrac{1}{s}\eta'^* b + \tfrac{1}{s^2} ab\right) F(\alpha,\beta) \\ &\quad \times \exp\left(-\tfrac{1}{4s^2}|\eta|^2 - \tfrac{1}{4s^2}|\eta'|^2 - \tfrac{1}{s}\eta a^\dagger - \tfrac{1}{s}\eta' b^\dagger + \tfrac{1}{s^2} a^\dagger b^\dagger\right) |00\rangle. \end{aligned} \quad (2.18)$$

This form of the Wigner function allows us to make an important argument to facilitate the comparison between the $|\eta\rangle_s$ and $|NOPA\rangle$ states.

By making the generic substitutions

$$\begin{aligned} \alpha &= \alpha' + A(\eta, s), \\ \beta &= \beta' + B(\eta', s), \end{aligned} \quad (2.19)$$

into $F(\alpha,\beta)$ in equation (2.18) (and using $A(\eta,s) = A, B(\eta,s) = B$) we find $F(\alpha',\beta')$:

$$\begin{aligned} F(\alpha',\beta') &= e^{2|\alpha'|^2 + 4\alpha' A + 2|A|^2} e^{2|\beta'|^2 + 4\beta' B + 2|B|^2} \\ &\quad \cdot e^{-2\alpha'^* a - 2A^* a} e^{-2\beta'^* a - 2B^* b} e^{2\alpha' a^\dagger + 2A a^\dagger} e^{2\beta' b^\dagger + 2B b^\dagger}. \end{aligned} \quad (2.20)$$

By comparing the terms in (2.20) with the Wigner function (2.18), we can see that setting

$$\begin{aligned} A(\eta,s) &= \frac{\eta}{2s}, \quad A^*(\eta,s) = \frac{\eta^*}{2s}, \\ B(\eta',s) &= \frac{\eta'}{2s}, \quad B^*(\eta',s) = \frac{\eta'^*}{2s}. \end{aligned} \quad (2.21)$$

will cancel the operator-dependent components of $|\eta,\eta'\rangle_s$. The remaining terms are not operator dependent and can be combined into a single function $E(\alpha',\beta',\eta,\eta')$, which does not impact on the behaviour of the Wigner function. We can express this as:

$$W_{\eta,\eta'}(\alpha',\beta') = E(\alpha',\beta',\eta,\eta') W_{0,0}(\alpha,\beta). \quad (2.22)$$

[6]Note that the prefactor $(\frac{2}{\pi})^2$ was omitted in [77].

That is, the Wigner function with the shifted parameters is equivalent to a function of the η- and shift-parameters multiplied by the original Wigner function (2.18) with η-parameters set to zero. Since the function $E(\alpha', \beta', \eta, \eta')$ does not impact on the Wigner function behaviour we can set its value to one. We can thus effectively set $\eta = \eta' = 0$ in $|\eta, \eta'\rangle_s$ without loss of generality. Taking $\eta = \eta' = 0$ therefore corresponds to a shift in the phase-space parameters of the displacement operators $\alpha' = \alpha - \frac{\eta}{2s}$, $\beta' = \beta - \frac{\eta'}{2s}$, which leads to:

$$|\eta = 0\rangle_s = N_2 \, e^{\frac{1}{s^2} a^\dagger b^\dagger} |00\rangle. \tag{2.23}$$

In order to compare the NOPA state (2.4) with the state (2.23), we follow [148] on reordering $SU(1,1)$ operators, to arrange (2.4) into the following form:

$$\begin{aligned} |NOPA\rangle &= e^{r(a^\dagger b^\dagger - ab)} |00\rangle \\ &= e^{r a^\dagger b^\dagger} e^{-2 \ln \cosh(r) \frac{1}{2}(a^\dagger a + b^\dagger b + 1)} e^{-rab} |00\rangle \\ &= \sqrt{1 - \tanh^2 r} \; e^{\tanh r \, a^\dagger b^\dagger} |00\rangle. \end{aligned} \tag{2.24}$$

Hence we arrive at the result that the $|\eta\rangle_s$ and $|NOPA\rangle$ methods of investigating the EPR limit approach equivalence, with $\tanh r = 1/s^2$.

The approach to equivalence between the NOPA and the η-states is also reflected in their application to the CHSH inequalities. In the NOPA case, the all-imaginary parameters $\alpha = \beta = i\sqrt{J}$, where J is a real displacement parameter $J \geq 0$, are substituted into equation (2.14) giving the value $B_2^{max} \approx 2.19$ [129, 15]. The same choice for α, β for the bipartite $|\eta\rangle_s$ (2.8) achieves, as expected, a maximum value of $B_2^{max} \approx 2.19$ as $s \to 1^+$ (explicit calculation of the Wigner functions is reserved for Section 2.3). This maximum value of B_2 is clearly the same value achieved for NOPA with $r \to \infty$ [15, 129]. A mesh plot of the B_2 value on a portion of the (J, s) plane is illustrated in Figure 2.1, which shows clearly that the value of $B2$ ($=B_2$) increases as $s \to 1^+$ and $J \to 0$ (graphical illustrations generated by Maple).

2.3 Tripartite states

Having established the similarity of the bipartite NOPA and η-states both in terms of their structure and CHSH-inequality violation, we extend the meth-

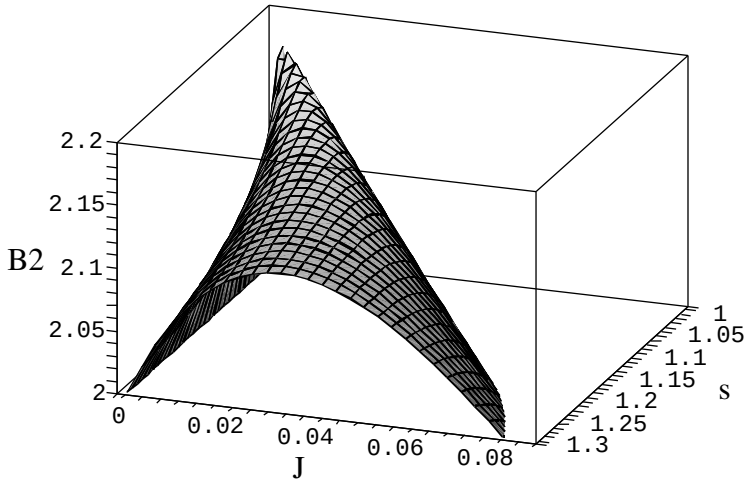

Figure 2.1: Plot of bipartite CHSH (2.14) using $|\eta\rangle_s$ (2.8), with an all-imaginary choice for α and β. Reaches a maximum value of $B_2^{max} \approx 2.19$ as $s \to 1$ and $J \to 0$. This is equivalent to the NOPA case.

ods to consider analogous tripartite states. We begin by introducing the tripartite Greenberger-Horne-Zeilinger (GHZ) NOPA-like state currently used in quantum optics, and compare it with the tripartite extension of the more direct regularised EPR transcription (2.8). The comparison reveals differences between the two approaches to the EPR limit that were not present in the bipartite example. The structure of the proposed tripartite $|\eta\rangle_s$ is therefore thoroughly investigated and explained in this section. In Subsection 2.3.1 we compare the tripartite Wigner functions of the tripartite NOPA and η-states, and we use these in Subsection 2.3.2 to compare behaviour and violations of tripartite CHSH inequalities.

The method for deriving the experimentally realizable tripartite NOPA-like states is described in [128], which involves the beamsplitter operation $B_{ab}(\theta)$, where θ is the angle of application[7]:

$$B_{ab}(\theta) : \begin{cases} a & \to & a\cos\theta + b\sin\theta \\ b & \to & -a\sin\theta + b\cos\theta. \end{cases} \tag{2.25}$$

Firstly, two phase-free beamsplitters $B_{23}(\theta)$ and $B_{12}(\theta)$ are applied at the respective angles $\theta = \pi/4$ and $\theta = \arccos(1/\sqrt{3})$. The operators a, b and c relate to the modes $1, 2$ and 3 as before, meaning that in this case (2.25) entails

[7] An additional overall relative sign (180° phase shift) between the two modes has been omitted; see for example [68].

the following transformations

$$B_{23}\left(\frac{\pi}{4}\right) \;:\; \left\{ \begin{array}{lcl} b & \rightarrow & \frac{1}{\sqrt{2}}(b+c) \\ c & \rightarrow & \frac{1}{\sqrt{2}}(c-b) \end{array} \right. ,$$
$$B_{12}(\arccos(1/\sqrt{3})) \;:\; \left\{ \begin{array}{lcl} a & \rightarrow & \frac{1}{3}(\sqrt{3}a+\sqrt{6}b) \\ b & \rightarrow & \frac{1}{3}(\sqrt{3}b-\sqrt{6}a) \end{array} \right. . \qquad (2.26)$$

The beamsplitters act on one momentum squeezed state and two position squeezed states of mode 1, 2 and 3 respectively, which may be written:

$$|NOPA^{(3)}\rangle = B_{23}\left(\frac{\pi}{4}\right) B_{12}\left(\arccos\frac{1}{\sqrt{3}}\right) \times \exp\Big(\frac{r}{2}\left(a^2-a^{\dagger 2}\right)\Big) \exp\left(\frac{-r}{2}\left(b^2-b^{\dagger 2}\right)\right) \exp\left(\frac{-r}{2}\left(c^2-c^{\dagger 2}\right)\right)|000\rangle. \qquad (2.27)$$

Note that expressions that have the form of the squeezing operator $S(z)$, where $z = e^{i\theta}$, can be written as a product of exponentials [125][8]:

$$\begin{aligned} S(z) &= \exp\big[\tfrac{1}{2}(za^{\dagger 2} - z^* a^2)\big] \\ &= \exp\big[\tfrac{1}{2}(e^{i\theta}\tanh r)a^{\dagger 2}\big] \\ &\quad \times \exp\big[-2(\ln\cosh r)(\tfrac{1}{2}a^\dagger a+\tfrac{1}{4})\big]\exp\big[-\tfrac{1}{2}(e^{-i\theta}\tanh r)a^2\big] , \end{aligned} \qquad (2.28)$$

using the BCH relations (2.17).

Applying the beamsplitter operations at the specified angles, and using manipulations of the form (2.28) we find the tripartite NOPA state (2.27) may be written in second-quantised form with an appropriate normalisation:

$$|NOPA^{(3)}\rangle = \big(1-\tanh^2(r)\big)^{3/4} \times \exp\big(-\tfrac{1}{6}\tanh r\big(a^{\dagger 2}+b^{\dagger 2}+c^{\dagger 2}\big)+\tfrac{2}{3}\tanh r\big(b^\dagger c^\dagger+a^\dagger b^\dagger+a^\dagger c^\dagger\big)\big)|000\rangle. \qquad (2.29)$$

By contrast, a suitable tripartite analogue of the bipartite $|\eta\rangle_s$-state (2.8) tending to the EPR limit, which we analyse in detail below, is defined by:

$$|\eta,\eta',\eta''\rangle_s = N_3\, e^{-\frac{1}{4s^2}|\eta|^2-\frac{1}{4s^2}|\eta'|^2-\frac{1}{4s^2}|\eta''|^2+\frac{1}{s}(\eta a^\dagger+\eta' b^\dagger+\eta'' c^\dagger)+\frac{1}{s^2}(a^\dagger b^\dagger+a^\dagger c^\dagger+b^\dagger c^\dagger)}|000\rangle, \qquad (2.30)$$

[8]Note the misprint in the sign of the last exponential in [125]; see [61].

with normalisation[9] $|N_3|^2 = \left|\frac{(s^4-1)\sqrt{s^4-4}}{s^6}e^{-F(\eta,\eta',\eta'')}\right|$, where $F(\eta,\eta',\eta'')$ is given in Appendix A.2. In the bipartite case discussed in Subsection 2.2.1, we used a shift in the parameters of the displacement operators in the Wigner functions for these states to show that it was possible to set $\eta = \eta' = 0$ in the η-state without loss of generality. When we set these parameters to zero we found that the expression for $|\eta\rangle_s$ approached the same EPR limit as the bipartite NOPA case. In the current tripartite case (2.30), we might expect that a similar shift could be possible and that a similar equivalence to the NOPA-like states would occur. With the parameters $\eta = \eta' = \eta'' = 0$ the tripartite EPR-like state becomes:

$$|\eta = \eta' = \eta'' = 0\rangle_s = N_3 e^{\frac{1}{s^2}(a^\dagger b^\dagger + a^\dagger c^\dagger + b^\dagger c^\dagger)}|000\rangle. \tag{2.31}$$

A direct comparison of (2.29) and (2.31) makes it clear that in this instance the NOPA- and η-states differ significantly. To understand the importance of these differences more fully, we analyse the structure of the tripartite $|\eta\rangle_s$ state in detail below.

Note here that, while the set of states (2.31) belong to the well known pure, fully symmetric three-mode Gaussian states, the more general state (2.30) where the parameters η, η' and η'' are retained is not symmetric, since the parameters can all differ. However, currently only Gaussian states are accessible experimentally. For discussion of Gaussian states in relation to entanglement in CV systems in general, see [2] and references therein.

Whereas the bipartite state (2.8) was a simultaneous eigenstate of $(X_1 - X_2)$ and $(P_1 + P_2)$, in the tripartite case (2.30) the choice of relative variables is no longer immediately apparent. In order to analyse its structure we follow the general method outlined in [54] for the construction of (2.6), extending to a regularised tripartite transcription. By acting separately on the state (2.30) with the annihilation operators a, b, c and using manipulations of the type:

$$ae^A = e^A\left\{a - [A,a] + \frac{1}{2}[A,[A,a]] + \ldots\right\}, \tag{2.32}$$

it is readily established that generically $|\eta,\eta',\eta''\rangle_s$ is an eigenstate of the fol-

[9] The value quoted in [77] was for the $\eta = 0$ case.

lowing combinations:

$$\begin{aligned}
\left(a-\frac{1}{s^2}\left(b^\dagger+c^\dagger\right)\right)|\eta,\eta',\eta''\rangle_s &= \frac{1}{s}\eta|\eta,\eta',\eta''\rangle_s,\\
\left(b-\frac{1}{s^2}\left(c^\dagger+a^\dagger\right)\right)|\eta,\eta',\eta''\rangle_s &= \frac{1}{s}\eta'|\eta,\eta',\eta''\rangle_s,\\
\left(c-\frac{1}{s^2}\left(a^\dagger+b^\dagger\right)\right)|\eta,\eta',\eta''\rangle_s &= \frac{1}{s}\eta''|\eta,\eta',\eta''\rangle_s.
\end{aligned} \tag{2.33}$$

From this we can deduce the different values of s that will dictate limiting cases for singular eigenvalues of various choices of relative variables. Keeping s general and substituting with the relevant phase-space operator equivalents of the mode operators using (2.7), the eigenvalue equations can be written:

$$\begin{aligned}
&\frac{1}{\sqrt{2}}\left(s+\frac{1}{s}\right)(X_1-X_2)+\frac{i}{\sqrt{2}}\left(s-\frac{1}{s}\right)(P_1-P_2)|\eta,\eta',\eta''\rangle_s = (\eta-\eta')|\eta,\eta',\eta''\rangle_s,\\
&\frac{1}{\sqrt{2}}\left(s+\frac{1}{s}\right)(X_2-X_3)+\frac{i}{\sqrt{2}}\left(s-\frac{1}{s}\right)(P_2-P_3)|\eta,\eta',\eta''\rangle_s = (\eta'-\eta'')|\eta,\eta',\eta''\rangle_s,\\
&\frac{1}{\sqrt{2}}\left(s-\frac{2}{s}\right)(X_1+X_2+X_3)+\frac{i}{\sqrt{2}}\left(s+\frac{2}{s}\right)(P_1+P_2+P_3)|\eta,\eta',\eta''\rangle_s =\\
&\qquad\qquad (\eta+\eta'+\eta'')|\eta,\eta',\eta''\rangle_s.
\end{aligned} \tag{2.34}$$

By inspecting (2.34) it is clear that the singular cases will occur for $s=1$ and $s=\sqrt{2}$. For the case $s=1$ we evidently have a singular eigenstate of the relative coordinates, while remaining a *squeezed* state [134] of the total momentum. Conversely, for $s=\sqrt{2}$ we have a singular eigenstate of the total momentum, but a squeezed state of the relative coordinates.

If we construct mode operators corresponding to the Jacobi relative variables and the canonical centre-of-mass variables, say

$$\begin{aligned}
\mathfrak{a}_{rel} &= \frac{1}{2}(X_1-X_3)+\frac{i}{2}(P_1-P_3),\\
\mathfrak{b}_{rel} &= \frac{1}{2\sqrt{3}}(X_1+X_3-2X_2)+\frac{i}{2\sqrt{3}}(P_1+P_3-2P_2),\\
\mathfrak{a}_{cm} &= \frac{1}{\sqrt{6}}(X_1+X_2+X_3)+\frac{i}{\sqrt{6}}(P_1+P_2+P_3),
\end{aligned} \tag{2.35}$$

then we find, from (2.34) for general s:

$$\begin{aligned}
\left(s\mathfrak{a}_{rel}+\frac{1}{s}\mathfrak{a}^{\dagger}_{rel}\right)|\eta,\eta',\eta''\rangle_s &= \frac{1}{\sqrt{2}}\left(\eta-\eta''\right)|\eta,\eta',\eta''\rangle_s,\\
\left(s\mathfrak{b}_{rel}+\frac{1}{s}\mathfrak{b}^{\dagger}_{rel}\right)|\eta,\eta',\eta''\rangle_s &= \frac{1}{\sqrt{6}}\left(\eta-2\eta'+\eta''\right)|\eta,\eta',\eta''\rangle_s,\\
\left(s\mathfrak{a}_{cm}-\frac{2}{s}\mathfrak{a}^{\dagger}_{cm}\right)|\eta,\eta',\eta''\rangle_s &= \frac{1}{\sqrt{3}}\left(\eta+\eta'+\eta''\right)|\eta,\eta',\eta''\rangle_s. \qquad (2.36)
\end{aligned}$$

By inspection of (2.36) it is again obvious that for $s=1$ or $s=\sqrt{2}$, canonical combinations arise in the first two, and last cases respectively. On the other hand, the non-canonical combinations appearing for $s=1$ in the third, and $s=\sqrt{2}$ in the first two cases, allows us to calculate the squeezing parameter z in each instance. Using the notation of [134] to find the squeezing parameter $z=re^{2i\phi}$, the squeezing operator $S(z)=\exp(\frac{1}{2}(z^*a^2-za^{\dagger 2}))$ gives the following transformations of creation and annihilation operators:

$$\begin{aligned}
S^{\dagger}(z)aS(z) &= a\cosh(r)-a^{\dagger}e^{-2i\phi}\sinh(r)\\
S^{\dagger}(z)a^{\dagger}S(z) &= a^{\dagger}\cosh(r)-ae^{2i\phi}\sinh(r). \qquad (2.37)
\end{aligned}$$

For a generic normalised combination of creation and annihilation operators with coefficients α and β as in (2.36), we set the phase $\phi=\pi/2$ in (2.37) to get

$$\frac{\alpha a+\beta a^{\dagger}}{\sqrt{\alpha^2-\beta^2}}=\cosh(z)a+\sinh(z)a^{\dagger}, \qquad (2.38)$$

from which we can find the squeezing parameter:

$$\begin{aligned}
z &= \ln(e^z)=\ln(\cosh(z)+\sinh(z))\\
&= \ln\left(\frac{\alpha+\beta}{\sqrt{\alpha^2-\beta^2}}\right)\\
&= \frac{1}{2}\ln\left(\frac{\alpha+\beta}{\alpha-\beta}\right). \qquad (2.39)
\end{aligned}$$

Clearly the values $\alpha=\sqrt{2},\beta=1/\sqrt{2}$ in the first two cases of (2.36) and $\alpha=1,\beta=2$ in the last case show that the squeezing parameters have the values $z=\frac{1}{2}\ln 3$ in each instance.

Having established the structure of the tripartite EPR-like states (2.30), we shall now examine their behaviour when applied to Wigner functions, and the consequences of using these states in CHSH inequalities.

2.3.1 Tripartite Wigner functions

We have determined that the tripartite $|\eta,\eta',\eta''\rangle_s$ state (2.30) differs significantly from the tripartite NOPA-like state (2.29) in its structure, and will now compare and contrast their respective Wigner function behaviours. The Wigner function (2.11) for (2.30) becomes

$$\begin{aligned} W(\alpha,\beta,\gamma) \;=\; & \left(\tfrac{2}{\pi}\right)^3 N_3^2\, e^{-\frac{1}{2s^2}|\eta|^2-\frac{1}{2s^2}|\eta'|^2-\frac{1}{2s^2}|\eta''|^2} \\ & \times\langle 000|\exp\left(\tfrac{1}{s}\left(\eta^* a+\eta'^* b+\eta''^* c\right)+\tfrac{1}{s^2}\left(ab+ac+bc\right)\right) \\ & \times\, e^{\alpha a^\dagger-\alpha^* a}e^{\beta b^\dagger-\beta^* b}e^{\gamma c^\dagger-\gamma^* c}\,(-1)^{n_a+n_b+n_c}\,e^{\alpha^* a-\alpha a^\dagger}e^{\beta^* b-\beta b^\dagger}e^{\gamma^* c-\gamma c^\dagger} \\ & \times\, \exp\left(\tfrac{1}{s}\left(\eta a^\dagger+\eta' b^\dagger+\eta'' c^\dagger\right)+\tfrac{1}{s^2}\left(a^\dagger b^\dagger+a^\dagger c^\dagger+b^\dagger c^\dagger\right)\right)|000\rangle. \end{aligned} \tag{2.40}$$

By commuting creation and annihilation mode operators with the parity operator $(-1)^{n_a+n_b+n_c}$ we can rearrange (2.40) into anti-normal ordered form using BCH-type identities (2.17) to become:

$$\begin{aligned} W(\alpha,\beta,\gamma) \;=\; & \left(\tfrac{2}{\pi}\right)^3 N_3^2\, e^{-\frac{1}{2s^2}|\eta|^2-\frac{1}{2s^2}|\eta'|^2-\frac{1}{2s^2}|\eta''|^2} \\ & \times\langle 000|\exp\left(\tfrac{1}{s}\left(\eta^* a+\eta'^* b+\eta''^* c\right)+\tfrac{1}{s^2}\left(ab+ac+bc\right)\right) \\ & \times\, e^{2|\alpha|^2}e^{2|\beta|^2}e^{2|\gamma|^2}e^{-2\alpha^* a}e^{-2\beta^* b}e^{-2\gamma^* c}e^{2\alpha a^\dagger}e^{2\beta b^\dagger}e^{2\gamma c^\dagger} \\ & \times\, \exp\left(\tfrac{1}{s}\left(\eta a^\dagger+\eta' b^\dagger+\eta'' c^\dagger\right)+\tfrac{1}{s^2}\left(a^\dagger b^\dagger+a^\dagger c^\dagger+b^\dagger c^\dagger\right)\right)|000\rangle. \end{aligned} \tag{2.41}$$

As mentioned in Section 2.2, annihilation operators acting directly on the vacuum to the right would annihilate the state, and similarly creation operators acting directly on the vacuum to the left annihilate the state. To avoid this, we can insert a complete set of coherent states

$$\iiint |u,v,w\rangle\langle u,v,w|\frac{d^2u d^2v d^2w}{\pi}, \tag{2.42}$$

between the annihilation and creation operators in their anti-normal ordered form. This means we can make use of the properties of coherent states:

$$\begin{array}{ll} \langle u,v,w|a^\dagger = u^*\langle u,v,w|, & a|u,v,w\rangle = u|u,v,w\rangle \\ \langle u,v,w|b^\dagger = v^*\langle u,v,w|, & b|u,v,w\rangle = v|u,v,w\rangle \\ \langle u,v,w|c^\dagger = w^*\langle u,v,w|, & c|u,v,w\rangle = w|u,v,w\rangle \end{array}\;, \tag{2.43}$$

and

$$\langle 000|u,v,w\rangle\langle u,v,w|000\rangle = e^{-|u|^2-|v|^2-|w|^2}. \tag{2.44}$$

After inserting (2.42) into (2.41) and using (2.43) and (2.44), the Wigner function becomes:

$$\begin{aligned} W(\alpha,\beta,\gamma) &= \left(\tfrac{2}{\pi}\right)^3 N_3^2\, e^{-\frac{1}{2s^2}|\eta|^2-\frac{1}{2s^2}|\eta'|^2-\frac{1}{2s^2}|\eta''|^2} \\ &\quad\times\iiint \exp\left(\tfrac{1}{s}\left(\eta^* u+\eta'^* v+\eta''^* w\right)+\tfrac{1}{s^2}\left(uv+uw+vw\right)\right) \\ &\quad\times\ \exp(2|\alpha|^2+2|\beta|^2+2|\gamma|^2-2\alpha^* u-2\beta^* v-2\gamma^* w) \\ &\quad\times\ \exp(-|u|^2-|v|^2-|w|^2)\exp(2\alpha u^*+2\beta v^*+2\gamma w^*) \\ &\quad\times\ \exp\left(\tfrac{1}{s}\left(\eta u^*+\eta' v^*+\eta'' w^*\right)+\tfrac{1}{s^2}\left(u^*v^*+u^*w^*+v^*w^*\right)\right) \\ &\quad\times\frac{d^2u d^2v d^2w}{\pi}. \end{aligned} \tag{2.45}$$

The exponential factors within the integral may now be manipulated into a form suitable for use in the formula [25, 53]:

$$\begin{aligned} &\int\prod_i^n\left[\frac{d^2z_i}{\pi}\right]\exp\left(-\frac{1}{2}(z,z^*)\begin{pmatrix} A & B\\ C & D\end{pmatrix}\begin{pmatrix} z\\ z^*\end{pmatrix}+(\mu,\nu^*)\begin{pmatrix} z\\ z^*\end{pmatrix}\right) \\ &\qquad=\left[\det\begin{pmatrix} C & D\\ A & B\end{pmatrix}\right]^{-\frac{1}{2}}\exp\left[\frac{1}{2}(\mu,\nu^*)\begin{pmatrix} A & B\\ C & D\end{pmatrix}^{-1}\begin{pmatrix}\mu\\ \nu^*\end{pmatrix}\right] \\ &\qquad=\left[\det\begin{pmatrix} C & D\\ A & B\end{pmatrix}\right]^{-\frac{1}{2}}\exp\left[\frac{1}{2}(\mu,\nu^*)\begin{pmatrix} C & D\\ A & B\end{pmatrix}^{-1}\begin{pmatrix}\nu^*\\ \mu\end{pmatrix}\right], \end{aligned} \tag{2.46}$$

where matrices A and D must be symmetrical, and matrix $C = B^T$. In order for (2.45) to satisfy this form, we find that the generic vectors (z, z^*) and (μ, ν^*) must in this case be:

$$\begin{aligned} (z,z^*) &= (u,v,w,u^*,v^*,w^*)\,, \\ (\mu,\nu^*) &= \left(\tfrac{1}{s}\eta^*-2\alpha^*,\tfrac{1}{s}\eta'^*-2\beta^*,\tfrac{1}{s}\eta''^*-2\gamma^*,-\tfrac{1}{s}\eta+2\alpha,-\tfrac{1}{s}\eta'+2\beta,-\tfrac{1}{s}\eta''+2\gamma\right). \end{aligned}$$

Furthermore, we have the matrix

$$\begin{pmatrix} C & D\\ A & B\end{pmatrix}=\begin{pmatrix} 1 & 0 & 0 & 0 & -\frac{1}{s^2} & -\frac{1}{s^2}\\ 0 & 1 & 0 & -\frac{1}{s^2} & 0 & -\frac{1}{s^2}\\ 0 & 0 & 1 & -\frac{1}{s^2} & -\frac{1}{s^2} & 0\\ 0 & -\frac{1}{s^2} & -\frac{1}{s^2} & 1 & 0 & 0\\ -\frac{1}{s^2} & 0 & -\frac{1}{s^2} & 0 & 1 & 0\\ -\frac{1}{s^2} & -\frac{1}{s^2} & 0 & 0 & 0 & 1\end{pmatrix}, \tag{2.47}$$

which has inverse

$$\begin{pmatrix} C & D \\ A & B \end{pmatrix}^{-1} = \frac{s^4}{(s^4-4)(s^4-1)} \begin{pmatrix} s^4-3 & 1 & 1 & 2\,s^{-2} & \frac{s^4-2}{s^2} & \frac{s^4-2}{s^2} \\ 1 & s^4-3 & 1 & \frac{s^4-2}{s^2} & 2\,s^{-2} & \frac{s^4-2}{s^2} \\ 1 & 1 & s^4-3 & \frac{s^4-2}{s^2} & \frac{s^4-2}{s^2} & 2\,s^{-2} \\ 2\,s^{-2} & \frac{s^4-2}{s^2} & \frac{s^4-2}{s^2} & s^4-3 & 1 & 1 \\ \frac{s^4-2}{s^2} & 2\,s^{-2} & \frac{s^4-2}{s^2} & 1 & s^4-3 & 1 \\ \frac{s^4-2}{s^2} & \frac{s^4-2}{s^2} & 2\,s^{-2} & 1 & 1 & s^4-3 \end{pmatrix} \tag{2.48}$$

Note also that

$$\left[\det \begin{pmatrix} C & D \\ A & B \end{pmatrix}\right]^{-\frac{1}{2}} = \left[(s^{12} - 6s^7 + 9s^4 - 4)/s^{12}\right]^{-\frac{1}{2}}, \tag{2.49}$$

such that the N_3^2 cancel in the Wigner function when $\eta = \eta' = \eta'' = 0$.

By direct extension of the argument in Subsection 2.2.1, we can show that it is possible to set $\eta = \eta' = \eta'' = 0$ without impacting on the Wigner function behaviour by considering the following shifts in phase space parameters:

$$\alpha' = \alpha - \frac{\eta}{2s}, \quad \beta' = \beta - \frac{\eta'}{2s}, \quad \gamma' = \gamma - \frac{\eta''}{2s}. \tag{2.50}$$

This is equivalent to expressing the Wigner function as

$$\begin{aligned} W_{\eta,\eta',\eta''}(\alpha',\beta',\gamma') &= E(\alpha',\beta',\gamma',\eta,\eta',\eta'')W_{0,0,0}(\alpha,\beta,\gamma) \qquad (2.51) \\ E(\alpha',\beta',\gamma',\eta,\eta',\eta'') &= \exp\left(\tfrac{1}{s}(\alpha'\eta^* + \alpha'^*\eta + \beta'\eta'^* + \beta'^*\eta' + \gamma'\eta''^* + \gamma'^*\eta'')\right). \end{aligned}$$

We are again free to choose instances where $E(\alpha',\beta',\gamma',\eta,\eta',\eta'') = 1$ as it is not operator dependent, which corresponds to setting $\eta = \eta' = \eta'' = 0$ in the Wigner function. We shall henceforth assume $\eta = \eta' = \eta'' = 0$ unless otherwise stated, and write simply $W(\alpha,\beta,\gamma)$ to avoid the cumbersome dashed notation of the shifted parameters. With this shift, the Wigner function for our tripartite state becomes:

$$\begin{aligned} W(\alpha,\beta,\gamma) &= \tfrac{8}{\pi^3}\exp\Big(\tfrac{1}{(s^4-4)(s^4-1)}\left[C_1(|\alpha|^2 + |\beta|^2 + |\gamma|^2)\right. \\ &+ C_2(\alpha\beta + \alpha\gamma + \beta\gamma + \alpha^*\beta^* + \alpha^*\gamma^* + \beta^*\gamma^*) \\ &+ C_3(\alpha\beta^* + \alpha\gamma^* + \beta\alpha^* + \beta\gamma^* + \gamma\alpha^* + \gamma\beta^*) \\ &+ \left. C_4(\alpha^2 + \beta^2 + \gamma^2 + \alpha^{*2} + \beta^{*2} + \gamma^{*2})\right]\Big), \qquad (2.52) \end{aligned}$$

where

$$C_1 = -2(s^8 - s^4 - 4)\,, \quad C_2 = 4s^2(s^4 - 2)\,, \quad C_3 = -4s^4\,, \quad C_4 = 4s^2. \quad (2.53)$$

We may now compare this Wigner function with the corresponding function for the tripartite GHZ NOPA-like states (2.29). This may be obtained by substituting (2.29) into (2.11) and rearranging the exponentials into a form suitable for manipulation by (2.46). The Wigner function $W^N(\alpha, \beta, \gamma)$ for the tripartite NOPA-like state then becomes:

$$\begin{aligned} W^N(\alpha,\beta,\gamma) \;=\; & \left(\frac{2}{\pi}\right)^3 \exp\left\{\left(2 - \frac{4}{1-\tanh^2 r}\right)\left(|\alpha|^2 + |\beta|^2 + |\gamma|^2\right)\right. \\ & -\frac{2\tanh r}{3\,(1-\tanh^2 r)}\left(\alpha^{*2} + \beta^{*2} + \gamma^{*2} + \alpha^2 + \beta^2 + \gamma^2\right) \\ & \left.+\frac{8\tanh r}{3\,(1-\tanh^2 r)}\left(\alpha\beta + \beta\gamma + \gamma\alpha + \alpha^*\beta^* + \beta^*\gamma^* + \gamma^*\alpha^*\right)\right\} \\ =\; & \frac{8}{\pi^3}\exp\left\{(-2\cosh(2r))\left(|\alpha|^2 + |\beta|^2 + |\gamma|^2\right)\right. \\ & -\frac{1}{3}\sinh(2r)\left(\alpha^{*2} + \beta^{*2} + \gamma^{*2} + \alpha^2 + \beta^2 + \gamma^2\right) \\ & \left.+\frac{4}{3}\sinh(2r)\left(\alpha\beta + \beta\gamma + \gamma\alpha + \alpha^*\beta^* + \beta^*\gamma^* + \gamma^*\alpha^*\right)\right\}. \quad (2.54) \end{aligned}$$

This is the result quoted by van Loock and Braunstein in [129], and further explication can be found in that paper.

Comparing the Wigner functions (2.52) and (2.54) for the $|\eta, \eta', \eta''\rangle_s$ and NOPA-like states respectively, the most important point to note is the emergence of mixed conjugate/non-conjugate pairs (e.g. $\alpha\beta^*$) in (2.52), which do not appear with the second-quantised NOPA-like optical analogue (2.54). As such it may be reasonable to expect that the differences propagate to become important in application to the CHSH inequalities and the violation of locality. This will be examined in the following subsection.

2.3.2 Tripartite CHSH inequalities

Having calculated the Wigner functions for the tripartite NOPA and η-states, these may now be used as components for generating their respective CHSH

inequalities. The tripartite CHSH inequality appears analogously to (2.14) [15, 129]:

$$B_3 = \Pi(0,0,\gamma) + \Pi(0,\beta,0) + \Pi(\alpha,0,0) - \Pi(\alpha,\beta,\gamma), \tag{2.55a}$$

$$|B_3| \leq 2, \tag{2.55b}$$

in which $\Pi(\alpha,\beta,\gamma)$ again represents the expectation value of the displaced parity operator (2.12). Whereas we knew that in the bipartite case the limits for the NOPA and $|\eta\rangle_s$ states both tended to the same EPR ideal for specific values of their regularisation parameters, there are a wealth of other choices that may extremise the CHSH inequality in the tripartite case. To make the behaviour of the Wigner function (2.52) in the asymptotic region clearer, the parameters α, β and γ are written in polar form, $\alpha = |\alpha|e^{i\phi_\alpha}$ etc. The Wigner function for the tripartite η-state thus becomes:

$$\begin{aligned} W(\alpha,\beta,\gamma) = \frac{8}{\pi^3}\exp\Bigg(\frac{1}{(s^4-4)(s^4-1)}\big[&C_1\left(|\alpha|^2+|\beta|^2+|\gamma|^2\right) \\ &+2C_2(|\alpha||\beta|\cos(\phi_\alpha+\phi_\beta)+|\beta||\gamma|\cos(\phi_\beta+\phi_\gamma)+|\gamma||\alpha|\cos(\phi_\gamma+\phi_\alpha)) \\ &+2C_3(|\alpha||\beta|\cos(\phi_\beta-\phi_\alpha)+|\beta||\gamma|\cos(\phi_\gamma-\phi_\beta)+|\gamma||\alpha|\cos(\phi_\gamma-\phi_\alpha)) \\ &+2C_4\big(|\alpha|^2\cos(2\phi_\alpha)+|\beta|^2\cos(2\phi_\beta)+|\gamma|^2\cos(2\phi_\gamma)\big)\big]\Bigg), \end{aligned} \tag{2.56}$$

where C_1, C_2, C_3 and C_4 are given by (2.53).

Examining (2.56) facilitates the search for choices that will minimize the last term in (2.55a). In the bipartite case, we approached the EPR limit $s \to 1^+$ by choosing all-imaginary parameters $\alpha,\beta = i\sqrt{J}$. In this tripartite case (2.56), since $\alpha = |\alpha|e^{i\phi_\alpha}$, this corresponds to choosing all phases $\phi_\alpha = \phi_\beta = \phi_\gamma = \frac{\pi}{2}$, and all magnitudes $|\alpha| = |\beta| = |\gamma| = \sqrt{J}$. The tripartite CHSH inequality (2.55a) will then be constructed using (2.11) from a combination of the following four Wigner functions:

$$\begin{aligned} W(i\sqrt{J},0,0) = W(0,i\sqrt{J},0) = W(0,0,i\sqrt{J}) &= \frac{8}{\pi^3}\exp\left(-\frac{J(s^4-s^2+2)}{(s^2+1)(s^2-2)}\right), \\ W(i\sqrt{J},i\sqrt{J},i\sqrt{J}) &= \frac{8}{\pi^3}\exp\left(-\frac{3J(s^2+2)}{s^2-2}\right). \end{aligned} \tag{2.57}$$

Consequently B_3 (2.55a) becomes:

$$B_3 = 3\exp\left\{-\frac{J(s^4-s^2+2)}{(s^2+1)(s^2-2)}\right\} - \exp\left\{-\frac{3J(s^2+2)}{(s^2-2)}\right\}. \tag{2.58}$$

In the region $s \to 1^+$, B_3 never reaches a value greater than 2 (Figure 2.2), meaning the inequality is not violated in this region for this parameter choice. Nevertheless, a violation corresponding to the EPR limit $s \to 1^+$ can be found by making the choice $\alpha = -\beta = -\sqrt{J}$; $\gamma = 0$, for which (2.56) gives:

$$\begin{aligned} W(-\sqrt{J},0,0) = W(0,\sqrt{J},0) &= \exp\left\{-\frac{J\left(s^4+s^2+2\right)}{\left(s^2-1\right)\left(s^2+2\right)}\right\}, \\ W(-\sqrt{J},\sqrt{J},0) &= \frac{8}{\pi^3}\exp\left(-\frac{2J(s^2+1)}{(s-1)(s+1)}\right), \\ W(0,0,0) &= 1, \end{aligned} \tag{2.59}$$

and B_3 becomes (Figure 2.3):

$$B_3 = 1 + 2\exp\left\{-\frac{J\left(s^4+s^2+2\right)}{\left(s^2-1\right)\left(s^2+2\right)}\right\} - \exp\left\{-\frac{2J\left(s^2+1\right)}{\left(s^2-1\right)}\right\}. \tag{2.60}$$

In this case, as $s \to 1^+$, $J \to 0$, the maximum value is $B_3^{max} \approx 2.09$, which can be checked both analytically and numerically.

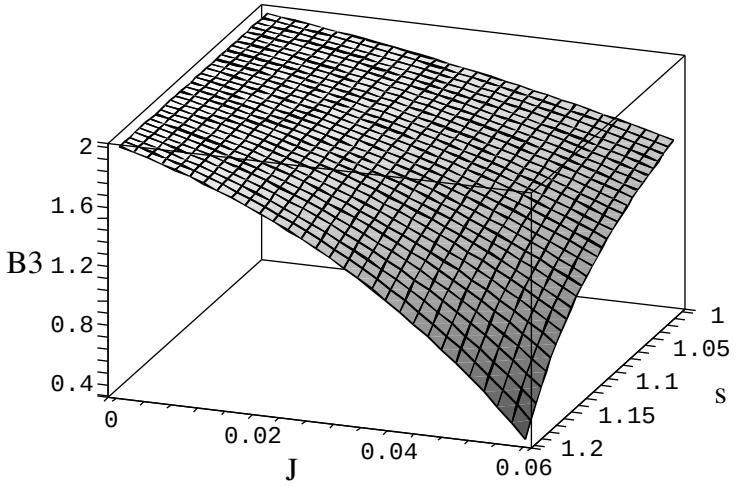

Figure 2.2: Tripartite s-modified CHSH. With an all-imaginary choice for α, β and γ, B_3 never reaches a value greater than 2 as $s \to 1$.

However, what is more interesting still is exploring an auxiliary regime of the regulator, $s \to \sqrt{2^+}$, in equation (2.58). This is shown in Figure 2.4. Analytically, we can approximate the maximum of (2.58) for $s \to \sqrt{2^+}$ to the lowest order in $s - \sqrt{2} = \epsilon$. We note that a pole exists in (2.58) at $(s^2 - 2)$ and therefore substitute $s = \sqrt{2^+}$ such that $B_3 = 3x - x^\lambda$, where $x = \exp(-4J/3\epsilon^2)$, and $\lambda = 9$. To find the value of x at which B_3 reaches its maximum value we

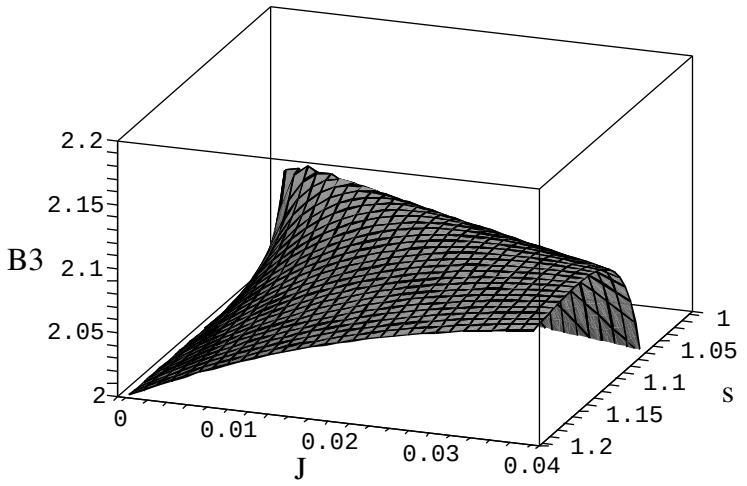

Figure 2.3: Tripartite s-modified CHSH. With $\alpha = -\beta = -\sqrt{J}$, $\gamma = 0$, B_3 reaches a maximum value of ≈ 2.09 as $s \to 1^+$ and $J \to 0$.

find the derivative $dB_3/dx = 0$ which shows $x = \left(\frac{3}{\lambda}\right)^{\frac{1}{\lambda-1}}$. At this value of x we find the maximum value

$$B_3^{max} \cong (\lambda - 1)\left(\frac{3}{\lambda}\right)^{\frac{\lambda}{\lambda-1}} \cong 2.32. \tag{2.61}$$

This can be confirmed numerically for $s \to \sqrt{2^+}$, $J \to 0$. The values of B_3^{max} correspond exactly to those calculated for the experimentally verified NOPA-like states, whose maximisation as $r \to \infty$ is also governed by (2.61).

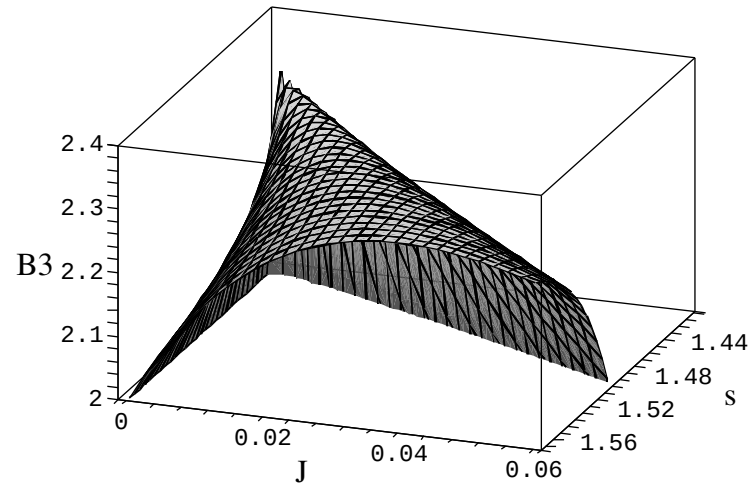

Figure 2.4: Tripartite s-modified CHSH. With an all imaginary choice for α, β and γ, B_3 reaches a maximum value of ≈ 2.32 as $s \to \sqrt{2^+}$ and $J \to 0$.

2.4 Discussion and further pursuits

In this new era of experimental realisation and utilization of CV EPR states, we have shown here that a rigorous framework from first principles in the bipartite case can be extended naturally to tripartite states. Given the necessity of working with normalisable states which still approximate the ideal EPR-type limit for practical implementation of CHSH inequalities, we examined a family of such regulated states parameterized by a regulating parameter s. This family of states was compared with those relating to multipartite NOPA-like states. The NOPA states have been shown to manifest CHSH violations, and have the advantage of being directly accessible by experiment via standard quantum optics protocols such as multiparametric heterodyne detection techniques and beam splitter operations. However, as an extension of a direct transcription of the EPR paradox, this new η-family of regularised states provides an alternative, systematic description of the approach to the ideal EPR states for relative variables.

In the bipartite case, we showed that the NOPA and η-states can be transcribed to approach equivalence with $\tanh r = 1/s^2$, with equivalent violation of the CHSH inequality in this limit. In developing the regularised tripartite state analysis we found expressions for their eigenstates. It became apparent that there are two regimes of the regularisation parameter in which these states become singular: in one case ($s \to 1$) we have a singular eigenstate of the relative coordinates while remaining squeezed in the total momentum; in the other limit ($s \to \sqrt{2}$) we have a singular eigenstate of the total momentum, but squeezed in the relative coordinates. In these two regimes we have explored CHSH inequalities via Wigner functions regarded as expectation values of displaced parity operators. Violations of the tripartite CHSH bound ($B_3 \leq 2$) are established analytically and numerically, with $B_3 \cong 2.09$ in the canonical regime ($s \to 1^+$), as well as $B_3 \cong 2.32$ in the auxiliary regime ($s \to \sqrt{2^+}$). This maximal violation is the same as the maximal violation achieved with the NOPA-like states.

Related tripartite entangled states have recently been constructed by Fan [56]. However, despite those states being accessible by standard quantum optics techniques, they are not true generalisations of ideal 'EPR' states. That is,

while they diagonalise one centre-of-mass variable (for example, $X_1+X_2+X_3$), they are *coherent* states [85] of the remaining relative Jacobi observables (that is, they diagonalise their annihilation mode operators $\mathfrak{a}$, $\mathfrak{b}$). This is different from the $s \to \sqrt{2}$ limit of our EPR-type tripartite states, which as stated above turn out to be *squeezed* states of these relative degrees of freedom (eigenstates of a linear combination $\frac{1}{\sqrt{3}}(2\mathfrak{a}+\mathfrak{a}^\dagger)$, $\frac{1}{\sqrt{3}}(2\mathfrak{b}+\mathfrak{b}^\dagger)$ in the relative mode operators, with the value $\frac{1}{2}\ln 3$ for the squeezing parameter). Moreover, in the case of the tripartite entangled states of [56], no regularisation has been given.

The Wigner functions for the tripartite NOPA-like states (2.29) show peaks at zeroes of $X_i - X_j$ and $P_i + P_j$ for all distinct pairs i, j [16], which may not appear to be consistent with simultaneous diagonalisation of commuting observables. It can, however, be inferred from the agreement between (2.29) and a recent complementary proposal for the construction of true multipartite entangled states [57, 55] that do approach the ideal EPR limit, that the two constructions are in agreement. The second-quantised form for the tripartite entangled state proposed in [55] is

$$|p,\xi_2,\xi_3\rangle = \frac{1}{\sqrt{3}\pi^{\frac{3}{4}}}\exp\Big[A+ \frac{i\sqrt{2}p}{3}\sum_{i=1}^3 a_i^\dagger + \frac{\sqrt{2}\xi_2}{3}(a_1^\dagger - 2a_2^\dagger + a_3^\dagger) + \frac{\sqrt{2}\xi_3}{3}(a_1^\dagger + a_2^\dagger - 2a_3^\dagger) + S^\dagger\Big]|000\rangle,$$

$$\begin{aligned} A &\equiv -\frac{p^2}{6} - \frac{1}{3}(\xi_2^2 + \xi_3^2 - \xi_2\xi_3), \\ S &\equiv \frac{2}{3}\sum_{i<j=1}^3 a_i a_j - \frac{1}{6}\sum_{i=1}^3 a_i^2, \end{aligned} \tag{2.62}$$

from which we can deduce that in the infinite squeezing limit $\tanh(r) = 1$, the tripartite NOPA state (2.29) approaches the same EPR limit as (2.62) for the case $p = \xi_2 = \xi_3 = 0$.

We have discussed the composition of the NOPA-like states, which are constructed with a view to experimental realisability, and, in the bipartite case, to manufacture specific properties of the Wigner function. In this sense, the new suggestions for regularised states stemming from a direct transcription of the EPR paradox in terms of the simultaneous diagonalisation of commuting observables can be seen as a more general or fundamental description. As the regularised tripartite EPR-type state proposed in this chapter produces

a different Wigner function from the NOPA-type, with two singular limits rather than one, this new regularisation may potentially suggest that alternative experimental ways to achieve violations of the CHSH inequalities are possible. The current construction of EPR-type states also considers in more detail the structure of tripartite EPR-type states, compared to the comprehensive [55] which finds n-partite representations of entangled states through their Gaussian-form completeness relation without exploring regularisations, Wigner function behaviour and CHSH inequality violation. For a review of Gaussian states, and discussions of the realisability of entangled states, we refer to [2, 1, 59, 14], and references therein.

In further work, it would be worth establishing the full experimental ramifications of the constraints placed on the choices of displacement parameters entailed by the shift in η. The current discussion might also easily be extended to include a presentation of the alternative bipartite starting point of conjugate variable choice $X_1 + X_2$ and $P_1 - P_2$, and its tripartite counterpart. Furthermore, one can extend the analysis to an N-partite generalisation, where one might reasonably expect the mode combination to take the form $\left[\exp\left(\frac{1}{s^2}\left(\sum_{i<j} a_i^\dagger a_j^\dagger\right)\right)\right]$ (see for example [123], which discusses the canonical combinations for any number of modes). We also discussed the choice of regularisation for the η-states, which introduced a single regularisation parameter for each mode. In this case these all took the same value $1/s$, which was the simplest possible choice that preserved the symmetry of the state. One could, however, consider alternative regularisations, which could potentially suggest a whole family of previously uninvestigated experimentally accessible entangled states.

Since the publication of this work in [77], the practical implementation of many of the ideas considered herein have been discussed with the experimental quantum optics group at the Australian National University (ANU), headed by Prof. Hans Bachor, and work on this is ongoing. Unfortunately the ANU facility does not have the sensitive photon counter equipment necessary to test the η-state locality violation directly. However, there is great interest in finding a clear transcription between current experimental EPR variance calculations and the single Bell operator parameter (B_2, B_3, etc) discussed in this thesis. The experimental variance calculations rely on a combination of

the variance for the level of squeezing achieved and the variance for equipment efficiencies (see [14] for an introduction to the practicalities of experiments in quantum optics). On measuring combinations of variables such as $X_1 - X_2$, there will be an associated variance from the inaccuracies of the measurement. The variances are combined in a way to produce a number between 0 and 1, which is called 'EPR' in quantum optics terms, where the number less than 1 indicates how close one is to the perfect EPR state and thus the degree of non-locality achieved.

In experimental quantum optics, attempts to increase the degree of violation are currently concentrated on improving the level of squeezing. The two regions of violation $s \to 1$ and $s \to \sqrt{2}$ demonstrated by the regularised tripartite η-state might indicate that a different way of achieving violation is possible, which would have immediate implications for production, measurement and implementation. For further development of these ideas it is necessary to define clearly the relationship between the regularisation parameter 's' and the experimental measurement factors and variance parameters.

Note also that this work was recently cited in connection with the construction of a generalized multi-mode bosonic realization of the $SU(1,1)$ algebra and its corresponding squeezing operator [147]. There, the Wigner function representations of their multi-mode squeezed vacuum states are used to examine CHSH inequality violations in the same manner as discussed herein. This underscores the utility of the method of analysis of entangled states, and broadens its field of application to non-linear optical processes and Bose-Einstein condensation in dilute gases.

In this chapter we have examined the structure and interpretation of entanglement through its role in the EPR paradox, which is only one approach among many in a vast literature on the subject. Nevertheless, the information presented here contributes considerable detail to one of the most famous experiments in fundamental quantum mechanics. We have presented a rigorous extension of Fan and Klauder's general EPR-like states to the regularised tripartite CV case for relative variables, and we have discovered an interesting new structure. The CHSH inequalities constructed with component Wigner functions for this case show significant violation of the classical bound, which we have compared with current quantum optics implementations and have

identified a number of differences and areas for further investigation. Having seen some of the drastic consequences of the quantum phenomenon of entanglement on classical interpretation, we can now ask what the effect of a classical phenomenon is on quantum interpretation, which we shall address in the coming chapters.

Chapter 3

Quantum Dissipative Systems

The exposition of this chapter follows the development of two specific quantum system-environment models, namely the Spin-Boson and Kondo models, before describing the construction of a new dissipative system starting from an anisotropic Coqblin-Schrieffer model. Using the tools of constructive bosonisation and exact solvability, it is shown that the Spin-Boson model is equivalent to the XXZ-type anisotropic Kondo model, and a new observation is made about the structure of the fully anisotropic XYZ-type Kondo model. The methods are extended to three-component fermions, which presents a new, exactly solvable three-level dissipative system. The main results of this chapter have been published in a condensed form in [78] and supplementary results are being prepared for submission.

3.1 Introduction

In Chapter 2 we examined one of the most baffling features of entanglement – the apparent violation of locality by systems of two (or more) quantum particles. The example highlighted the gulf between current theory and a satisfactory description of what is by now an easily reproducible and experimentally accessible phenomenon. The EPR experiment and its related proofs demonstrate that one cannot preserve both the postulates of quantum mechanics and special relativity. The experiment is therefore deserving of its status as a paradox, given our otherwise dependable reliance on these theories in fundamental physics. Despite nearly a century of sustained effort to find a

consistent theory that can avoid this paradox, there is still little consensus in the literature. Clues to a more complete theory can be found by looking closely at the interaction between quantum and classical systems, and consequently this chapter will expound in detail certain elements of that interface.

Several branches of both classical and quantum physics address the challenge of many-body interactions. In three-dimensional mechanics it is believed that the problem cannot be solved exactly for three or more bodies, but for lower dimensions many models may be solved precisely. This chapter will investigate a subclass of one-dimensional exactly solvable models in detail, in which a quantum particle interacts with a dissipative bath. Specifically, we will demonstrate the connection between fermion gas-impurity models and quantum dissipative systems using the Spin-Boson (SB) and Kondo models, and by extension of the analysis we will also consider an Anisotropic Coqblin-Schrieffer (ACS) model, resulting in a new three-level exactly solvable dissipative system. More generally, it becomes evident that these workable system-environment models are an invaluable resource for investigating the quantum-classical boundary.

The origins of the SB model were discussed by Leggett et al in 1987 [95, 96]. The model is reviewed clearly and comprehensively therein, and more recently in [136]. The model describes a single two-state quantum system, such as a spin-half particle, interacting with a bath or reservoir of oscillators, which are described by bosonic statistics (hence the term Spin-Boson). This clearly makes the SB model an example of a two-level quantum dissipative system (2LQDS). Since the bath is only very weakly perturbed by the quantum system, the joint system's classical dynamics may be represented by linear equations. In [95] it is argued that the model for a double potential well (see figure 3.1) can be truncated to the Hamiltonian for an interacting two-state system. For this to be the case the thermal energy (proportional to k_BT, where k_B is the Boltzmann constant and T is the temperature) must be smaller than the energy between the excited states, so that we are concerned only with the ground states of the wells. These would now be linked only by any possibility of tunnelling between wells.

The Hamiltonian for the isolated two-state system may be written as $H = -\frac{1}{2}\hbar\Delta_0\sigma_x + \frac{1}{2}\epsilon\sigma_z$, with the eigenvalues of σ_z corresponding to the particle being in either the left or right wells. Δ_0 here indicates the 'bare' tunnelling

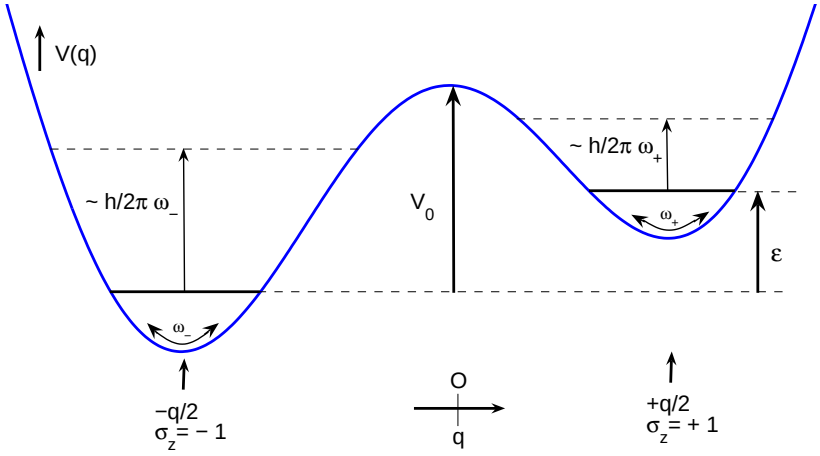

Figure 3.1: Double potential well with potential V(q) for extended coordinate q, showing the two-state limit. The eigenvalues of σ_z correspond to the particle being in either the left or right wells. ω_b is the smallest characteristic classical frequency and ϵ is the detuning parameter. The possibility of quantum tunnelling is accounted for in an effective tunnelling matrix element Δ discussed in-text. The Hamiltonian describing the overall system is given in (3.1b).

matrix element, but to take account of higher-frequency effects impacting on the system we shall later use a renormalised effective tunnelling matrix element Δ (see for example [136], section 18.1), where a physical cutoff parameter resolves the ultraviolet divergence of the renormalisation integral. The likelihood of tunnelling between the two potential wells (an entirely quantum phenomenon) is clearly dependent on the relative heights of the wells. The difference between the ground-state energies of the two wells when there is no tunnelling is the detuning (ϵ) of the system. It is clear then that the dynamics of the eigenstates of σ_z are dependent on this detuning parameter. In the symmetric well limit ($\epsilon = 0$), the probability of finding the system in the right well P_R minus the probability of finding it in the left well P_L becomes $P(t) = P_R - P_L = \cos(\Delta_0 t)$, meaning the eigenstates of the wells are delocalised and oscillating. That is, the system may be in either well by a superposition of their respective wave functions, providing an excellent workable model for entanglement and the loss of entanglement.

When a two-level system as described above interacts with an environment there is a suppression of the quantum features. These systems are considered to be "open" dissipative systems in that interactions between the system and the environment result in sharing of information with so many degrees of

freedom that it is unlikely that this information can all be recorded and the interaction reversed. This can be summarised in an entropy measure (which we shall discuss further in Chapter 4), and some authors attempt to use such explanations to rely on the second law of thermodynamics to explain the apparent directionality of time. However, it would seem such arguments are viciously circular as they already assume a preferred time direction in order for the system to 'evolve' in this way [76]. In this investigation we shall minimise our interaction with this philosophical minefield, and confine our discussion to more intricate details of the models concerned, with entropy used only as a relative measure between any two particular states of interest.

In the case of quantum systems in a superposition of states, it is well known that measurement reduces the system to a single eigenstate – commonly known as the wave function collapse, a suppression of the quantum features. Because system-environment models also present a suppression of quantum features, some authors refer to the systems as being "measured" by the environment, and that there is a similar "collapse" which describes this suppression. As mentioned in the Introduction, Kiefer and Joos [84] provide arguments to the contrary, warning that this reasoning assumes a premature conflation of the ideas of dissipation and decoherence. Explanations of the exact relationship between the two descriptions are not complete, but the following two chapters will provide some further insight into their interplay. The current chapter will describe in detail the construction of quantum dissipative systems, and Chapter 4 will investigate entanglement criteria in those models.

In the present case of the two-level quantum system, we shall suppose that the environment is a bath of harmonic oscillators, as is often the case in practical applications [34]. The overall system Hamiltonian then includes the sum of all the oscillator terms. It is argued in [34]-Appendix C (see also [35]), that the assumption of a harmonic oscillator environment is equivalent to the assumption of linear dissipation, so the Hamiltonian acquires a (linear) coupling term to describe the interaction between the system and the bath, resulting in the

overall SB Hamiltonian [95]:

$$H_{SB} = -\frac{1}{2}\hbar\Delta\sigma_x + \frac{1}{2}\epsilon\sigma_z + \sum_i \left(\frac{1}{2}m_i\omega_i^2 x_i^2 + \frac{p_i'^2}{2m_i}\right) + \frac{1}{2}q_0\sigma_z\sum_i C_i' x_i \quad (3.1a)$$

$$\equiv -\frac{1}{2}\hbar\Delta\sigma_x + \frac{1}{2}\epsilon\sigma_z + \hbar\sum_i \omega_i\left(b_i^\dagger b_i + \frac{1}{2}\right) + \frac{1}{2}\sigma_z\hbar\sum_i C_i(b_i + b_i^\dagger). \quad (3.1b)$$

Here we have included the Hamiltonian with the traditionally recognisable harmonic oscillator terms in (3.1a), and its second quantised counterpart (3.1b), which is the notation that will be used throughout the rest of the chapter. The index i denotes the i^{th} harmonic oscillator, and q_0 is a measure of the distance between the two potential minima. We have used the standard relations

$$x_i = \sqrt{\frac{\hbar}{m_i\omega_i}}q_i, \;\; q_i = \frac{1}{\sqrt{2}}(b_i + b_i^\dagger), \;\; p_i' = \sqrt{\hbar m_i\omega_i}p_i, \;\; p_i = \frac{1}{i\sqrt{2}}(b_i - b_i^\dagger). \quad (3.2)$$

Note also that the zero-point energy ($\frac{1}{2}\hbar\sum_i\omega_i$) from the third term in (3.1b) is commonly ignored.

It is important to note the relationship between the coupling terms C_i' and C_i in (3.1a) and (3.1b), as the different conventions have resulted in different nomenclature being used in the literature. Clearly the coupling term C_i' has dimensions Joules per meter squared, and we can see that

$$C_i = \frac{q_o C_i'}{\sqrt{2\hbar m_i\omega_i}}$$

has dimensions of frequency. These coupling coefficients are used to create a single term to describe the interaction and dynamics of the overall system, commonly known as the spectral function. In fact, the term spectral function is often used for both the Spin-Boson case (3.1b) and for continuous models, because the two bear a simple relation. The spectral function for the case (3.1b) is given by the definition [34, 136]

$$G(\omega) := \sum_i C_i^2\delta(\omega - \omega_i), \quad (3.3)$$

which relates to the continuous spectral function $J(\omega)$ as follows [136]:

$$G(\omega) = \left(\frac{q_0^2}{\pi\hbar}\right)J(\omega) = \left(\frac{q_0^2}{\pi\hbar}\right)\frac{\pi}{2}\sum_i \frac{C_i'^2}{m_i\omega_i}\delta(\omega - \omega_i). \quad (3.4)$$

We can see that the function $G(\omega)$ has dimension frequency, and $J(\omega)$ has dimension mass times frequency squared.

In general, it is assumed that $J(\omega)$ varies as a power law of ω (with an exponential cutoff), and it is treated as a continuous and smooth function by assuming that the oscillator frequency spectrum is dense, and that there is nonpathological coupling and mass distribution [95]:

$$J(\omega) = A\gamma\omega^s e^{-\omega/\omega_c}. \tag{3.5}$$

The frequency ω will be affected by a cutoff frequency ω_c that is large compared to Δ, and the cutoff will be discussed in detail in Subsection 3.2.3. The power (s) of ω in $J(\omega)$ indicates whether the bath is Ohmic ($s = 1$), super-Ohmic ($s > 1$) or sub-Ohmic ($s < 1$) (see (3.65) for demonstration of Ohmic relation). For Hamiltonian (3.1b) we consider the Ohmic regime, for which one sets[1]

$$A = \frac{\pi\hbar}{q_0^2}. \tag{3.6}$$

The parameter γ in (3.5) is a dimensionless parameter (see Subsection 3.3.1) that now governs the system dynamics. In rough terms, the range $0 < \gamma < 1/2$ gives damped coherent oscillations, the value $\gamma = 1/2$ provides the crossover to incoherent oscillations, $1/2 < \gamma < 1$ gives exponential decay, and $1 < \gamma$ gives localisation.

The SB model, or 2LQDS, described above is closely related to the original Kondo model [87] (sometimes also referred to as the $s-d$ exchange model from its original formulation by Zener in 1951 [153]). The Kondo model describes the interaction between a single spin-half magnetic impurity and otherwise non-interacting electrons (i.e. one spin-half system in a bath of fermions – a spin-fermion model, if you will). Laflorencie et al discuss the relationship between the standard "free electron" Kondo model and the Kondo effect for a chain of spins [91]. The Kondo model has been studied in great detail as it is readily accessible by experiment, but the analysis has often been with a different objective than to investigate the quantum-classical transition. With such a wealth of literature to consider however, the Kondo model is a highly useful, practical way in which to study the effect of external environments on small, controlled systems.

[1]It has been argued that this choice for A is directly proportional to the classically measurable friction coefficient of the extended system, at least in the case of "strictly linear" dissipation [34].

In the case of Ohmic coupling between the quantum system and its environment, it can be shown [95, 44] that the standard anisotropic Kondo Hamiltonian is equivalent to the SB Hamiltonian (see Subsection 3.3.1 for details). This equivalence relies on the methods of constructive bosonisation (see Section 3.2) and unitary transformation, and the example highlights the importance of these principles in relating fermion gas-impurity models to their dissipative system counterparts. Indeed we shall use these methods in this chapter to show that similar links exist between more examples of this family of models.

The Kondo problem is one of a class of several models investigating the theory of magnetism, as originally proposed by Werner Heisenberg in 1928 [71]. The isotropic Heisenberg Hamiltonian treats the spins of the magnetic systems quantum mechanically, with each spin sitting on a lattice point:

$$H = -J \sum_{l=1}^{N} S_l^x S_{l+1}^x + S_l^y S_{l+1}^y + S_l^z S_{l+1}^z - 2h \sum_{l=1} S_l^z, \tag{3.7}$$

where h is the magnetic field aligned in the z-direction. The ground state has all spins aligning spin-up, and the total z-component of spin S^z is $N/2$. In a similar manner, the original isotropic Kondo Hamiltonian, which will be discussed in detail in Section 3.3, often takes the form:

$$H_K = \sum_{\boldsymbol{k},\sigma} \epsilon(\boldsymbol{k}) c_{\boldsymbol{k}\sigma}^\dagger c_{\boldsymbol{k}\sigma} + J\boldsymbol{S} \cdot \boldsymbol{s}(0). \tag{3.8}$$

In this standard form of the Hamiltonian, the magnetic field component $g\mu_B h S_z$ is omitted, where g is the gyromagnetic ratio and μ_B the Bohr magneton. The indices on the spin operators in the Kondo model are dropped to subscripts, providing a more consistent notation for subsequent sections, where there is no summation over lattice points. The coupling parameter in the Kondo model is given the symbol J, and its value dictates the regime of the model: $J > 0$ indicates the anti-ferromagnetic regime, and $J < 0$ indicates the ferromagnetic regime (note that individual authors may use different sign conventions of the model (3.8), as some authors prefer to keep the Heisenberg form of negative J). Depending on the level of isotropy in the coupling parameter J, we can identify these simplified one-dimensional models with labels pertaining to the anisotropy of the internal (spin) degrees of freedom. These broader models are labelled XXX for the isotropic case, and XXZ and XYZ for the anisotropic

Kondo models (AKM), just as they were for the original Heisenberg chains. The Kondo Hamiltonian (3.8) and its related anisotropic models will be discussed in detail later in this chapter, and further comment will be reserved for such sections.

In order to investigate the asymptotic limits of the models and to determine the precise effect of the parameters, we shall restrict our analysis to completely integrable systems – that is, those systems which are exactly solvable by the star-triangle (or now more widely know as the Yang-Baxter) equation. The exact solution for the ferromagnetic XXX model was found as early as 1931, by Hans Bethe using his now famous Bethe Ansatz [26]. The Ansatz is used to find energy eigenstates of one-dimensional versions of interacting, localized spin-half particles in Heisenberg models of solids, where nearest neighbours can interact, with periodic boundary conditions. In general, the N-body wavefunction is written as a linear combination of $N!$ plane waves with N quasi-momenta which must satisfy the Bethe Ansatz equations. By solving these equations one can find the energy density (energy per unit length), and most thermodynamical quantities of interest. In 1966, Yang and Yang [145] showed that the method was applicable to the XXZ model, and it was confirmed through Baxter's so-called six-vertex model [21]. In 1972, Baxter [17] solved the XYZ model by a generalisation of the Bethe Ansatz, through its link to the related eight-vertex model [18, 19, 20]. Unbeknown to Baxter [21], Sutherland had shown in 1970 [117] that the transfer matrix of any zero-field eight-vertex model commutes with an XYZ operator Hamiltonian (thus having the same eigenvectors). A little later, Takhtadzhan and Faddeev neatly related the XYZ model to the quantum inverse problem [119].

Having established some important features and problems with entanglement as part of a consistent fundamental physical theory in Chapters 1 and 2, this chapter will investigate the interaction between the simple quantum systems outlined above and a medium which suppresses the quantum features. The investigation will require a re-examination of the well-known bosonisation method and its application to anisotropic Kondo models, which we do in Sections 3.2 and 3.3. The detailed re-examination unveils some previously unreported results regarding the structure of the elliptic XYZ-type Kondo model, which is explained in Subsection 3.3.2. In Section 3.4 the methods

are comprehensively extended to a new three-level model, and we show that this model is exactly solvable (main results published in [78]). Such solvable many-body interaction systems are extremely rare and important in condensed matter systems, and we suggest a range of potential applications and directions for further work in Section 3.5. Some further extensions of the models and discussion of their relationship to entanglement will be reserved for Chapter 4.

3.2 Constructive bosonisation

We begin the analysis of fermion gas-impurity models with an introduction to the method of constructive bosonisation. Although this is an established method, often used in quantum field theory and condensed matter for example, we shall go on to show that the approach warrants re-examination in its application to a wide variety of models, and gives access to a range of previously unknown results.

It has long been known that fermion fields have a bosonic description, with the original field theoretic formulation often accredited to Tomonaga (1950) [122]. We shall be using the so-called 'constructive bosonisation' approach of Haldane, from 1981 [67]. In condensed matter physics, bosonisation and refermionisation is often used to diagonalise Hamiltonians, but the method has a more general utility, despite some criticism of the approximations used in the method (see [66] and Section 3.3 for further comment). The simplifications afforded by a bosonic description, such as the use of bosonic density fluctuations, are especially important for the case of one-dimensional models where Landau Fermi liquid theory fails. For the models considered herein, however, the greatest asset of the bosonic transcription is to present the model as exactly solvable. The emphasis is on the bosonisation enabling a mapping from interesting models that have not been solved analytically, to systems for which the dynamics and thermodynamics are either already known or allow for solutions easily.

The comprehensive paper on the dynamics of the dissipative two-level system by Leggett et al [95] introduces dissipation of two-state systems through coupling to bosons in the SB model. The Kondo model, on the other hand,

describes a spin-half impurity interacting with a fermion bath. At the time of writing, a complete and exact mapping between the Spin-Boson and the Kondo model had not been established, but [95] outlines a clear physical correspondence nevertheless. The relationship between the 2LQDS and the Kondo model is shown by the equivalence of the models through the bosonisation of the XXZ-type AKM. This equivalence had been discussed some time earlier by Anderson and Yuval [8, 149], and Blume, Emery and Luther [27, 50] using the alternative partition function description. The partition function is found as a power series by analogy with transitions caused by an X-ray knocking an electron from a low-lying atomic level of a solid [50] (see also Chakravarty [38], and Bray and Moore [33]). We will not investigate this method further here, but note that the method is a useful alternative way of deriving dynamical and thermodynamical properties.

Although Leggett et al show the bosonisation only heuristically, the full bosonisation is done by taking proper account of the Klein factors (see Subsection 3.2.2), as in [44, 151][2]. Aside from the inclusion of Klein factors, the procedure outlined by Costi and Zaránd in [44] is identical to [95]. The result is that a unitary transformation of the bosonised XXZ-type anisotropic Kondo Hamiltonian corresponds to the standard SB Hamiltonian: $UH^B_{XXZ}U^\dagger \equiv H_{SB}$. The reason for this seemingly fortuitous correspondence is that the fermion field $\psi_\alpha(x)$ acting on the ground state of the Fermi sea is an eigenstate of the bosonic operators which create the boson field, such that it has a coherent state representation in terms of the bosonic operators.

3.2.1 Creation and annihilation operators and operator normal ordering

Before detailing the bosonisation procedure, we review briefly the relationship and differences between fermionic and bosonic notation for creation and annihilation operators, as well as the concept of normal ordering. Creation and annihilation operators act on physically realisable many-particle states and retain the symmetry of the state they act on (taking account of normal ordering). The multi-particle space is a direct sum of the tensor product of

[2]Note that the paper by Zaránd and von Delft [151] was published as an eprint in its extended form, with an abridged version appearing in Physical Review B [152].

single-particle states, and the inner product of states with different particle numbers is orthogonal. The bosonic operators b_p and $b_p^\dagger$ satisfy the usual Bose commutation relations $[b_p, b_{p'}^\dagger] = \delta_{pp'}$, whereas fermionic operators satisfy the corresponding anticommutation relations:

$$\begin{aligned} \left\{c_i, c_j^\dagger\right\} &= c_i c_j^\dagger + c_j^\dagger c_i = \delta_{ij} \\ \left\{c_i, c_j\right\} &= \left\{c_i^\dagger, c_j^\dagger\right\} = 0. \end{aligned} \tag{3.9}$$

While the bosonic creation operator maps an N-particle state to an $N+1$ state, a fermionic creation operator will map to zero if that state is already occupied, due to the Pauli exclusion principle (i.e. $(c_i^\dagger)^2|0\rangle = 0$). Application of fermionic operators is accompanied by a change of sign, and an increase or decrease of the particle number in the orbital specified by the index 'i'.

The number of particles N_i in any given state $|\psi\rangle$ is found by applying the number operator to that state, which takes the same form for both fermionic and bosonic operators, generically denoted by $\widehat{N}_i = a_i^\dagger a_i$, where a_i reduces the number of particles in that state by one and $a_i^\dagger$ increases it by one back to the original. This means that $\widehat{N}_i|\psi\rangle = N_i|\psi\rangle$, and the total number of particles in the space is found by $N = \sum_i N_i$ for the eigenvalues N_i. The number operator is clearly a diagonal matrix with elements N_i, which are the eigenvalues for the operator equation. Note now that the reverse-ordered operator $\widehat{\mathcal{N}}_i = a_i a_i^\dagger$ is also a diagonal matrix, but in this case will have different eigenvalues for bosons and fermions, respectively given by:

$$b_i b_i^\dagger \to \mathcal{N}_i + 1, \quad c_i c_i^\dagger \to 1 - \mathcal{N}_i. \tag{3.10}$$

The ordering of the operators is thus of great importance, and yields different results for fermionic and bosonic operators.

A crucial identification for the bosonisation procedure is the transcription of an infinite number of fermionic modes of species α to bosonic modes by the bilinear combinations (see for example [132]):

$$\begin{aligned} b_{p\alpha}^\dagger = (b_{p\alpha})^\dagger &= i n_p^{-1/2} \sum_{k=-\infty}^{\infty} c_{k+p\,\alpha}^\dagger c_{k\alpha} \\ b_{p\alpha} &= -i n_p^{-1/2} \sum_{k=-\infty}^{\infty} c_{k-p\,\alpha}^\dagger c_{k\alpha}. \end{aligned} \tag{3.11}$$

For finite system length L, the fermionic wavenumbers k are quantized as

$$k = \frac{2\pi}{L}(n_k - \delta_n/2), \tag{3.12}$$

where δ_n is 0 for complete periodicity, or 1 for antiperiodicity. It is clear that the fermionic operators rely on the discrete k's being unbounded from below, while the bosonic operators themselves are only defined for discretised *positive* wave number $p = 2\pi n_p/L$. In most practical situations, implementing the procedure will result in non-normal ordered expressions.

Normal ordering requires the ordering of creation and annihilation operators to annihilate the 'vacuum', which in many cases demands that the standard creation operators be to the left of the annihilation operators. Normal ordering is indicated by the notation $: \ldots :$, with the expression between the two colons being normal ordered. The procedure is the same for both fermions and bosons, although they annihilate different states: fermions annihilate the vacuum state, or Fermi sea, denoted by $|0\rangle_0$ or $|F\rangle$, while 'vacuum' state for bosonic operators may be regarded as the ground-state $|N_i\rangle_0$. Explicitly we have

$$\begin{aligned} c_{k\alpha}|0\rangle_0 &= 0 \quad \text{for } k > 0, \\ c^\dagger_{k\alpha}|0\rangle_0 &= 0 \quad \text{for } k \leq 0, \\ b_{p\alpha}|N_i\rangle_0 &= 0, \end{aligned} \tag{3.13}$$

where $b_{p\alpha}$ is defined for $p > 0$ only. The case $k = 0$ is on the Fermi surface, and indicates the highest filled level of $|0\rangle_0$. As an example of normal ordering, the number operator $\widehat{N}_\alpha$ for electrons of species α would be written explicitly as:

$$\widehat{N}_\alpha = \sum_{k=-\infty}^{\infty} : c^\dagger_{k\alpha} c_{k\alpha} := \sum_{k=-\infty}^{\infty} [c^\dagger_{k\alpha} c_{k\alpha} - {}_0\langle 0|c^\dagger_{k\alpha} c_{k\alpha}|0\rangle_0]. \tag{3.14}$$

Normal ordering is often equivalent to the "point-splitting" regularisation technique used in field theory in that their electron densities $: (\psi^\dagger_\alpha(z)\psi_\alpha(z)) :$ agree [132]. Point splitting evaluates the products at points a short distance apart and subtracts the divergence, a superfluous mechanism in normal ordering.

3.2.2 Klein factors

The Klein factors $\mathcal{F}_\alpha$ are unitary laddering operators between N-particle Hilbert spaces, raising or lowering the fermion number by one (see e.g. [132]). They ensure different species of fermion fields anticommute, and they commute with all bosonic operators. The effect is to alter the ground state (but not the set of bosonic excitations) to contain either more or less α-fermions. Consequently, they must obey the relations

$$\begin{array}{ll} \left\{\mathcal{F}_\alpha^\dagger, \mathcal{F}_{\alpha'}\right\} = 2\delta_{\alpha\alpha'} & \text{for all } \alpha, \alpha' \\ \{\mathcal{F}_\alpha^\dagger, \mathcal{F}_{\alpha'}^\dagger\} = \{\mathcal{F}_\alpha, \mathcal{F}_{\alpha'}\} = 0 & \alpha \neq \alpha' \\ [\mathcal{F}_\alpha, b_{p\alpha'}] = [\mathcal{F}_\alpha, b_{p\alpha'}^\dagger] = 0 & \text{for all } \alpha, \alpha' \\ [N_\alpha, \mathcal{F}_{\alpha'}^\dagger] = \delta_{\alpha\alpha'}\mathcal{F}_{\alpha'}^\dagger & \\ [N_\alpha, \mathcal{F}_{\alpha'}] = -\delta_{\alpha\alpha'}\mathcal{F}_{\alpha'}. & \end{array} \tag{3.15}$$

Moreover we can deduce that, when $i \neq k$ and the shorthand $\mathcal{F}_{ji} = \mathcal{F}_j^\dagger \mathcal{F}_i$:

$$[\mathcal{F}_{ji}, \mathcal{F}_{kj}] = -2\mathcal{F}_k^\dagger \mathcal{F}_i \tag{3.16}$$

$$\{\mathcal{F}_{ji}, \mathcal{F}_{kj}\} = 0. \tag{3.17}$$

Klein factors can be ignored only when the Hamiltonian conserves the number of every species α, such that the correlation functions are non-zero, with equal numbers of $\psi_\alpha^\dagger$ and ψ_α. The factors are often written as an exponential of a phase-type operator $\mathcal{F}_\alpha^\dagger \equiv e^{i\theta_\alpha}$, but as von Delft and Schoeller highlight [132], this notation leads to mistakes. In the Kondo model, if these phase operators were to be absorbed into the boson field, a linear transformation would be meaningless, as these factors would then be ill-defined. Further information about the origins, action and importance of these operators may be found in [132] and references therein.

3.2.3 Bosonisation procedure

This subsection outlines the important considerations for creating the explicit identification between fermionic and bosonic fields, which occurs at the level of operators on Fock space, and further useful expressions pertinent to the procedure that will be implemented in the remainder of the chapter.

One dimensional multicomponent local fermion fields $\psi_\alpha(x)$ can be written in terms of the fermionic annihilation operator $c_{k\alpha}$ using Fourier series as follows:

$$\psi_\alpha(x) = \sqrt{\frac{2\pi}{L}} \sum_k e^{-ikx} c_{k\alpha}. \tag{3.18}$$

Consequently, the fermionic annihilation and creation operators are respectively found by:

$$\begin{aligned} c_{k\alpha} &= (2\pi L)^{-1/2} \int_{-L/2}^{L/2} e^{ikx} \psi_\alpha(x) dx, \\ c^\dagger_{k\alpha} &= (2\pi L)^{-1/2} \int_{-L/2}^{L/2} e^{-ikx} \psi^\dagger_\alpha(x) dx. \end{aligned} \tag{3.19}$$

The normalisation for these expressions can vary in the literature. Here the fermion fields are normalised to 2π as in [132], as opposed to 1 as in [44]. Fermion fields normalised to 2π result in correlation functions normalised to 1.

As demonstrated in Subsection 3.2.1, there exists a formal transcription between an infinite number of such fermionic modes and bosonic operators, which may now be conferred upon the respective fermionic and bosonic fields ($\psi_\alpha(x)$ and $\varphi_\alpha(x)$ respectively). The corresponding bosonic field in one dimension is:

$$\varphi_\alpha(x) = -\sum_{p>0} \sqrt{\frac{2\pi}{L}} (e^{-ipx} b_{p\alpha} + e^{ipx} b^\dagger_{p\alpha}), \tag{3.20}$$

yielding the identification at the level of operators on Fock space:

$$\psi_\alpha(x) = \sqrt{\frac{2\pi}{L}} \mathcal{F}_\alpha : e^{-i\varphi_\alpha(x)} :, \tag{3.21}$$

which includes the Klein factors $\mathcal{F}_\alpha$ to ladder between states with different fermion numbers and ensure correct anticommutation relations between fermionic operators (see Subsection 3.2.2).

In order to regulate the non-normal ordered expressions that arise on implementation of the bosonisation procedure, we introduce a regularisation parameter $a \to 0$ for the ultraviolet divergent momentum states in the non-normal ordered expressions (see Subsection 3.2.1). The regularisation then sets the scale for the suppression of contributions from wavenumbers $|k| \gtrsim a^{-1}$ away

from the Fermi surface and maintains the rigorous fermion-boson correspondence and isomorphism of Hilbert spaces. The parameter is introduced at the quantum field level by modifying (3.20) to become

$$\varphi_\alpha(x) = -\sum_p \sqrt{\frac{2\pi}{L}}(e^{-ipx}b_{p\alpha} + e^{ipx}b^\dagger_{p\alpha})e^{-ap/2}. \tag{3.22}$$

Importantly, this lets us re-express the normal-ordered (3.21) in terms of ordinary operator products in an expansion in powers of a:

$$\psi_\alpha(x) = \lim_{a\to 0}\left(\frac{\mathcal{F}_\alpha}{\sqrt{a}}e^{-i\varphi_\alpha(x)}\right). \tag{3.23}$$

The parameter a is sometimes referred to, perhaps misleadingly, as the lattice spacing because it can be of the order $1/k_F$, where k_F is the wave number at the Fermi surface. However, since its inception Haldane stressed that the parameter itself is not intended to play the role of a 'cutoff length' [67]. Instead, the bosonic 'momentum cutoff' comes in the form $\exp(-ap/2)$ as in (3.22). Von Delft and Schoeller suggest that perhaps effective bandwidth is a more appropriate description ([132], p16). Gulacsi [66] rejects this notion, asserting instead that it measures the minimum wavelength of the density fluctuations which satisfy the bosonic commutation relations. He maintains this would include the effective bandwidth as a special case, specifically in the one-component model, and the interpretation can be extended to systems with two components.

Clearly equation (3.23) does not hold for the case $a = 0$. In this instance it is necessary to use the strictly normal-ordered expressions for the Fermi field [132]:

$$\psi_\alpha \;=\; \mathcal{F}_\alpha\left(\frac{2\pi}{L}\right)^{1/2} e^{-i\frac{2\pi}{L}(\widehat{N}_\alpha - \frac{1}{2}\delta_n)x}e^{-i\phi^\dagger_\alpha(x)}e^{-i\phi_\alpha(x)}. \tag{3.24}$$

This expression contains charge-dependent phase factors deriving from the number operator $\widehat{N}_\alpha$, which implies that (3.23) is valid as an operator identity only when acting on the zero fermion number sectors of the fermionic Hilbert spaces. It is often the case that the phases tend to cancel, because the bosonisation transcription entails expressions that are bilinear with respect to fermions and field quantities evaluated locally at $x = 0$ and so may

in general be ignored. However, some further discussion on the $\widehat{N}_\alpha$-dependent terms and their treatment in relation to the three-level case is included in the appendix, B.1. The case $a = 0$ itself will not be considered further here.

Using (3.11), (3.18) and (3.22), the electron density may be expressed as:

$$\frac{1}{2\pi} : \psi^\dagger_\alpha(x)\psi_\alpha(x) := \frac{1}{2\pi}\partial_x\varphi_\alpha(x) + \frac{N_\alpha}{L}. \tag{3.25}$$

Note that we may write $\varphi_\alpha(x) = \phi_\alpha(x) + \phi^\dagger_\alpha(x)$, where

$$\phi^\dagger_\alpha(x) = (\phi_\alpha(x))^\dagger \equiv -\sum_p n_p^{-1/2} e^{ipx} b^\dagger_{p\alpha} e^{-ap/2}, \tag{3.26}$$

for which we have the following useful commutation relations [132]:

$$\begin{aligned}
\big[\phi_\alpha(x), \phi_{\alpha'}(x')\big] &= \big[\phi^\dagger_\alpha(x), \phi^\dagger_{\alpha'}(x')\big] = 0, && (3.27)\\
\big[\phi_\alpha(x), \phi^\dagger_{\alpha'}(x')\big] &= \delta_{\alpha\alpha'} \sum_p \frac{1}{n_p} e^{-p(i(x-x')+a)} \\
&= -\delta_{\alpha\alpha'} \ln\big[1 - e^{-i2\pi/L(x-x'-ia)}\big] \\
&\overset{L\to\infty}{\to} -\delta_{\alpha\alpha'} \ln\big[i2\pi/L(x-x'-ia)\big], && (3.28)
\end{aligned}$$

i.e. in the limit of large L only terms of the order $1/L$ contribute to the expansion of the exponential.

The commutator of the bosonic field with its derivative is commonly expressed as $[\varphi_\alpha(x), \partial_{x'}\varphi'_\alpha(x')] = 2\pi i\delta(x-x')$, but occasionally it is necessary to consider the order of the limits $a \to 0$ and $L \to \infty$ for a more careful analysis. For these cases we have [132]:

$$\begin{aligned}
[\varphi_\alpha(x), \partial_{x'}\varphi'_\alpha(x')] &\overset{a\to 0, L\to\infty}{\to} 2\pi i\,(\delta(x-x') - 1/L)\,\delta_{\alpha\alpha'} && (3.29a)\\
&\overset{L\to\infty, a\to 0}{\to} \delta_{\alpha\alpha'} 2\pi i(\sum_{n\in Z}\delta(x-x'-nL) - 1/L). && (3.29b)
\end{aligned}$$

Moreover, there is a clear problem of evaluation at $x = 0$, where one would not take the limit $a \to 0$, but use a smeared delta function [151].

The principles outlined above will be utilised in an illustrative example in Subsection 3.3.1, showing the well-known equivalence between the Spin-Boson and Kondo models. Subsequently the method will be used to find new results for the XYZ-type AKM in Subsection 3.3.2, and the new three-level model in Section 3.4.

3.3 Spin-1/2 Kondo Models

The original Kondo model [87] was designed to describe conduction electron resistivity in dilute magnetic alloys. In simple metals and non-magnetic alloys the resistivity decreases monotonically with temperature T, but for dilute magnetic alloys resistivity instead passes through a minimum before rising as $T \to 0$, meaning the impurity or impurities dramatically change the macroscopic properties of the whole system. A perfect lattice should have infinite conductivity at zero temperature. However, phonons resulting from a finite temperature in the system will cause some scattering, and hence dissipation of the electron current (resistivity). There are fewer phonons at lower temperature, so as $T \to 0$ scattering with any impurities begins to dominate. Looking at the $s-d$ model with perturbative techniques, Kondo verified [87] that there is a difference in scattering at third order perturbation: for simple metals, electron-phonon backscattering dominates, whereas there is singular, divergent spin scattering between conduction electrons and impurity at third order. Kondo cites experimental evidence suggesting the resistance minimum is due to a spin interaction, rather than any other impurity features and moreover shows it to be proportional to impurity concentration.

The perturbational approach breaks down at low temperatures, which prompted the development of several many-body techniques to solve this low-temperature 'Kondo Problem' (see Hewson [72] for a brief history of magnetic impurities in metals[3]). Anderson [7] applied a 'poor man's scaling' approach to the task. While this was also perturbational, meaning it still broke down at low temperatures, it could be assumed by analogy to other models that the results could be extended into the low-temperature region. This suggested that there would be infinite coupling between the impurity and one of the conduction electrons to form a magnetically neutral spin-singlet state[4] at low temperatures. This

[3]Hewson's title "The Kondo Problem to Heavy Fermions" refers to so-called 'Heavy fermion' models, which include, for example, Ce or Yb with Tm impurities, where the definition of 'heavy' is in this context a mass ratio $m/m_e \sim 100 - 1000$.

[4]A spin singlet describes the case where particles combine into a correlated state with total angular momentum zero, as discussed in Chapter 2. If two electrons, for example, combine they can form a state with spin 0, which is called the singlet state, or spin 1, which is called the triplet state. (The electron itself would be referred to as a doublet, having two possible spin values $\pm 1/2$.) Note that the term singlet state can also refer to a particle with vanishing spin.

result was corroborated by Wilson's numerical renormalization group methods [144], for which he received the Nobel prize in 1982, and later verified separately by Andrei [9] (see also his extensive summary [10]) and Wiegmann [141, 142, 60, 58] using the exact Bethe Ansatz solutions to the Kondo model. A comprehensive summary and explanation is also given in [127]. The 'Kondo Temperature' T_K is a measure of the temperature below which these singlets may form (below the conduction electron bandwidth). It is the temperature at which the series included in Kondo's perturbative approach becomes divergent, and is found by the relation [72]

$$k_B T_K \sim D e^{-1/2J\rho_0}, \tag{3.30}$$

where D and ρ_0 are the conduction electron bandwidth and density of states respectively, k_B is the Boltzmann constant and J the usual coupling coefficient. (The expression (3.30) is found by the Bethe Ansatz, while some other methods predict an additional factor $|2J\rho_0|^{1/2}$ [72], where the missing $\sqrt{J}$ factor is thought to be due to the ad-hoc nature of the Bethe Ansatz cut-off scheme).

As mentioned in the introduction to this chapter, the isotropic Kondo Hamiltonian is often written as (3.8):

$$H_K = \sum_{\boldsymbol{k},\alpha} \epsilon(\boldsymbol{k}) c^\dagger_{\boldsymbol{k}\alpha} c_{\boldsymbol{k}\alpha} + J\boldsymbol{S}\cdot\boldsymbol{s}(0).$$

This expression uses dimensionless spin operators $\boldsymbol{S} = \frac{1}{2}\boldsymbol{\sigma}$ ($\boldsymbol{\sigma}$ being the vector of 2×2 Pauli matrices (2.1)) and $\boldsymbol{s}(0) = \frac{1}{2}\sum_{\boldsymbol{k},\boldsymbol{k'},\alpha,\alpha'} c^\dagger_{\boldsymbol{k}\alpha}\boldsymbol{\sigma}_{\alpha\alpha'}c_{\boldsymbol{k'}\alpha'}$, which indicates that the position of the impurity is at the origin. It is otherwise common for spin operators to have dimension $\hbar$, and thus the second term in (3.8) can sometimes be seen in the literature with a denominator of $\hbar$. The use of dimensionless spin operators therefore entails a change in the dimensions of the coupling parameter J from frequency to Joules, and we shall follow this convention here. The operator $c^\dagger_{\boldsymbol{k}\alpha}$ creates an electron with spin label α and wave vector $\boldsymbol{k}$. Equation (3.8) assumes antiferromagnetic coupling $J > 0$, and as discussed in the introduction, the second term of the Hamiltonian may be split into components relating to the anisotropy of the internal (spin) degrees of freedom. The resultant split to three coupling parameters thus dictates the labels for the formulations of the model: XXX for the istotropic (3.8) and XXZ or XYZ for the anisotropic models, demonstrated respectively in (3.33)

and (3.34). Moreover, the different anisotropy labels broadly correspond to the rational, trigonometric and elliptic R-matrices respectively in the exactly solvable cases (see later sections). It is well-known that the spin-$\frac{1}{2}$ AKM is exactly solvable through the relation to these R-matrices [21, 127].

As is explained carefully in [95], the construction of (3.8) assumed only s-wave scattering (pointlike exchange interactions). Thus when the plane electronic waves are expanded in spherical waves about the impurity ($c^\dagger_{\boldsymbol{k}\alpha} = \sum_l \sum_{lm=-l}^{l} Y_{lm}(\boldsymbol{k}/k) c^\dagger_{klm\alpha}$), only electrons with angular momentum quantum numbers $l = m = 0$ will be affected. This means the states may be characterised by the magnitude of the wave vector $|\boldsymbol{k}|$, rendering the model essentially one dimensional. Furthermore, it is assumed that the interaction amplitudes are small, and uses the Fermi surface value (k_F) as the momentum reference. Since the dominant excitations are closest to the Fermi surface for long times and low temperatures, the dispersion relation can be linearised around the Fermi energy ϵ_F:

$$\epsilon(\boldsymbol{k}) = \epsilon_F + \hbar v_F(|\boldsymbol{k}| - k_F). \tag{3.31}$$

Therefore, with the new momentum reference $\widetilde{k} = |\mathbf{k}| - k_F$, the free fermion Hamiltonian is

$$H_0^F = \hbar v_F \sum_{\widetilde{k}\alpha} \widetilde{k} c^\dagger_{\widetilde{k}\alpha} c_{\widetilde{k}\alpha}, \tag{3.32}$$

where the operator $c^\dagger_{\widetilde{k}\alpha}$ creates an electron with spin label α and momentum $|\mathbf{k}| = \widetilde{k} + k_F$, and clearly $\widetilde{k}$ cannot be less than $(-k_F)$.

In modifying the model to XXZ-type anisotropy, one splits the coupling term from (3.8) into parallel and perpendicular terms to find the XXZ-type Hamiltonian[5]:

$$\begin{aligned} H^F_{XXZ} &= H^F_0 + H^F_{||} + H^F_{\perp} \\ &= \hbar v_F \sum_{\widetilde{k},\alpha=1,2} \widetilde{k} c^\dagger_{\widetilde{k}\alpha} c_{\widetilde{k}\alpha} + \frac{J_{||}}{2} \sum_{\widetilde{k},\widetilde{k}'} (c^\dagger_{\widetilde{k}\uparrow} c_{\widetilde{k}'\uparrow} - c^\dagger_{\widetilde{k}\downarrow} c_{\widetilde{k}'\downarrow}) S_z \\ &\quad + \frac{J_\perp}{2} \sum_{\widetilde{k},\widetilde{k}'} \left(\sigma_+ c^\dagger_{\widetilde{k}\uparrow} c_{\widetilde{k}'\downarrow} + \sigma_- c^\dagger_{\widetilde{k}\downarrow} c_{\widetilde{k}'\uparrow} \right). \end{aligned} \tag{3.33}$$

[5]Note that we will use the second quantised notation throughout, although the method was very new when Bethe was originally working with the XXX Heisenberg model. Dirac developed second quantisation for Bose statistics in 1927, and a year later Wigner and Jordan extended it to fermionic particles.

Notice that in this representation the dual notation for the spin labels $\alpha, \beta = 1, 2$ indicates that the values enumerated by $1, 2$, correspond directly to the explicit $\uparrow, \downarrow$ eigenvalues of σ_z, such that $1 \equiv\uparrow$, $2 \equiv\downarrow$. The sign of $J_\perp$ is irrelevant, since it can be compensated for by a rotation of the impurity spin. Similarly, to obtain the XYZ-type anisotropic Hamiltonian one separates the internal, spin degrees of freedom into three coupling components:

$$\begin{aligned} H^F_{XYZ} &= \hbar v_F \sum_{\widetilde{k},\alpha=1,2} \widetilde{k} c^\dagger_{\widetilde{k}\alpha} c_{\widetilde{k}\alpha} + \frac{J_x}{2} \sum_{\widetilde{k},\widetilde{k}'} \left(c^\dagger_{\widetilde{k}\uparrow} c_{\widetilde{k}'\downarrow} + c^\dagger_{\widetilde{k}\downarrow} c_{\widetilde{k}'\uparrow} \right) S_x \\ &\quad + \frac{J_y}{2i} \sum_{\widetilde{k},\widetilde{k}'} \left(c^\dagger_{\widetilde{k}\uparrow} c_{\widetilde{k}'\downarrow} - c^\dagger_{\widetilde{k}\downarrow} c_{\widetilde{k}'\uparrow} \right) S_y + J_z \sum_{\widetilde{k},\widetilde{k}'} \left(c^\dagger_{\widetilde{k}\uparrow} c_{\widetilde{k}'\uparrow} - c^\dagger_{\widetilde{k}\downarrow} c_{\widetilde{k}'\downarrow} \right) S_z. \end{aligned} \tag{3.34}$$

A Kondo impurity in the bulk of a metal can be viewed as a single quantum spin interacting with an ideal electron gas via an antiferromagnetic coupling (i.e. $J > 0$ in this convention), a point which shall be important in later sections. The equivalence of the Kondo problem and the ground state of a spin $S = \frac{1}{2}$ interacting with a free electron gas was demonstrated by Anderson and Yuval [8]. The interaction gives rise to singular scattering at the Fermi surface while at the same time screening the impurity spin with the conduction electron spins. One should remember, however, that this particular equivalence holds only provided we linearise the momentum states around the Fermi surface, such that only states near the Fermi surface contribute – what Tsvelick and Wiegmann call the 'long-time' approximation [127]. With this linearisation approximation, one may also make the simplification that charge and spin density waves do not interact and the charge excitations are free particles [127]. Gulacsi [66] highlights the general problem with the linearisation approximation, where any finite interaction strength will clearly introduce an energy excitation a finite distance from the Fermi surface and result in finite errors. He cites Haldane as establishing that these non-linear dispersion effects destroy the exactly solvable nature of simple models, and cites Matveenko and Brazovskii in determining the loss of absolute spin-charge separation. For our purposes, the linearisation is nevertheless a suitable approximation, and we show in detail, where appropriate, that the models remain exactly solvable.

3.3.1 Equivalence of Spin-Boson and XXZ-type Anisotropic Kondo Model

The spin-$\frac{1}{2}$ XXZ-type Anisotropic Kondo Model (AKM) is widely discussed in the literature, and here we outline the standard working to demonstrate the equivalence of the XXZ-type AKM and the SB models. For reference we include some further details of the working in Appendix B.2. This example emphasises the role of the bosonisation and unitary transformation procedure, clarifying the methods before applying them to the XYZ-type and three level models in later sections. The equivalence illustrated below is for zero detuning (ϵ), or bias, which corresponds to zero magnetic field in the Kondo case.

Recall from Section 3.2 that formal fermion-boson correspondence relies on the fermionic wavenumbers being unbounded from below, whereas the $\widetilde{k}$ in (3.33) and (3.34) cannot be less than $(-k_F)$. In establishing the equivalence between the SB and Kondo models then, the practice is to extend the limit on $\widetilde{k}$ downwards to negative infinity, such that it can be denoted by the usual fermion wave number k, and imposing a high energy cutoff of the order of the bandwidth. This cutoff corresponds to the bosonic momentum cutoff discussed in Subsection 3.2.3, which introduced the regularisation parameter a. The implication for the oscillator frequency ω_k is the imposition of a cutoff frequency $\omega_c = v_F/a$, which should be remembered when considering the Fermi velocity $v_F = \omega_k/k$ in (3.31), for example. In practice, as the Kondo model is the large Coulomb repulsion limit of the Anderson model [6, 72], this can be used to determine the scale of the high energy cutoff.

Having extended the limit of $\widetilde{k}$ to become k, we may bosonise (3.33) using the procedure described in Subsection 3.2.3. As a result, the kinetic, free Hamiltonian (3.32) becomes:

$$\begin{aligned} H_0^F &= \hbar v_F \sum_{k,\alpha} k c_{k\alpha}^\dagger c_{k\alpha} \\ (H_0^B) &= \hbar v_F \sum_{p>0} p(b_{p\uparrow}^\dagger b_{p\uparrow} + b_{p\downarrow}^\dagger b_{p\downarrow}) \qquad (3.35) \\ &= \hbar v_F \int_{-L/2}^{L/2} \frac{dx}{2\pi} \frac{1}{2} : (\partial_x \varphi_\alpha(x))^2 : \qquad (3.36) \\ &= \hbar v_F \int_{-L/2}^{L/2} \frac{dx}{2\pi} \frac{1}{2} : (\partial_x \varphi_C)^2 + (\partial_x \varphi_S)^2 : . \qquad (3.37) \end{aligned}$$

As indicated in Subsection 3.2.3, the bosonisation also entails fermion-number-dependent terms. Further comment as to their resolution is reserved for Section 3.4 and B.1. The subscripts S and C indicate a spin/charge combination as $\varphi_S = \frac{1}{\sqrt{2}}(\varphi_\uparrow - \varphi_\downarrow)$ and $\varphi_C = \frac{1}{\sqrt{2}}(\varphi_\uparrow + \varphi_\downarrow)$, and similarly for bosonic operator combinations which will be denoted b_S, b_C later. The equivalence between (3.32), (3.35) and (3.36) is the one used in the literature (see for example [95, 44, 132]). A careful working of the details between equations (3.35) and (3.36) is given in Appendix B.2.1 and reveals that there would in general be an exponential damping term dependent on the regularisation parameter. However, as discussed in [95], the cutoff may be imposed on the interaction terms of the Hamiltonian, while leaving the momenta unrestricted in the free Hamiltonian. Consequently this factor has been ignored in keeping with this convention.

Bosonising the perpendicular coupling term in the Hamiltonian (3.33) involves straightforward substitution with (3.19) and (3.23) to get[6]

$$\begin{aligned} H_\perp^F &= \frac{J_\perp}{2}\sum_{k,k'}\left(\sigma_+ c_{k\uparrow}^\dagger c_{k'\downarrow} + \sigma_- c_{k\downarrow}^\dagger c_{k'\uparrow}\right) \\ (H_\perp^B) &= \frac{J_\perp L}{4\pi a}\left(\mathcal{F}_\uparrow^\dagger \mathcal{F}_\downarrow e^{i\sqrt{2}\varphi_S(0)} S_- + \mathcal{F}_\downarrow^\dagger \mathcal{F}_\uparrow e^{-i\sqrt{2}\varphi_S(0)} S_+\right), \end{aligned} \tag{3.38}$$

where $S_\pm = S_x \pm i S_y$.

Furthermore, using (3.19) and the electron density (3.25) produces the bosonised parallel coupling Hamiltonian:

$$\begin{aligned} H_{||}^F &= \frac{J_{||}}{4}\sigma_z \sum_{k,k'}\left(c_{k\uparrow}^\dagger c_{k'\uparrow} + c_{k\downarrow}^\dagger c_{k'\downarrow}\right) \\ (H_{||}^B) &= \frac{J_{||} L}{2\pi} S_z \sqrt{2}\partial_x \varphi_S(0). \end{aligned} \tag{3.39}$$

Having bosonised the individual terms in the XXZ-type AKM Hamiltonian, the mapping to the SB model proceeds by applying the unitary operator $U = e^{i\sqrt{2}S_z\varphi_S(0)}$ to these terms. Unitary transformation of the kinetic term (3.37) makes use of the Hadamard lemma for this formulation of the Baker-Campbell-

[6]Note that a common transcription of the standard two-level Kondo/Spin-Boson equivalence uses Wannier operator notation, where the coupling constant dimensions are scaled by a factor proportional to the system size (see for example [95]).

Hausdorff (BCH) formula:

$$e^A B e^{-A} = B + [A,B] + \frac{1}{2!}[A,[A,B]] + \frac{1}{3!}[A,[A,[A,B]]] \dots \quad (3.40)$$

and gives (further details in Appendix B.2.2):

$$\begin{aligned} UH_0U^\dagger &= H_0 + \left[i\sqrt{2}S_z\varphi_S(0), H_0 \right] \\ &= H_0 - 2iv_F\hbar S_z \sum_{p>0} \sqrt{\frac{\pi p}{L}} e^{-ap/2} \left(b_{pS} - b_{pS}^\dagger \right). \end{aligned} \quad (3.41)$$

Applying the BCH rule in the unitary transformation of the perpendicular component (3.38) removes the exponential factors (further details in Appendix B.2.2) to give

$$UH_\perp U^\dagger = \frac{J_\perp L}{4\pi a} \left(\mathcal{F}_\uparrow^\dagger \mathcal{F}_\downarrow S_- + \mathcal{F}_\downarrow^\dagger \mathcal{F}_\uparrow S_+ \right). \quad (3.42)$$

Using (3.16) and (3.17) we find that operators of the form $S'_+ = \mathcal{F}_\downarrow^\dagger \mathcal{F}_\uparrow S_+$, $S'_- = \mathcal{F}_\uparrow^\dagger \mathcal{F}_\downarrow S_-$ have the appropriate commutation relations to express

$$UH_\perp U^\dagger = \frac{J_\perp L \sigma_x}{4\pi a}. \quad (3.43)$$

Unitary transformation of the parallel component of the Hamiltonian (3.39) is straightforward and can be expressed (see (B.4)):

$$\begin{aligned} UH_{||}U^\dagger &= H_{||} + \text{constant} \\ &= \frac{J_{||} L S_z \sqrt{2}}{2\pi} \partial_x \varphi_S(0) + \text{constant} \\ &= \frac{J_{||} L}{\pi} S_z \sum_{p>0} \sqrt{\frac{\pi p}{L}} e^{-ap/2}\ i\ (b_{pS} - b_{pS}^\dagger) + \text{constant}. \end{aligned} \quad (3.44)$$

Combining and rearranging the expressions (3.41), (3.43) and (3.44), the fully transformed bosonised XXZ-type Hamiltonian becomes:

$$\begin{aligned} UH^B_{XXZ}U^\dagger = {} & v_F\hbar \sum_{p>0} p(b_{p\uparrow}^\dagger b_{p\uparrow} + b_{p\downarrow}^\dagger b_{p\downarrow}) + \frac{J_\perp L \sigma_x}{4\pi a} \\ & + \left(\frac{J_{||} L}{2\pi} - v_F\hbar \right) \sqrt{2} S_z \sum_{p>0} \sqrt{\frac{2\pi p}{L}} e^{-ap/2} \left(b_{pS} + b_{pS}^\dagger \right) + \text{const.}, \end{aligned} \quad (3.45)$$

which is written in the conventional coordinate-coupled form of $(b+b^\dagger)$ rather than the imaginary momentum combination $i(b-b^\dagger)$ by employing a canonical transformation $b^\dagger \to -ib^\dagger$, $b \to ib$. By making the following identifications, it is evident that this model is equivalent to the SB model (3.1b):

$$-\frac{\hbar\Delta}{2} = \frac{J_\perp L}{4\pi a}, \quad -\sqrt{\gamma} = \frac{J_{||} L}{2\pi v_F \hbar} - 1, \quad \omega_p = v_F p, \quad \omega_c = \frac{v_F}{a}, \tag{3.46}$$

where we identify the coupling coefficient $C_i = C_p$, with

$$C_p \;=\; -\sqrt{2}\sqrt{\gamma}\left(\frac{2\pi v_F \omega_p}{L}\right)^{1/2} e^{-\omega_p/2\omega_c}. \tag{3.47}$$

This leaves a dimensionless coupling parameter $\gamma = (1-\rho L J_{||})^2$, where $\rho = (2\pi\hbar v_F)^{-1}$ is the density of states of the conduction electrons. This identification of the parameter γ indicates that the critical value $\gamma_c = 1$ separates the ferromagnetic and anti-ferromagnetic regions. Note that the identifications (3.46) and (3.47) appear slightly differently to several appearances in the wider literature which often make use of the Wannier operator convention as mentioned above, and a tendency to set $\hbar = 1$. However, we have avoided these conventions in this exposition to be explicit about the dimensionality of each term and their relationship to each other.

3.3.2 Spin-$\frac{1}{2}$ XYZ-type Anisotropic Kondo Model

Applying the same procedure of bosonisation and unitary transformation outlined in Subsection 3.3.1 above to the spin-$\frac{1}{2}$ XYZ-type AKM (3.34) will produce once again a connection to a two-level dissipative system. As in the previous example, the XYZ-type model is well-known to be exactly solvable. However, despite the wealth of literature that exists on this more complex generalisation of the XXZ model, re-analysis via bosonisation exposes a peculiarity of the model which has not been mentioned previously. These results are currently being prepared for submission for publication.

Recall the spin-$\frac{1}{2}$ XYZ-type AKM Hamiltonian of (3.34):

$$\begin{aligned} H^F_{XYZ} \;=\; & \hbar v_F \sum_{k,\alpha=1,2} k c^\dagger_{k\alpha} c_{k\alpha} + \frac{J_x}{2}\sum_{k,k'}\left(c^\dagger_{k\uparrow}c_{k'\downarrow} + c^\dagger_{k\downarrow}c_{k'\uparrow}\right) S_x \\ & + \frac{J_y}{2i}\sum_{k,k'}\left(c^\dagger_{k\uparrow}c_{k'\downarrow} - c^\dagger_{k\downarrow}c_{k'\uparrow}\right) S_y + J_z \sum_{k,k'}\left(c^\dagger_{k\uparrow}c_{k'\uparrow} - c^\dagger_{k\downarrow}c_{k'\downarrow}\right) S_z. \end{aligned}$$

The bosonisation of the free component of the Hamiltonian will proceed as in the previous section (3.37), so we will concentrate here on the *interaction* part of the Hamiltonian ${}^{\rm int}H^F_{XYZ}$. On substitution with (3.19) we find

$$\begin{aligned} {}^{\rm int}H^F_{XYZ} &= \frac{J_x L}{4\pi}\left(\psi^\dagger_\uparrow(0)\psi_\downarrow(0)+\psi^\dagger_\downarrow(0)\psi_\uparrow(0)\right)S_x \\ &+\frac{J_y L}{4\pi i}\left(\psi^\dagger_\uparrow(0)\psi_\downarrow(0)-\psi^\dagger_\downarrow(0)\psi_\uparrow(0)\right)S_y \\ &+\frac{J_z L}{2\pi}\left(\psi^\dagger_\uparrow(0)\psi_\uparrow(0)-\psi^\dagger_\downarrow(0)\psi_\downarrow(0)\right)S_z. \end{aligned} \tag{3.48}$$

We can now substitute the fermion field expressions in terms of their bosonic field expressions in the usual way (3.23), noting that the Klein factors commute with the boson creation and annihilation operators, giving:

$$\begin{aligned} {}^{\rm int}H^B_{XYZ} &= \frac{J_x L}{4\pi a}(\mathcal{F}^\dagger_\uparrow\mathcal{F}_\downarrow e^{i\sqrt{2}\varphi_S(0)}+\mathcal{F}^\dagger_\downarrow\mathcal{F}_\uparrow e^{-i\sqrt{2}\varphi_S(0)})S_x \\ &+\frac{J_y L}{4i\pi a}(\mathcal{F}^\dagger_\uparrow\mathcal{F}_\downarrow e^{i\sqrt{2}\varphi_S(0)}-\mathcal{F}^\dagger_\downarrow\mathcal{F}_\uparrow e^{-i\sqrt{2}\varphi_S(0)})S_y \\ &+\frac{J_z L\sqrt{2}}{2\pi}\partial_x\varphi_S(0)S_z. \end{aligned} \tag{3.49}$$

An alternative arrangement of (3.49) uses the notation $J' = (J_x - J_y)/2, J_\perp = (J_x + J_y)/2, J_{||} = J_z$, and combines operators into $S''_+ = \mathcal{F}^\dagger_\uparrow\mathcal{F}_\downarrow S_+$, $S''_- = \mathcal{F}^\dagger_\downarrow\mathcal{F}_\uparrow S_-$, $S'_+ = \mathcal{F}^\dagger_\downarrow\mathcal{F}_\uparrow S_+$, $S'_- = \mathcal{F}^\dagger_\uparrow\mathcal{F}_\downarrow S_-$ from which the reduction to the XXZ-type model when $J_x = J_y$ is clear (see (3.38) and (3.39)):

$$\begin{aligned} {}^{\rm int}H^B_{XYZ} &= \frac{J' L}{4\pi a}\left(e^{i\sqrt{2}\varphi_S(0)}S''_+ + e^{-i\sqrt{2}\varphi_S(0)}S''_-\right) \\ &+\frac{J_\perp L}{4\pi a}\left(e^{i\sqrt{2}\varphi_S(0)}S'_- + e^{-i\sqrt{2}\varphi_S(0)}S'_+\right) \\ &+\frac{J_{||} L\sqrt{2}}{2\pi}\partial_x\varphi_S(0)S_z. \end{aligned} \tag{3.50}$$

Unitary transformation of the Hamiltonian (3.50) with the operator $U = \exp(i\sqrt{2}S_z\varphi_S(0))$ produces

$$\begin{aligned} U\,{}^{\rm int}H^B_{XYZ}U^\dagger &= \frac{J'}{4\pi a}\left(e^{i2\sqrt{2}\varphi_S(0)}S''_+ + e^{-i2\sqrt{2}\varphi_S(0)}S''_-\right) \\ &+\frac{J_\perp}{4\pi a}\left(S'_- + S'_+\right) + \frac{J_z\sqrt{2}}{2\pi}\partial_x\varphi_S(0)S^z. \end{aligned} \tag{3.51}$$

Recall that in the XXZ case unitary transformation removed the residual exponential terms accompanying the $J_\perp$ in (3.38). This is still the case; however,

the same operation in the present XYZ case instead *reinforces* the exponentials in the J' term. The result is a Hamiltonian with non-minimal system-bath interactions between the upper and lower states (in contrast to the interactions discussed in [95]), which we shall call bath-mediated tunnelling. The new coupling coefficients D_p are found using (3.20) for the coefficients of the exponential multiplying the new $S''_\pm$ operators in the J' term:

$$\begin{aligned} J' \;\propto\; & S''_+ \exp(i2\sqrt{2}\varphi_S(0)) + h.c. \\ & = S''_+ \exp\left(-2i\sum_p n_p^{-1/2} e^{-ap/2}(b_{pS} + b_{pS}^\dagger)\right) + h.c. \\ & = S''_+ \exp\left(-i\sum_p D_p(b_{pS} + b_{pS}^\dagger)\right) + h.c. \end{aligned} \tag{3.52}$$

That is, the coupling coefficients are $D_p = 2(n_p)^{-1/2}e^{-ap/2}$.

Figure 3.2 clarifies and emphasizes the role of the Klein factors in these systems. The application of the standard spin operators $S_\pm$ indicates a vertical shift to a different eigenvalue of S_z, whereas application of a combination of Klein operators introduces a shift to the left or the right on the lattice. Consequently, application of the compound operators $S'_\pm$ and $S''_\pm$ result in shifts along the diagonal lines indicated in the diagram.

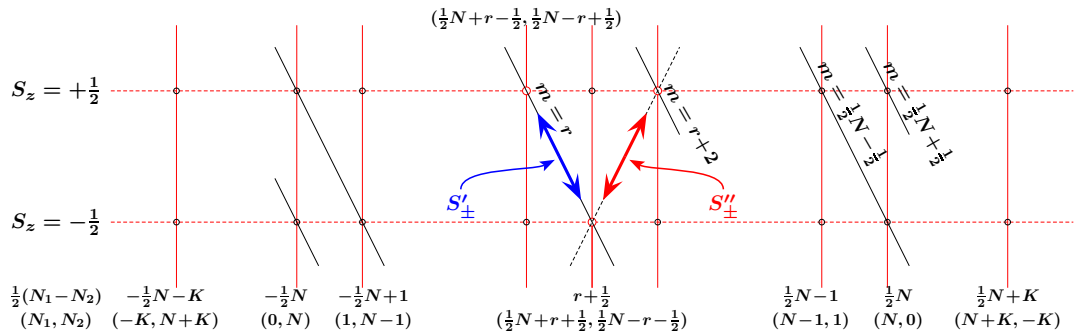

Figure 3.2: The figure illustrates the compound operator projections $S''_\pm$ and $S'_\pm$ on a lattice. Application of the standard spin operators $S_\pm$ introduces a vertical shift to a different eigenvalue of S_z, while application of a combination of Klein operators represents a horizontal shift. N is the sum of the number of particles $(N_1 + N_2)$, while r is a parameter representing an arbitrary line of constant $m = \frac{1}{2}(N_1 - N_2) \pm S_z$. The parameter $K \to \infty$. (Figure adapted from private communication with P.D. Jarvis.)

The Klein-dressed operators S'_+ and S'_- together with S_z generate $SU(2)$ on

states of fixed N, m, S_z and oscillator quantum numbers $|N, m; \alpha, \{n_p\}\rangle$. The total number of particles N is the sum of the number of particles of each species α: $N = \sum_\alpha N_\alpha$ with $N_\alpha = \sum_{p,p'} : c^\dagger_{p\alpha} c_{p'\alpha} :$. We have defined $m = \frac{1}{2}M + \alpha$, with $M = N_\uparrow - N_\downarrow$ being the difference in number between the different species. By contrast, the Klein-dressed compound operators S''_+ and S''_- that appear in the XYZ case have the same matrix elements in spin space as $S_\pm$, while simultaneously shifting m by ± 2, as can be seen from Figure 3.2. The XYZ-type Hamiltonian therefore does not conserve $\frac{1}{2}(N_\uparrow - N_\downarrow) + S_z$ such that in this case, as opposed to the XXZ-case, projection onto a single eigenvalue is not possible. As mentioned in the introduction it is well known that also the XYZ model is exactly solvable, so it is evident that it in fact corresponds to an exactly solvable, extended two-level system with the upper and lower levels having infinite degeneracy. This particular peculiarity of the bosonised elliptic case, which shows a more intricate structure than might be inferred from the simpler XXZ-type case, has not been discussed in the literature previously. This new structure could, for example, aid the development of new models for (continuous time) quantum random walks [4, 83]. In particular, since the charge sectors have infinite extension to the left and right in Fig.3.2, the walker is not restricted to a walk in a confined domain. In this case the Bethe Ansatz methods for giving explicit solutions to the model could potentially provide new analytic insight into the walk behaviour.

3.4 Anisotropic Coqblin-Schrieffer Model

In this section, the methods of bosonisation and unitary transformation are applied to another fermion gas system – an anisotropic Coqblin-Schrieffer model – resulting in a new model for a three-level exactly solvable quantum dissipative system. This result was first announced in the paper [78]. Models of solvable dissipative systems are both rare and important, with many practical applications, especially in the field of condensed matter systems. This section will describe in full the intricacies of the model, as well as providing explicit detail of the relevant calculations.

The starting point is an equivalent of the spin-$\frac{1}{2}$ XXZ-type AKM (see Subsection 3.3.1) for *three* component fermions rather than spin-$\frac{1}{2}$. The Coqblin-

Schrieffer model [43] describes isotropic, magnetic, multicomponent fermion systems. For the new system, we extend the interactions between the local and 'impurity' spins to include *anisotropic* components, resulting in an Anisotropic Coqblin-Schrieffer (ACS) model. The associated fermionic Hamiltonian is the direct analogue of the XXZ-type Kondo Hamiltonian (3.33), with kinetic and magnetic terms, as well as transverse and longitudinal interactions at the origin (complex phases $\zeta_{\alpha\beta}$ are included for generality):

$$\begin{aligned} H^F_{ACS} &= \sum_{k,\alpha=1}^{3} \hbar v_F k \,{:}c^\dagger_{k\alpha}c_{k\alpha}{:} + \sum_{\alpha} h_\alpha S_{\alpha\alpha} \\ &\quad + \sum_{k,k',\alpha} J_\parallel \,{:}c^\dagger_{k\alpha}c_{k'\alpha}{:}S_{\alpha\alpha} + J_\perp \sum_{k,k',\alpha<\beta} \left(e^{i\zeta_{\alpha\beta}} c^\dagger_{k\alpha}c_{k'\beta}S_{\beta\alpha} + \text{h.c.}\right). \end{aligned} \tag{3.53}$$

In equation (3.53), the labels $\alpha, \beta = 1, 2, 3$ correspond to the three independent fermionic components, while k is the fermion wavenumber as before. The magnetic impurity operators $S_{\alpha\beta}$ are generators of the $SU(3)$ Lie algebra for $\alpha, \beta = 1, 2, 3$, provided $S_{11} + S_{22} + S_{33} = 0$. However, we may drop this condition and regard the 9 *independent* operators $S_{\alpha\beta}$ as generators of $U(3)$. In fact, it is useful to reparametrise the modes and couplings with a relabelling from the double-index notation to a set employing the standard Gell-Mann matrix labels $\lambda_{\mathtt{A}}$ for diagonal and off-diagonal matrices ($\mathtt{A} = \mathtt{3}, \mathtt{8}, \mathtt{0}$ for the diagonals, and $\mathtt{A} = \mathtt{1}, \mathtt{2}, \mathtt{4}, \mathtt{5}, \mathtt{6}, \mathtt{7}$ for the off-diagonals – see Appendix B.3 for further notational explanation). In this case, diagonal quantities $x_{\alpha\beta}$, $\alpha, \beta = 1, 2, 3$ would be expressed using the standard Jacobi three-body combinations:

$$x_{\mathtt{3}} = \tfrac{1}{\sqrt{2}}(x_{11} - x_{22}), \;\; x_{\mathtt{8}} = \tfrac{1}{\sqrt{6}}(x_{11} + x_{22} - 2x_{33}), \;\; x_{\mathtt{0}} = \tfrac{1}{\sqrt{3}}(x_{11} + x_{22} + x_{33}).$$

The magnetic term would be expressible as:

$$\sum_{\alpha=1}^{3} h_\alpha S_{\alpha\alpha} \equiv h_{\mathtt{3}} S_{\mathtt{3}} + h_{\mathtt{8}} S_{\mathtt{8}} + h_{\mathtt{0}} S_{\mathtt{0}}. \tag{3.54}$$

Similarly, reparametrising the kinetic term of (3.53) and bosonising (see Subsection 3.2.3) produces:

$$\sum_{k,\alpha=1}^{3} \hbar v_F k \,{:}c^\dagger_{k\alpha}c_{k\alpha}{:} = \sum_{p>0} \hbar v_F p \left(b^\dagger_{\mathtt{3}p} b_{\mathtt{3}p} + b^\dagger_{\mathtt{8}p} b_{\mathtt{8}p} + b^\dagger_{\mathtt{0}p} b_{\mathtt{0}p}\right). \tag{3.55}$$

As in (3.37), we would expect fermion number-dependent terms in (3.55). However, the absence of the terms will be explained at the end of this section, with additional details in Appendix B.1.

The transverse 'spin' interaction terms of (3.53) remain off-diagonal on bosonisation, and are not affected by normal ordering, leading to the three-level analogue of (3.38):

$$\frac{L}{2\pi a}J_\perp\sum_{\alpha<\beta}\left(e^{i\zeta_{\alpha\beta}}e^{-i(\varphi_\alpha(0)-\varphi_\beta(0))}\mathcal{F}_\beta^\dagger\mathcal{F}_\alpha S_{\alpha\beta}+e^{-i\zeta_{\alpha\beta}}e^{i(\varphi_\alpha(0)-\varphi_\beta(0))}\mathcal{F}_\alpha^\dagger\mathcal{F}_\beta S_{\beta\alpha}\right). \quad (3.56)$$

By contrast, the longitudinal 'spin' couplings (with diagonal fermion bilinears) simply become combinations of the oscillator modes themselves when the bosonisation is implemented, in a similar manner to (3.39), in the form

$$\begin{aligned}J_\parallel\sum_{k,k',\alpha}{:}c_{k\alpha}^\dagger c_{k'\alpha}{:}S_{\alpha\alpha} \;=\; & J_\parallel\sum_{p>0}\sqrt{\frac{pL}{2\pi}}e^{-pa/2}\\ & \times i\left(S_{\mathsf{3}}(b_{\mathsf{3}p}-b_{\mathsf{3}p}^\dagger)+S_{\mathsf{8}}(b_{\mathsf{8}p}-b_{\mathsf{8}p}^\dagger)+S_{\mathsf{0}}(b_{\mathsf{0}p}-b_{\mathsf{0}p}^\dagger)\right) \quad (3.57)\end{aligned}$$

– again together with additional terms proportional to fermion-number.

As in the two-level case, a unitary transformation of the model allows it to be brought into a QDS form (see Subsection 3.3.1). The analogue three-level operator to perform the conjugation is in this instance

$$U=\exp(i\textstyle\sum_\alpha\varphi_\alpha(0)S_{\alpha\alpha})\equiv\exp(i(\varphi_{\mathsf{3}}(0)S_{\mathsf{3}}+\varphi_{\mathsf{8}}(0)S_{\mathsf{8}}+\varphi_{\mathsf{0}}(0)S_{\mathsf{0}})). \quad (3.58)$$

From the $U(3)$ Lie algebra relations $[S_{\alpha\alpha},S_{\alpha\beta}]=S_{\alpha\beta}$, $[S_{\beta\beta},S_{\alpha\beta}]=-S_{\alpha\beta}$ (with $\alpha\neq\beta$), (3.40) and the exponential expansion, it is straightforward to show that the action on an operator $S_{\alpha\beta}$ will be

$$\begin{aligned}US_{\alpha\beta}U^{-1} &= \exp(i\textstyle\sum_\alpha\varphi_\alpha(0)S_{\alpha\alpha})S_{\alpha\beta}\exp(-i\sum_\alpha\varphi_\alpha(0)S_{\alpha\alpha})\\ &= S_{\alpha\beta}+[i\textstyle\sum_\alpha\varphi_\alpha(0)S_{\alpha\alpha},S_{\alpha\beta}]\\ &\qquad +\tfrac{1}{2!}[i\textstyle\sum_\alpha\varphi_\alpha(0)S_{\alpha\alpha},[i\sum_\alpha\varphi_\alpha(0)S_{\alpha\alpha},S_{\alpha\beta}]]+\ldots\\ &= \exp(i(\varphi_\alpha-\varphi_\beta))S_{\alpha\beta}. \quad (3.59)\end{aligned}$$

As such, applying the unitary transformation to the transverse coupling terms of (3.56) will *cancel* the corresponding scalar exponentials. The longitudinal term (3.57), however, commutes with U, returning only itself in the form of (3.57).

The kinetic terms (3.55) acquire an additional commutator contribution from the BCH-type rearrangements, which is of the same overall structure as the longitudinal terms. A further term arising from the double commutator in the conjugation by the exponential yields a power series in a whose sum can be removed as an additional overall constant. Explicitly, the transformation of the kinetic terms becomes:

$$U\sum_{p>0}\hbar v_F p\big(b^\dagger_{3p}b_{3p}+b^\dagger_{8p}b_{8p}+b^\dagger_{0p}b_{0p}\big)\,U^{-1} = \sum_{p>0}\hbar v_F p\big(b^\dagger_{3p}b_{3p}+b^\dagger_{8p}b_{8p}+b^\dagger_{0p}b_{0p}\big) \\ -\hbar v_F\sum_{p>0}\sqrt{\frac{2\pi p}{L}}e^{-pa/2}\,i\Big(S_3(b_{3p}-b^\dagger_{3p})+S_8(b_{8p}-b^\dagger_{8p})+S_0(b_{0p}-b^\dagger_{0p})\Big)\,. \tag{3.60}$$

The fully transformed transcription of the ACS Hamiltonian (3.53) is therefore the combination of the magnetic (3.54), transverse (3.56) with exponential coupling terms exorcised, longitudinal (3.57) (which we can write in the coordinate-coupled convention in the same way as (3.45)) and kinetic terms (3.60):

$$\begin{aligned} UH^B_{ACS}U^\dagger &= h_3S_3+h_8S_8+h_0S_0+\sum_{p>0}\hbar v_F p\big(b^\dagger_{3p}b_{3p}+b^\dagger_{8p}b_{8p}+b^\dagger_{0p}b_{0p}\big) \\ &\quad +\frac{L}{2\pi a}J_\perp\sum_{\alpha<\beta}\Big(e^{i\zeta_{\alpha\beta}}\mathcal{F}^\dagger_\beta\mathcal{F}_\alpha S_{\alpha\beta}+e^{-i\zeta_{\alpha\beta}}\mathcal{F}^\dagger_\alpha\mathcal{F}_\beta S_{\beta\alpha}\Big) \\ &\quad +\sum_{p>0}\sqrt{\frac{2\pi p}{L}}v_F\hbar e^{-pa/2}\left(1-\frac{J_{||}L}{2\pi\hbar v_F}\right) \\ &\quad\quad \cdot\Big(S_3(b_{3p}+b^\dagger_{3p})+S_8(b_{8p}+b^\dagger_{8p})+S_0(b_{0p}+b^\dagger_{0p})\Big)\,. \end{aligned} \tag{3.61}$$

By analysing this bosonised and transformed Hamiltonian, the first link to quantum dissipative systems is found by considering the composite operators composed of the combination of Klein operators and the off-diagonal generators of $U(3)$, $S_{\alpha\beta}$, $\alpha\neq\beta$. It is straightforward to check that, provided the $S_{\alpha\beta}$ are *elementary* 3×3 matrices so that the operator condition $e_{ij}e_{kl}=\delta_{jk}e_{il}$ can be applied, the composite operators defined by

$$S'_{\alpha\beta}:=-\mathcal{F}^\dagger_\beta\mathcal{F}_\alpha S_{\alpha\beta},\quad S'_{\alpha\alpha}:=\mathcal{F}^\dagger_\alpha\mathcal{F}_\alpha S_{\alpha\alpha}=S_{\alpha\alpha} \tag{3.62}$$

fulfil the usual $U(3)$ commutation relations and can be identified with operators acting between the states of the quantum three-level system in the QDS

interpretation (see (B.13)). This calculation is included in Appendix B.3.1 for reference.

The operator S_0 is proportional to the 3×3 identity matrix (provided the original doubly indexed operators are indeed represented with elementary matrices) and one can recognise that it is the linear Casimir invariant of $U(3)$. Consequently, terms involving b_{0p} and $b_{0p}^\dagger$ are entirely quadratic or linear. Completing the square for these displaced oscillator modes combines their contribution into a sum of kinetic energy terms for an infinite set of oscillator modes, together with an unimportant (infinite) shift in the energy. These do not interact with the remainder of the system, so can be dropped from the final model. The same reasoning applies to the magnetic term, allowing $h_0 S_0$ to be dropped as well.

By employing the standard 3×3 Gell-Mann matrices $\lambda_{\mathtt{A}}$, $\mathtt{A} = \mathtt{1},\cdots,\mathtt{8}$ as a basis for the $SU(3)$ generators in the fundamental representation (these would play the role of the Pauli matrices in the similar two-level case – see Appendix B.3) the transformed ACS (3.61) can be written in a clear QDS form:

$$\begin{aligned} H^B_{QDS} \;:=\; & \varepsilon_3\lambda_3 + \varepsilon_8\lambda_8 + \Delta(\lambda_1+\lambda_4+\cos\zeta\lambda_6 + \sin\zeta\lambda_7) + \\ & \sum_p \hbar\omega_p(b^\dagger_{3p}b_{3p}+b^\dagger_{8p}b_{8p}) + \sum_p \hbar C_{3p}\lambda_3(b_{3p}+b^\dagger_{3p}) + \hbar C_{8p}\lambda_8(b_{8p}+b^\dagger_{8p}). \end{aligned} \tag{3.63}$$

The detuning parameters ε_3 and ε_8 correspond directly to h_3 and h_8 respectively. From the kinetic terms it is evident that the oscillator baths have frequency spectrum $\omega_p = v_F p$ provided $\omega \ll \omega_c$, where ω_c is the cutoff frequency $\omega_c = v_F/a$. The tunnelling matrix elements are given in terms of the transverse coupling strength of the original model, $\Delta \equiv -J_\perp L/2\pi a$, modulated by a complex phase. By an appropriate basis choice, this phase may be shifted on to the $2,3$ spin-label sector, and expressed in the Cartesian basis by a combination of the corresponding Gell-Mann matrices, namely λ_6 and λ_7, rotated by angle $\zeta := \zeta_{23} - \zeta_{13} + \zeta_{12}$ (see (3.53) and also (3.68), (3.70) below).

It is evident that the overall dissipative coupling coefficients C_{3p} and C_{8p} are equal, taking the form:

$$C_{3p} = C_{8p} \equiv C_p = v_F\sqrt{\frac{2\pi p}{L}}e^{-\omega_p/2\omega_c}\left(1 - \frac{J_\parallel L}{2\pi\hbar v_F}\right). \tag{3.64}$$

In the limit $a \to 0$ the spectral function $J(\omega)$ is found directly from (3.3) and (3.4) such that $J(\omega) = A\sum_i C_i^2 \delta(\omega - \omega_i)$, where A is given by (3.6). Thus, for any test function $f(\omega)$, remembering that the spectrum of bath frequencies $v_F p = \omega_p \equiv \omega_{n_p} = 2\pi v_F/L \cdot n_p$, we have:

$$\begin{aligned}\int J(\omega) f(\omega) d\omega = A\sum_{n_p} C_p^2 f(\omega_p) = \frac{2\pi v_F}{L}\sum_{n_p} A\gamma\omega_{n_p} e^{-\omega_{n_p}/\omega_c} f(\omega_{n_p}) \\ \to \frac{2\pi v_F}{L}\int dn_p\, A\gamma\omega_{n_p} e^{-\omega_{n_p}/\omega_c} f(\omega_{n_p}) \equiv \int d\omega \left(A\gamma\omega e^{-\omega/\omega_c}\right) f(\omega).\end{aligned} \tag{3.65}$$

This relies on the approximation that $f(\omega)$ is supported in the region $\omega \ll \omega_c$, and we can infer that the spectral function will have the Ohmic form with dimensionless coupling coefficient γ:

$$J(\omega) = \quad A\gamma\,\omega e^{-\omega/\omega_c}, \qquad \text{where} \qquad \gamma := \left(1 - \tfrac{J_\parallel L}{2\pi\hbar v_F}\right)^2. \tag{3.66}$$

The introduction of $S'_{\alpha\beta}$, with implicit Klein factors, as effective $U(3)$ generators implies that the three states of the quantum system in fact lie across different charge sectors. This situation, and at the same time the treatment of the residual fermion-number dependent terms, is resolved by noting that the original model (3.53) has three conserved quantum numbers $\widehat{N}_\alpha + S_{\alpha\alpha}$, $\alpha = 1, 2, 3$ or $\widehat{N}_3 + S_3$, $\widehat{N}_8 + S_8$, and $\widehat{N}_0 + S_0$ in terms of relative degrees of freedom. S_0 is proportional to the identity matrix, and so a projection onto an eigenspace with fixed eigenvalue M_0 is tantamount to fixing the total fermion number at N_0, which is a conserved quantity. Furthermore, the system admits a projection onto fixed eigenspaces of the remaining two operators with eigenvalues M_3 and M_8, which leaves the form of (3.63) unchanged. However, the detuning parameters $\varepsilon_3, \varepsilon_8$ need to be shifted from their orignial values h_3, h_8 to absorb additional M_3- and M_8-dependent contributions (see Appendix B.1 for details).

3.4.1 Exact solvability

In the last section it was demonstrated that by the method of constructive bosonisation and unitary transformation, the three component ACS Fermi gas-impurity model has a dissipative system counterpart. To underline its utility, this section will confirm that the starting model is exactly solvable.

The issue of integrability, or exact solvability, concerns the number of conserved quantities involved in the system: if the number of conserved quantities is greater than or equal to the number of degrees of freedom, then the system is integrable. The analysis for standard coordinate models is equivalent to that of the algebraic formulation for the associated XXZ and XYZ-type Heisenberg spin chains, which requires for integrability that the model admits an R-matrix satisfying the elegant star-triangle, or Yang-Baxter equation. Furthermore, this equation is a necessary condition for the factorisation of multiparticle scattering, or S-matrices, and when S-matrices are factorisable, conservation of particle number and momenta is ensured [17, 21]. Note that it was shown in [22] that R-matrices simultaneously satisfying conditions of automorphicity, crossing-symmetry, unitarity, specific behaviour at the asymptotes and structure at the poles will satisfy the Yang-Baxter equation, but this is not a necessary condition.

As demonstrated in [127], single particle-impurity scattering matrices S can be expressed as the exponential of the interaction component of the model Hamiltonian. This can in turn be reparametrised in terms of an R-matrix $R(x^{\gamma=1}, q)$ for some arbitrary but fixed value of the (additive) spectral parameter, say $\gamma = 1$, such that

$$\mathsf{S} = e^{iH_{int}(J_\parallel, J_\perp)} \equiv R(x^{\gamma=1}, q). \tag{3.67}$$

As such, the parameters x, q become functions of the couplings $J_\parallel, J_\perp$.

By this method we can find the scattering matrix for our particular system Hamiltonian, and compare this with a standard R-matrix that is known to satisfy the Yang-Baxter equation. If a mapping between the S- and R-matrices can be found then the system is indeed exactly solvable. For explicit evaluation of S for our system we use (3.53) and elementary 3×3 matrices $e_{\alpha\beta}$ to isolate the interaction Hamiltonian for the ACS model:

$$H_{int} = J_\parallel \sum_\alpha e_{\alpha\alpha} \otimes e_{\alpha\alpha} + J_\perp \sum_{\alpha<\beta} \left(e^{i\zeta_{\alpha\beta}} e_{\alpha\beta} \otimes e_{\beta\alpha} + e^{-i\zeta_{\alpha\beta}} e_{\beta\alpha} \otimes e_{\alpha\beta} \right),$$

which we shall write in terms of the matrices $\boldsymbol{P} = \sum_\alpha e_{\alpha\alpha} \otimes e_{\alpha\alpha}$ and $\boldsymbol{T} = \sum_{\alpha<\beta} \left(e^{i\zeta_{\alpha\beta}} e_{\alpha\beta} \otimes e_{\beta\alpha} + e^{-i\zeta_{\alpha\beta}} e_{\beta\alpha} \otimes e_{\alpha\beta} \right)$ for ease of calculation:

$$H_{int} = J_\parallel \boldsymbol{P} + J_\perp \boldsymbol{T}.$$

By (3.67) it is then straightforward to find the corresponding S matrix:

$$\begin{aligned}
\mathsf{S} &= e^{iJ_\parallel \boldsymbol{P}} e^{iJ_\perp \boldsymbol{T}} \\
&= \sum_{l=0}^{\infty} \frac{1}{l!}(iJ_\parallel \boldsymbol{P})^l \left(\sum_{k=1}^{\infty} \left(\frac{1}{(2k-1)!}(iJ_\perp)^{2k-1}\boldsymbol{T} + \frac{1}{(2k)!}(iJ_\perp)^{2k}(\boldsymbol{I}-\boldsymbol{P}) \right) + \boldsymbol{I} \right) \\
&= \left((e^{iJ_\parallel}-1)\boldsymbol{P} + \boldsymbol{I}\right)(i\sin(J_\perp)\boldsymbol{T} + (\cos(J_\perp)-1)(\boldsymbol{I}-\boldsymbol{P}) + \boldsymbol{I}) \\
&= e^{iJ_\parallel} \sum_\alpha e_{\alpha\alpha} \otimes e_{\alpha\alpha} + \cos J_\perp \sum_{\alpha\neq\beta} e_{\alpha\alpha} \otimes e_{\beta\beta} \\
&\quad + i \sin J_\perp \sum_{\alpha<\beta} \left(e^{i\zeta_{\alpha\beta}} e_{\alpha\beta} \otimes e_{\beta\alpha} + e^{-i\zeta_{\alpha\beta}} e_{\beta\alpha} \otimes e_{\alpha\beta} \right), \qquad (3.68)
\end{aligned}$$

where we have used $\boldsymbol{P}^2 = \boldsymbol{P}$, $\boldsymbol{PT} = 0$ and $\boldsymbol{I}$ is the identity matrix as usual.

Having established an explicit form of the S-matrix, we can compare this with the standard forms for trigonometric R-matrices of the appropriate dimension [79, 11] (see also [22]):

$$\begin{aligned}
R(x,q) = \quad & (qx - q^{-1}x^{-1}) \sum_\alpha e_{\alpha\alpha} \otimes e_{\alpha\alpha} + (x - x^{-1}) \sum_{\alpha\neq\beta} e_{\alpha\alpha} \otimes e_{\beta\beta} \\
& + (q - q^{-1}) \sum_{\alpha<\beta} \left(x e_{\alpha\beta} \otimes e_{\beta\alpha} + x^{-1} e_{\beta\alpha} \otimes e_{\alpha\beta} \right). \qquad (3.69)
\end{aligned}$$

By comparing expressions (3.68) and (3.69), it is clear that (3.69) has the correct structure to be identified with the scattering matrix S if $\zeta_{12} = \zeta_{13} = \zeta_{23}$ with phase factors identified with x. Since the interaction Hamiltonian is hermitian, we must have $x^{-1} = x^*$, and so we adopt the logarithmic parameters $x = e^{i\overline{f}}$, $q = e^{\overline{\mu}}$, where $\overline{f}$ and $\overline{\mu}$ are explicitly real parameters. We can see that this means $\zeta \equiv \overline{f}$, and the R-matrix is expressible, up to an overall factor of 2, as

$$\begin{aligned}
R(x,q) = \quad & \sinh(i\overline{f} + \overline{\mu}) \sum_\alpha e_{\alpha\alpha} \otimes e_{\alpha\alpha} + i \sin(\overline{f}) \sum_{\alpha\neq\beta} e_{\alpha\alpha} \otimes e_{\beta\beta} + \\
& + \sinh(\overline{\mu}) \sum_{\alpha<\beta} \left(e^{i\overline{f}} e_{\alpha\beta} \otimes e_{\beta\alpha} + e^{-i\overline{f}} e_{\beta\alpha} \otimes e_{\alpha\beta} \right). \qquad (3.70)
\end{aligned}$$

Following the method of [127], we compare the ratios of coefficients of the first two terms in (3.70) and (3.68) (or equally we can compare ratios of the first and third terms):

$$\frac{\sinh(i\overline{f} + \overline{\mu})}{\sinh(i\overline{f})} = \frac{\cos(J_\parallel)}{\cos(J_\perp)} + \frac{i\sin(J_\parallel)}{\cos(J_\perp)},$$

giving

$$\cosh(\overline{\mu}) - i\cot(\overline{f})\sinh(\overline{\mu}) \;=\; \frac{\cos(J_{\|})}{\cos(J_{\perp})} + \frac{i\sin(J_{\|})}{\cos(J_{\perp})}, \tag{3.71}$$

Equating real parts of (3.71) leads directly to the reparametrisation of $\overline{\mu}$ in terms of $J_{\|}$ and $J_{\perp}$, and equating imaginary parts and using $\sinh^2(\overline{\mu}) = \cosh^2(\overline{\mu}) - 1$ identifies the reparametrisation of $\overline{f}$:

$$\cosh(\overline{\mu}) = \frac{\cos J_{\|}}{\cos J_{\perp}}; \qquad \cot^2(\overline{f}) = \frac{\sin^2 J_{\|}}{\sin(J_{\perp}+J_{\|})\sin(J_{\perp}-J_{\|})}. \tag{3.72}$$

This demonstrates that the S-matrix of the three-level model admits a reparametrisation to, and hence equivalence with, the exactly solvable standard trigonometric R-matrix, confirming that this new 3LQDS belongs to the rare and important class of exactly solvable dissipative systems. It is worth noting that these transcriptions appear to be the opposite of the standard transcriptions in the XXZ-type case which are written as $\cos(\mu)$, $\coth^2(f)$ on the left hand side of (3.72) (see for example [127, 150, 44]), because we have written $\overline{f}$ and $\overline{\mu}$ to be explicitly real. For the specific values of $\zeta(\equiv \bar{f}) = 0$ and π, relating directly to measurements of specific tunnelling systems, the above generalised expressions (3.72) can be reduced to the isotropic case, while there is no apriori reason why ζ should be constrained to those values for physical systems in general.

Note that we have used the most common trigonometric R-matrix (3.69) which corresponds to the A_2^1 series of the generalised Toda systems describing one-dimensional lattice models with nearest-neighbour interactions. There are several alternative R-matrices which correspond to different series (see for example [79]). It is anticipated that scattering matrices from models related to the current three-level model will correspond to these alternative R-matrices, exhibiting solvable limits for particular parameters. The prospect of revealing other exactly solvable three-level dissipative systems with different applications thus shows the importance of further development of the work demonstrated here.

3.5 Discussion

This chapter has presented the method of constructive bosonisation and unitary transformation as a method for re-examining the detailed structure of fermion-gas impurity models and spin chains, exposing their connection to models for quantum dissipative systems. The focus has been on presenting the details of the interaction between a quantum system and its environment in these models. We began by introducing the standard spin-$\frac{1}{2}$ Spin-Boson and Kondo models, and outlined the well-known transcription between the two, which relies on the method of bosonisation. Subsection 3.3.2 extended the detailed analysis to the two-level XYZ-type generalisation of the AKM, and special emphasis was placed on the role of the Klein factors in physical interpretations of the resultant quantum dissipative system. The additional bath-mediated tunnelling present in the XYZ-type model exposed a structure that has not been reported previously. The analysis highlighted that the system in fact corresponds to an exactly solvable, extended two-level system with the upper and lower states having infinite degeneracy. This new insight into the otherwise well-discussed model may well facilitate development of new models for quantum random walks, where at each step the walker jumps to a neighbouring lattice site. Further investigation of the system might also reveal the details of the influence of the oscillator bath on the walker's performance.

Further emphasising the utility of the bosonisation method, the chapter concludes with a careful exposition of the new three-level model proposed in [78]. It is demonstrated that bosonisation and unitary transformation can be applied not only to existing models for further insight, but are invaluable tools in developing new exactly solvable quantum dissipative systems, such as the Anisotropic Coqblin-Schrieffer model discussed in Section 3.4. As a generalisation of the two-level Spin-Boson/Kondo model correspondence, this three-level analogue belongs to the same large family of related problems and models. The family of models has been studied extensively by a range of different methods, and it is beyond the scope of this thesis to provide detailed analysis of the relationship between the ACS model and these existing investigations. It would, however, be instructive to formalise the relationship between the ACS model and related ones, which would require explanations of crossover fields and language. For example, it is interesting to investigate the relationship to the

triangular lattices and quantum Brownian motion discussed in [3]. It appears that the transverse field terms in (3.63) are equivalent to hops on this triangular lattice. The model in [3] is shown to correspond to the two-dimensional 3-state Potts model with a boundary, meaning the link to integrable models is clear. However, the analysis and language of that paper is to investigate the critical behaviour derivable through $c = 2$ boundary conformal field theory, something which the present discussion of the ACS model does not consider. Furthermore, it has been pointed out that the ACS model bears connections to quantum wire junctions, the dissipative Hofstadter model and open string theory as presented in [39]. The ACS model contains further generalisations to these systems by including marginal operators coupled to the diagonal elements of the $SU(3)$ algebra. As such it could be argued that the two models stand in the same relation as the dissipative two-level system and the boundary sine-Gordon model.

It is clear then that such models are important in a range of fields, and the range of applications is equally diverse. Examples of three-level system-environment models where the ACS model might be applied include three-level quantum dots, single qubit systems addressed by an ancillary state, or qutrit states, triatomic triple well potentials, such as ammonia (NH_3) and the methyl ($-CH_3$), as well as Bose-Einstein condensate atomic transistors [115], which have a three well structure. The method of constructive bosonisation can be applied to other Fermi-gas Hamiltonians in attempts to find more exactly solvable dissipative systems and, as mentioned in Subsection 3.4.1, for particular parameters of related three-level models, solvable limits may be found by their correspondence with alternative R-matrices. Further study will reveal more insights into the physics of the system, and it would be of great interest to resolve the full spectrum and eigenstates of the Hamiltonian via the Bethe Ansatz [26]. This will enable calculation of a range of useful dynamical and thermodynamical quantities, such as magnetic susceptibility and specific heat (see for example [118] and [60]). Other authors have discussed vacuum sector dependence [132] and finite size effects [152] in the bosonisation of related models, and development along these lines may also be of interest. Finally, entanglement between quantum systems and dissipative environments [5, 101] may also be examined within this impurity-bath system, which will be addressed in the following chapter.

Chapter 4

Entanglement Criteria and Further Extensions to QDS and Fermi-gas Models

This chapter extends the investigation of the three-level quantum dissipative system discussed in Chapter 3 by finding the Rényi (and von Neumann) entropy as a criterion for entanglement in the model. Two different experimentally accessible approaches to finding entropy measures are discussed. In Section 4.2 we provide a careful extension of an existing variational method for calculating entanglement for the spin-$\frac{1}{2}$ Kondo model to the ACS case for three-component fermions. Utilising the exactly solvable nature of the ACS model, we find expressions for the exact values of the entropy using the Feynman-Hellmann Theorem in Section 4.3, and provide several comments and suggestions for further work in Section 4.4. The results of this chapter are being prepared for submission for publication.

4.1 Introduction

Calculating measures of the degree of entanglement is an interesting and important problem from both a theoretical and experimental perspective. As mentioned in Chapter 2, however, the differences in terminology and methodology in their approaches often does not always facilitate easy application of the results to both sectors. The use of quantum entropy measures, as we

shall investigate herein for the ACS model, provides a good approach that is both useful for the theoretician, and applicable to the experimentalist. In the introduction to this thesis we mentioned that an entanglement measure is simply any function of a quantum state that is zero for separable states and non-negative and real for other states, provided that the value of the function cannot increase under local operations and classical communication. As such, there are a myriad of different proposals for entanglement measures (see for example [5, 107] and references therein). In Chapter 2 we discussed the Bell and CHSH inequalities, and mentioned that these were not always an appropriate entanglement measure, since not all entangled states violate the inequalities. As a more definitive measure of entanglement, there is increasing propensity to use entropy. The von Neumann entropy [133] is arguably the most common of all entropy measures, and if multiplied by the Boltzmann constant k_B the von Neumann entropy gives the usual thermodynamic entropy. The von Neumann entropy is, however, a particular limiting case of the more general Rényi entropy, which has the quantum counterpart [74, 135, 121]:

$$S_R(\rho) := \frac{1}{1-\delta} \ln \mathrm{Tr}\left(\rho^\delta\right), \quad \delta > 1, \tag{4.1}$$

where ρ is the density matrix of the system in question. Using L'Hôpital's rule for $\delta = 1$ in (4.1) produces the von Neumann entropy as the limiting case:

$$S_{vN}(\rho) = -\mathrm{Tr}\left(\rho \ln \rho\right). \tag{4.2}$$

Note that in (4.1) and (4.2) we have used the natural logarithm following the convention of [74] for the Rényi entropy. However, it should be remembered that the Rényi and von Neumann entropies are generalisations of the classical Shannon entropy, which uses a logarithm to base 2, and so expressions such as (4.1) and (4.2) are often understood to be in units normalised to an overall factor of $\ln(2)$, since $\log_2(n) = \ln(n)/\ln(2)$ (see below for further discussion). This formality is often assumed implicitly in the literature, with statements such as appears in [101], that for $\rho = \frac{1}{2}\boldsymbol{I}$, the von Neumann entropy is $S(\rho) = -\mathrm{Tr}(\rho \ln \rho) = 1$, with no further indication of convention. Other authors (e.g. [92]) prefer to write $S(\rho) = -\mathrm{Tr}(\rho \log_2 \rho) = 1$ for the same case. Note also that for increasingly high δ in (4.1) the Rényi entropy measure is increasingly determined by only high probability events, whereas for low δ the events are weighted more equally.

A measure of the entanglement in terms of entropy is a relative measure between the fully mixed and the pure states, quantified by the way the entropy grows with spatial extent of the subsystem region (see for example [92]). If the overall system is in a pure state, then the entropy of one subsystem can be used as a measure of its degree of entanglement with the other subsystems. A pure state is indicated by an idempotent density matrix ($\rho^2 = \rho$), with trace equal to one. Thus we can see from (4.1) that the Rényi entropy is zero for pure states. Similarly, the von Neumann entropy is zero for pure states, since an idempotent density matrix would require $S_{vN}(\rho) = -\mathrm{Tr}(\rho \ln \rho) = -\mathrm{Tr}(2\rho \ln \rho)$.

Note that the use of the von Neumann and Rényi entropies for entanglement measures is still a somewhat controversial issue. Because these are quantum generalisations of the classical Shannon entropy, which assumes additivity and that properties of matter exist independently of measurement, it could be argued that this does not adequately account for the structure of entangled states. Furthermore, one could argue that a pure state with zero entropy fails to take account of intrinsic quantum uncertainties, and therefore the Rényi and von Neumann entropies are not appropriate measures. See [116], for example, for an argument for a minimum uncertainty pure state with non-zero entropy. For the current discussions the use of the Rényi entropy as a relative measure will, however, be adequate, since we are concerned with the entropy as an established entanglement criterion only, and not as a measure. We will also provide the von Neumann entropy for interest, and leave a fuller evaluation of the appropriate measures of entanglement to further work.

For any general composite system with density matrix ρ_{AB} and two subsystems A and B, the reduced density matrix for one subsystem, ρ_A say, requires the 'tracing out' of the other subsystem (B) from ρ_{AB}. This can be expressed as the sum of the expectation values of the composite system using the basis vectors $|j\rangle_B$ of B:

$$\rho_A = \mathrm{Tr}_B(\rho_{AB}) = \sum_j {}_B\langle j|\rho_{AB}|j\rangle_B. \tag{4.3}$$

For an explicit example, consider one of the standard Bell states (1.3). The density matrix for the entangled bipartite system is thus $\rho_{AB} = |\psi\rangle_{AB}{}_{AB}\langle\psi|$, and the reduced density matrix for the second subsystem ρ_B, say, is found by

tracing out all the degrees of freedom of the first subsystem (A):

$$\begin{aligned}\rho_B &= \mathrm{Tr}_B(\rho_{AB}) \\ &= \frac{1}{2}\left(\mathrm{Tr}\left(|0\rangle\langle 0|\right)|1\rangle\langle 1| - \mathrm{Tr}\left(|0\rangle\langle 1|\right)|1\rangle\langle 0| - \mathrm{Tr}\left(|1\rangle\langle 0|\right)|0\rangle\langle 1| + \mathrm{Tr}\left(|1\rangle\langle 1|\right)|0\rangle\langle 0|\right) \\ &= \frac{1}{2}\left(|1\rangle\langle 1| + |0\rangle\langle 0|\right) = \frac{1}{2}\boldsymbol{I}. \end{aligned} \tag{4.4}$$

Since the basis vectors of B are $\{|0\rangle, |1\rangle\}$ we see that we have used (4.3) in (4.4) with $a = 0, 1$ such that:

$$\mathrm{Tr}\left(|a\rangle\langle a|\right) = \sum_j \langle j|\left(|a\rangle\langle a|\right)|j\rangle = \langle 0|a\rangle\langle a|0\rangle + \langle 1|a\rangle\langle a|1\rangle = |\langle a|a\rangle|^2, \tag{4.5}$$

and in the case (4.4) our bases are orthonormal such that $|\langle a|a\rangle|^2 = \langle a|a\rangle = 1$.

We know that the Bell states are maximally entangled bipartite states, and these are well-known to have a von Neumann entropy of one in the 'binary' $\log_2$ sense (or $\ln(2)$ for natural logarithms), which we can verify for the above example using (4.4):

$$\begin{aligned} S_{vN}(\rho_B) &= -\mathrm{Tr_A}\rho\ln\rho \\ &= -\mathrm{Tr}\left(\frac{1}{2}\boldsymbol{I}\cdot\begin{pmatrix}\ln\frac{1}{2} & 0\\ 0 & \ln\frac{1}{2}\end{pmatrix}\right) \\ &= -\ln(\tfrac{1}{2}) = \ln(2). \end{aligned} \tag{4.6}$$

As mentioned above, using entropy as an entanglement measure is a relative gauge calculated from the change in entropy with spatial extent in the subsystem region. Its bounds are the fully mixed and pure states, and as demonstrated with the pure Bell state above, this means that for bipartite systems maximum entanglement is indicated by a von Neumann entropy $S_{vN}(\rho) = \ln(2)$ (4.6). For the more general Rényi entropy (4.1), the condition on entanglement is expressed as the violation of the following inequality, which has been shown to hold for all separable (non-entangled) states, and for all $\delta \geq 1$ [74]:

$$S_R(\rho) \geq \max\left(\mathrm{S}_R(\rho_A), \mathrm{S}_R(\rho_B)\right). \tag{4.7}$$

A violation of (4.7) for *any* $\delta \geq 1$ thus indicates entanglement for that δ.

The first step to finding entropy measures for the entanglement criterion is to acquire the density matrix of the system in question, which is in general

a difficult task. One way of achieving this is to first find the eigenstates of the model. For the ACS model in (3.4) we showed that the model is exactly solvable and that one can therefore in principle use the Bethe Ansatz [26] to find the exact eigenstates. As we outlined in Section 3.1, the procedure is to write the N-body wavefunction as a linear combination of $N!$ plane waves with N quasi-momenta, which must satisfy the Bethe Ansatz equations. The simpler ground state wave function is a sum of these wave functions acting on the 'vacuum' state of all the bath having spin-up, for example, with one impurity-spin lowering operator per impurity. There exists a vast literature on the Bethe Ansatz, and it is comprehensively reviewed in [127] for example, but in general it is difficult to implement. As a result, it is often avoided in favour of numerical approaches, despite the clear advantage of providing exact results. While we do not provide the Bethe Ansatz solution to the ACS model in this thesis, we will demonstrate both a possible approach for finding the density matrix and calculating the entropy numerically, as well as detailing a clear procedure for an exact measure.

In the first instance, we shall in Section 4.2 extend to the three-component case a variational method utilised previously by Oh and Kim [101] to find measures of the entanglement in the spin-$\frac{1}{2}$ Kondo model. One proceeds by proposing a possible ground state for the system, which includes variational parameters that can be optimised to achieve the lowest possible expectation value of the Hamiltonian, and thus the ground state energy of the system. This state is used to generate a reduced density matrix from which one can calculate the entropy and entanglement measures. The reliance of the method on variational parameters means that the results are not exact, but numerical calculations can be done to a high level of accuracy. To utilise the exactly solvable nature of the model we shall obtain in-principle exact results in Section 4.3. We find the density matrix for the system Hamiltonian directly using the Feynman-Hellmann theorem, which enables the calculation of exact expressions for the entropy. The entropy measures found by both these experimentally accessible methods provide criteria for entanglement in the three-level system via the violation of (4.7). The chapter concludes with a summary of the findings in the Discussion section 4.4, and suggests further work to continue the investigation into entanglement in the three-level model.

4.2 Variational approach to entanglement

Oh and Kim [101] examined entanglement in the single (spin-$\frac{1}{2}$) impurity Kondo model by a variational Ansatz (as proposed by Yosida [146]). In general, the variational principle is used to estimate the ground state energy E_g from the expectation value of a Hamiltonian H, using $\langle H \rangle \geq E_g$. It assumes a form for the normalised wavefunction that relies on variational parameters. These parameters can then be optimised to find the value producing the lowest possible expectation value, so the method clearly provides an upper bound for the ground state energy. The variational method is not an ideal way to establish entanglement measures, since *exact* solutions would be available from the Bethe Ansatz. However, it is informative to follow the method of [101] to provide the three-level analogue analysis to Oh and Kim's two-level entanglement measures. The result is an interesting extension to generalised states that permits a strong condition on entanglement through the Rényi entropy (4.1).

In the two-level case, Oh and Kim proposed that when the impurity spin and the Fermi sea are maximally entangled the state is represented by the Kondo singlet:

$$|\Psi_s\rangle = \frac{1}{\sqrt{2}} \left(|\omega_\downarrow\rangle|\chi_\uparrow\rangle - |\omega_\uparrow\rangle|\chi_\downarrow\rangle \right). \tag{4.8}$$

Here $|\omega_\downarrow\rangle$ and $|\omega_\uparrow\rangle$ denote conduction electron states with one extra down- and up-spin respectively, and $|\chi_\uparrow\rangle$ and $|\chi_\downarrow\rangle$ are the impurity spin-up and down states (i.e. $|\omega_\downarrow\rangle$ has $N/2$ up-spin and $N/2+1$ down-spin conduction electrons) [72]. Using real variational parameters Γ_k, the conduction electron states $|\omega_\downarrow\rangle$ and $|\omega_\uparrow\rangle$ can be written

$$|\omega_\alpha\rangle = \frac{1}{\sqrt{M}} \sum_{k>k_F} \Gamma_k c_{k\alpha}^\dagger |F\rangle, \tag{4.9}$$

where $|F\rangle$ is the filled Fermi sphere (introduced in Subsection 3.2.1 and discussed further below), M is some normalisation constant and $c_{k\alpha}^\dagger$ are the usual creation operators for fermions (3.9) with wave number k and spin $\alpha = 1, 2$ having the same dual notation as used in Chapter 3 where $1 \equiv\uparrow$, $2 \equiv\downarrow$. The impurity spin states $|\chi_\uparrow\rangle$ and $|\chi_\downarrow\rangle$ are defined in a second-quantised notation by introducing creation operators $\hat{\chi}_\sigma^\dagger$ for the impurity with spin $\sigma = 1, 2$ (where

again $1 \equiv\uparrow$, $2 \equiv\downarrow$) as:

$$|\chi_\sigma\rangle = \hat{\chi}_\sigma^\dagger|0\rangle. \tag{4.10}$$

In this two-level case, the variational parameters can be found to be dependent on the Kondo temperature T_K (see (3.30)), wave number k, Boltzmann constant k_B and the single particle energy ϵ_k via the relation: $\Gamma_k = 1/(\epsilon_k + k_B T_K)$ [101].

Oh and Kim used the variational estimate for the ground state wavefunction (4.8) to find measures of the entanglement present in the standard spin-$\frac{1}{2}$ AKM [101]. The results presented therein report that the impurity spin is maximally entangled with all the conduction electrons, while the entanglement within the conduction electron screening cloud[1] is barely affected by the impurity. This is in contrast to the conventional belief that the entanglement is generated by consecutive interaction with the impurity [89], and the authors suggest the entanglement is instead due to the Pauli exclusion principle. Furthermore, the two-spin reduced density matrix of the impurity and one conduction electron is found to be a Werner state [137], and hence it is relatively straightforward to rearrange the parameters characterising the state to demonstrate whether it is separable or entangled. In that case the regime of parameters is such that the entanglement vanishes between the impurity and a single conduction electron, and it was suggested that this is because there are so many conduction electrons that entanglement to any single one is negligible.

In this section we will use the variational principle to suggest a possible ground state for the three-level model from Chapter 3, and use this to find the reduced density matrices of the system. In this generalised case it is not immediately clear whether the reduced density matrices of the three-level system can be brought into a Werner state form but they can, nevertheless, be used to investigate entanglement criteria in terms of the entropy, as discussed in the introduction to this chapter.

[1] See [31] and references therein for calculation of measures of this screening cloud as impurity-spin-conduction-electron-spin correlation functions. [31] also shows that any finite temperature introduces an energy scale beyond which the Kondo correlations vanish exponentially.

4.2.1 Extension to three-component fermions

In the spin-$\frac{1}{2}$ case discussed in Section 4.2 above, one could instead have analysed the alternative ground state possibilities such as the triplet state with total spin $s = 1$ rather than the singlet case (4.8) with $s = 0$. For the generalisation to three-component fermions we shall consider one ground state possibility in direct analogue with the singlet-state analysis presented in [101]. Allowing for three possible "spin" values for the labels $\alpha, \beta = 1, 2, 3$ as in Chapter 3, the three-component singlet state analogue now becomes an antisymmetric triplet:

$$|\Psi\rangle = \frac{1}{\sqrt{2}} \left(|\omega_\alpha\rangle|\chi_\beta\rangle - |\omega_\beta\rangle|\chi_\alpha\rangle \right), \tag{4.11}$$

taking $\alpha \neq \beta$ by definition.

To find an entropy measure for use in the entanglement criterion (4.7), we first find the density matrix of the entire system:

$$\begin{aligned} \rho &= |\Psi\rangle\langle\Psi| \\ &= \frac{1}{2} \left(|\omega_\alpha\rangle|\chi_\beta\rangle\langle\chi_\beta|\langle\omega_\alpha| - |\omega_\alpha\rangle|\chi_\beta\rangle\langle\chi_\alpha|\langle\omega_\beta| \right. \\ &\quad \left. -|\omega_\beta\rangle|\chi_\alpha\rangle\langle\chi_\beta|\langle\omega_\alpha| + |\omega_\beta\rangle|\chi_\alpha\rangle\langle\chi_\alpha|\langle\omega_\beta| \right). \end{aligned} \tag{4.12}$$

The reduced density matrix for the impurity ρ_{im} is found by tracing out all the fermionic bath degrees of freedom in direct analogy with (4.4) to give:

$$\begin{aligned} \rho_{\text{im}} &= \text{Tr}_{\text{bath}}(\rho) \\ &= \frac{1}{2} \left(|\chi_\alpha\rangle\langle\chi_\alpha| + |\chi_\beta\rangle\langle\chi_\beta| \right). \end{aligned} \tag{4.13}$$

For $\alpha = 1, \beta = 2$ this gives:

$$\rho_{\text{im}} = \frac{1}{2}\text{diag}(1, 1, 0), \tag{4.14}$$

and other particular α, β subsystems will give a permutation of the diagonal elements. These reduced density matrices will again have a von Neumann entropy $S_{vN}(\rho_{\text{im}}) = \ln(2)$, as in (4.6), showing that the impurity spin is maximally entangled with the Fermi gas since this is a direct analogue of the standard bipartite situation. This is thus an expected result as we started with a singlet state analogue. However, it provides an important upper bound

for the criterion (4.7) when we find the condition for entanglement between the impurity and a single conduction fermion below. The proposed wavefunction (4.11) is of course only one of many possible starting points for such analysis, but here we will follow the direct analogue to the standard bipartite spin-$\frac{1}{2}$ situation as it is an illustrative example revealing the details of the method and highlights some important generalisations and complications. Some discussion of alternative approximations to the ground state behaviour will be included in Section 4.4.

Reduced density matrix for impurity and one bath fermion

In order to find the criterion for entanglement between the impurity and a single fermion from the environmental bath, we follow the general method of [101], although the procedure for finding the reduced density matrix increases significantly in complexity. This involves the tracing out of all degrees of freedom except for the impurity spin and one conduction spin from the joint system density matrix (4.12). In effect, this leaves a reduced density matrix ρ^{red} for one conduction fermion at an arbitrary position r and the impurity, which we shall choose to be at the origin. As we will show below, the elements that populate this reduced density matrix can be found by the following expectation value expression:

$$\rho^{\text{red}}_{\sigma\gamma,\sigma'\gamma'}(r) = \frac{1}{2}\langle\Psi|\hat{\psi}^{\dagger}_{\gamma'}(r)\hat{\chi}^{\dagger}_{\sigma'}(0)\hat{\chi}_{\sigma}(0)\hat{\psi}_{\gamma}(r)|\Psi\rangle. \tag{4.15}$$

In the one-dimensional case that we are considering here, the creation operator for *one* fermion of spin γ' at position r in the bath is:

$$\hat{\psi}^{\dagger}_{\gamma'}(r) = \frac{1}{\sqrt{V}}\left(\sum_{l\leq k_F} e^{il.r}c^{\dagger}_{l\gamma'} + \sum_{l>k_F} e^{il.r}c^{\dagger}_{l\gamma'}\right), \tag{4.16}$$

where V is the volume of the Fermi gas. The creation operator $\hat{\chi}^{\dagger}_{\sigma'}$ for the impurity at the origin is still as given in (4.10). We shall demonstrate (4.15) to be true by considering the following example for bipartite basis states

$\{|\alpha a\rangle \equiv |\alpha\rangle \otimes |a\rangle\}$. For wavefunctions of the form

$$|\psi\rangle = \sum_{\alpha,a} \psi_{\alpha a}|\alpha\rangle|a\rangle, \tag{4.17}$$

we have the inner product

$$\langle \beta b|\psi\rangle = \psi_{\beta b}. \tag{4.18}$$

The reduced density matrix for the first space corresponding to this state is found by tracing over space (2) in a similar fashion to that used to obtain (4.13), with $\rho_{(1)} = \mathrm{Tr}_{(2)}\rho$. Using (4.3) and (4.18), the expectation value of the reduced density matrix $\rho_{(1)}$ thus becomes the general

$$\langle \alpha|\rho_{(1)}|\beta\rangle = \sum_a \langle \alpha a|\psi\rangle\langle\psi|a\beta\rangle = \sum_a \psi_{\alpha a}\psi^\dagger_{\beta a}. \tag{4.19}$$

We can represent the current three-level case by writing the components of the basis vectors in the above example as $|\alpha\rangle = \hat{\chi}^\dagger_\alpha|0\rangle$, $|a\rangle = \hat{\psi}^\dagger_a|F\rangle$, where $|F\rangle$ is a pseudo-vacuum first introduced in Subsection 3.2.1. Consequently, the expectation value of generic impurity operators $\hat{\chi}^\dagger_c\hat{\chi}_d$ becomes:

$$\begin{aligned}
\langle \hat{\chi}^\dagger_c\hat{\chi}_d\rangle &= \langle\psi|\hat{\chi}^\dagger_c\hat{\chi}_d|\psi\rangle \\
&= \sum_{\alpha,a,\alpha',a'} \psi^\dagger_{\alpha' a'}\langle a'\alpha'|\hat{\chi}^\dagger_c\hat{\chi}_d|\alpha a\rangle\psi_{\alpha a} \\
&= \sum_{\alpha,a,\alpha',a'} \psi^*_{\alpha' a'}\langle 0F|\hat{\psi}_{a'}\hat{\chi}_{\alpha'}\hat{\chi}^\dagger_c\hat{\chi}_d\hat{\chi}^\dagger_\alpha\hat{\psi}^\dagger_a|F0\rangle\psi_{\alpha a} \\
&= \sum_{\alpha,a,\alpha',a'} \psi^\dagger_{\alpha' a'}\psi_{\alpha a}\delta_{a' a}\delta_{\alpha' c}\delta_{d\alpha} \\
&= \sum_a \psi^\dagger_{ca}\psi_{da}.
\end{aligned} \tag{4.20}$$

From (4.19) and (4.20) we can thus see that this leads to the rule

$$\langle \alpha|\rho_{(1)}|\beta\rangle \equiv \langle \hat{\chi}^\dagger_\alpha\hat{\chi}_\beta\rangle. \tag{4.21}$$

This is equivalent to equation (4.15), in which particular matrix elements of the reduced density matrix are obtained by calculating the expectation values of impurity operators $\hat{\chi}^\dagger_{\sigma'}(0)\hat{\chi}_\sigma(0)$, and the fermionic operators $\hat{\psi}_\gamma(r)$ and $\hat{\psi}^\dagger_{\gamma'}(r)$ pick out the single bath fermion at position r.

The generalised equation (4.15) for calculating the elements of the reduced density matrix of the three-level system can thus be found using (4.9), (4.10), (4.11) and (4.16) to be expressible as:

$$\begin{aligned}\rho^{\mathrm{red}}_{\sigma\gamma,\sigma'\gamma'}(r) &= \frac{1}{2MV}\sum_{k>k_F}\Gamma_k\left(\langle 0|\langle F|\chi_\beta c_{k\alpha} - \langle 0|\langle F|\chi_\alpha c_{k\beta}\right)\\ &\cdot\left(\sum_{l\le k_F} e^{il.r}c^\dagger_{l\gamma'} + \sum_{l>k_F} e^{il.r}c^\dagger_{l\gamma'}\right)\chi^\dagger_{\sigma'}\chi_\sigma\\ &\cdot\left(\sum_{m\le k_F} e^{-im.r}c_{m\gamma} + \sum_{m>k_F} e^{-im.r}c_{m\gamma}\right)\\ &\cdot\sum_{p>k_F}\Gamma_p\left(c^\dagger_{p\alpha}\chi^\dagger_\beta|F\rangle|0\rangle - c^\dagger_{p\beta}\chi^\dagger_\alpha|F\rangle|0\rangle\right), \end{aligned} \tag{4.22}$$

where we have dropped the circumflex ($\hat{}$) notation for convenience as we shall be dealing with operators throughout.

Expanding all the terms in (4.22) produces a form from which we can deduce which elements of the reduced density matrix are non-zero. We remember that in the notation $|F\rangle|0\rangle \equiv |F\rangle \otimes |0\rangle \equiv |F0\rangle$, the Fermi sea $|F\rangle$ acts as a pseudo-vacuum, which we shall discuss in more detail below. We write all four sums implicitly in a simplified notation that combines sums for elements either above or below (and on) the Fermi surface. Consequently, the expanded form of (4.22) becomes (see overleaf):

$$\rho^{\mathrm{red}}_{\sigma\gamma,\sigma'\gamma'}(r) = \frac{1}{2MV}\Bigg(\sum_{k,p>k_F} \sum_{l,m\leq k_F} \Gamma_k\Gamma_p e^{il.r} e^{-im.r} \langle \chi_\beta c_{k\alpha} c^\dagger_{l\gamma'} \chi^\dagger_{\sigma'} \chi_\sigma c_{m\gamma} c^\dagger_{p\alpha} \chi^\dagger_\beta \rangle \quad (4.23a)$$

$$- \sum_{k,p>k_F} \sum_{l,m\leq k_F} \Gamma_k\Gamma_p e^{il.r} e^{-im.r} \langle \chi_\beta c_{k\alpha} c^\dagger_{l\gamma'} \chi^\dagger_{\sigma'} \chi_\sigma c_{m\gamma} c^\dagger_{p\beta} \chi^\dagger_\alpha \rangle \quad (4.23b)$$

$$+ \sum_{k,m,p>k_F} \sum_{l\leq k_F} \Gamma_k\Gamma_p e^{il.r} e^{-im.r} \langle \chi_\beta c_{k\alpha} c^\dagger_{l\gamma'} \chi^\dagger_{\sigma'} \chi_\sigma c_{m\gamma} c^\dagger_{p\alpha} \chi^\dagger_\beta \rangle \quad (4.23c)$$

$$- \sum_{k,m,p>k_F} \sum_{l\leq k_F} \Gamma_k\Gamma_p e^{il.r} e^{-im.r} \langle \chi_\beta c_{k\alpha} c^\dagger_{l\gamma'} \chi^\dagger_{\sigma'} \chi_\sigma c_{m\gamma} c^\dagger_{p\beta} \chi^\dagger_\alpha \rangle \quad (4.23d)$$

$$+ \sum_{k,l,p>k_F} \sum_{m\leq k_F} \Gamma_k\Gamma_p e^{il.r} e^{-im.r} \langle \chi_\beta c_{k\alpha} c^\dagger_{l\gamma'} \chi^\dagger_{\sigma'} \chi_\sigma c_{m\gamma} c^\dagger_{p\alpha} \chi^\dagger_\beta \rangle \quad (4.23e)$$

$$- \sum_{k,l,p>k_F} \sum_{m\leq k_F} \Gamma_k\Gamma_p e^{il.r} e^{-im.r} \langle \chi_\beta c_{k\alpha} c^\dagger_{l\gamma'} \chi^\dagger_{\sigma'} \chi_\sigma c_{m\gamma} c^\dagger_{p\beta} \chi^\dagger_\alpha \rangle \quad (4.23f)$$

$$+ \sum_{k,l,m,p>k_F} \Gamma_k\Gamma_p e^{il.r} e^{-im.r} \langle \chi_\beta c_{k\alpha} c^\dagger_{l\gamma'} \chi^\dagger_{\sigma'} \chi_\sigma c_{m\gamma} c^\dagger_{p\alpha} \chi^\dagger_\beta \rangle \quad (4.23g)$$

$$- \sum_{k,l,m,p>k_F} \Gamma_k\Gamma_p e^{il.r} e^{-im.r} \langle \chi_\beta c_{k\alpha} c^\dagger_{l\gamma'} \chi^\dagger_{\sigma'} \chi_\sigma c_{m\gamma} c^\dagger_{p\beta} \chi^\dagger_\alpha \rangle \quad (4.23h)$$

$$- \sum_{k,p>k_F} \sum_{l,m\leq k_F} \Gamma_k\Gamma_p e^{il.r} e^{-im.r} \langle \chi_\alpha c_{k\beta} c^\dagger_{l\gamma'} \chi^\dagger_{\sigma'} \chi_\sigma c_{m\gamma} c^\dagger_{p\alpha} \chi^\dagger_\beta \rangle \quad (4.23i)$$

$$+ \sum_{k,p>k_F} \sum_{l,m\leq k_F} \Gamma_k\Gamma_p e^{il.r} e^{-im.r} \langle \chi_\alpha c_{k\beta} c^\dagger_{l\gamma'} \chi^\dagger_{\sigma'} \chi_\sigma c_{m\gamma} c^\dagger_{p\beta} \chi^\dagger_\alpha \rangle \quad (4.23j)$$

$$- \sum_{k,m,p>k_F} \sum_{l\leq k_F} \Gamma_k\Gamma_p e^{il.r} e^{-im.r} \langle \chi_\alpha c_{k\beta} c^\dagger_{l\gamma'} \chi^\dagger_{\sigma'} \chi_\sigma c_{m\gamma} c^\dagger_{p\alpha} \chi^\dagger_\beta \rangle \quad (4.23k)$$

$$+ \sum_{k,m,p>k_F} \sum_{l\leq k_F} \Gamma_k\Gamma_p e^{il.r} e^{-im.r} \langle \chi_\alpha c_{k\beta} c^\dagger_{l\gamma'} \chi^\dagger_{\sigma'} \chi_\sigma c_{m\gamma} c^\dagger_{p\beta} \chi^\dagger_\alpha \rangle \quad (4.23l)$$

$$- \sum_{k,l,p>k_F} \sum_{m\leq k_F} \Gamma_k\Gamma_p e^{il.r} e^{-im.r} \langle \chi_\alpha c_{k\beta} c^\dagger_{l\gamma'} \chi^\dagger_{\sigma'} \chi_\sigma c_{m\gamma} c^\dagger_{p\alpha} \chi^\dagger_\beta \rangle \quad (4.23m)$$

$$+ \sum_{k,l,p>k_F} \sum_{m\leq k_F} \Gamma_k\Gamma_p e^{il.r} e^{-im.r} \langle \chi_\alpha c_{k\beta} c^\dagger_{l\gamma'} \chi^\dagger_{\sigma'} \chi_\sigma c_{m\gamma} c^\dagger_{p\beta} \chi^\dagger_\alpha \rangle \quad (4.23n)$$

$$- \sum_{k,l,m,p>k_F} \Gamma_k\Gamma_p e^{il.r} e^{-im.r} \langle \chi_\alpha c_{k\beta} c^\dagger_{l\gamma'} \chi^\dagger_{\sigma'} \chi_\sigma c_{m\gamma} c^\dagger_{p\alpha} \chi^\dagger_\beta \rangle \quad (4.23o)$$

$$+ \sum_{k,l,m,p>k_F} \Gamma_k\Gamma_p e^{il.r} e^{-im.r} \langle \chi_\alpha c_{k\beta} c^\dagger_{l\gamma'} \chi^\dagger_{\sigma'} \chi_\sigma c_{m\gamma} c^\dagger_{p\beta} \chi^\dagger_\alpha \rangle \Bigg). \quad (4.23p)$$

All the operators involved in (4.23) are fermionic and must therefore necessarily adhere to the standard fermionic anticommutation relations (3.9). The impurity and bath operators act on separate fermionic spaces, meaning we can

write all sixteen of the fermionic strings in (4.23) as two blocks of the generic form

$$\langle 0|\chi_a\chi_b^\dagger\chi_c\chi_d^\dagger|0\rangle\langle F|c_e c_f^\dagger c_g c_h^\dagger|F\rangle. \tag{4.24}$$

By using the fermionic anticommutation relations we can write any particular combination of fermionic operators in this arrangement as

$$\begin{aligned}\langle\chi_a\chi_b^\dagger\chi_c\chi_d^\dagger\rangle &= \langle(\delta_{ab}-\chi_b^\dagger\chi_a)(\delta_{cd}-\chi_d^\dagger\chi_c)\rangle \\ &= \langle\delta_{ab}\delta_{cd}-\delta_{ab}\chi_d^\dagger\chi_c-\delta_{cd}\chi_b^\dagger\chi_a+\delta_{ad}\chi_b^\dagger\chi_c-\chi_b^\dagger\chi_d^\dagger\chi_a\chi_c\rangle \\ &= \delta_{ab}\delta_{cd}. \end{aligned}\tag{4.25}$$

The last line uses the definition of normal ordering (see Subsection 3.2.1), which demands that the vacuum expectation value of normal ordered operators is zero. Note that Wick's theorem [140] makes this deduction much simpler for longer strings of products of creation and annihilation operators, in the case where the model is extended to more than one impurity, for example.

In deducing which terms of (4.23) are non-zero for any particular $\rho^{\mathrm{red}}_{\sigma\gamma,\sigma'\gamma'}(r)$ matrix element, the first step is to note that both parties of any operator pairing in the delta-function combinations indicated by (4.25) must be either both above or both below the Fermi sea. This means we can immediately halve the number of terms in (4.23) by ignoring (4.23c,d,e,f,k,l,m,n), which we can see from the summation convention involve terms with only one operator below (or on) the Fermi surface (e.g. $c_{l\gamma'}^\dagger$ in (4.23c)).

For the remaining terms in (4.23), consider first the impurity space. It is clear from (4.25) that the possible outcomes are

$$\langle\chi_\beta\chi_{\sigma'}^\dagger\chi_\sigma\chi_\beta^\dagger\rangle = \delta_{\beta\sigma'}\delta_{\sigma\beta}, \tag{4.26a}$$

$$\langle\chi_\beta\chi_{\sigma'}^\dagger\chi_\sigma\chi_\alpha^\dagger\rangle = \delta_{\beta\sigma'}\delta_{\sigma\alpha}, \tag{4.26b}$$

or the symmetrically opposite outcomes in α,β, remembering that $\alpha\neq\beta$ by definition from (4.11). These are the conditions for the expectation values of the string of impurity operators to be non-zero. From (4.24) it is clear that the conditions (4.26) must coincide with the instances where the expectation values of the fermionic bath operators are also non-zero. We can apply the same reasoning for the bath operators as for (4.25) to get:

$$\langle c_{k\alpha}c_{l\gamma'}^\dagger c_{m\gamma}c_{p\alpha}^\dagger\rangle = \delta_{kl}\delta_{mp}, \tag{4.27a}$$

$$\langle c_{k\alpha}c_{l\gamma'}^\dagger c_{m\gamma}c_{p\beta}^\dagger\rangle = \delta_{kl}\delta_{mp}, \tag{4.27b}$$

and again with the symmetrically opposite expressions in α, β. Note that for (4.27a) to be non-zero, we must also have $\gamma' = \gamma = \alpha$, and similarly (4.27b) demands $\gamma' = \alpha$; $\gamma = \beta$. For the equations (4.27) it is again important to consider the position of the operators relative to the Fermi sea. That is, (4.27) is only non-zero for the terms (4.23g,h,o,p) where all operators are above the Fermi sea. It would seem that we should have to discount the terms (4.23a,b,i,j), because (4.27) demands $\delta_{kl}\delta_{mp}$, which we know must yield zero since k and p are above the Fermi surface while l and m are both below (or equal to) k_F. However, we must consider the implications of the Fermi sea itself. Because the bath operators in reality act on the Fermi sea and not the vacuum, we will show below that for (4.23a,j) it is possible to pair the operators $c^\dagger_{l\gamma'}$ and $c_{m\gamma}$ with their counterparts from the Fermi sea, leaving the possibility of $c_{k\alpha}$ to pair with $c^\dagger_{p\alpha}$. The terms (4.23b,i) can, however, never exist even in this instance, because it results in an attempt to pair $c_{k\alpha}$ with $c^\dagger_{p\beta}$ (and $c_{k\beta}$ with $c^\dagger_{p\alpha}$), which is precluded by the fact that $\alpha \neq \beta$ by definition.

Until now we have considered the Fermi sea $|F\rangle$ to be a pseudo-vacuum, whereas in fact it is a product of fermionic operators up to the Fermi surface, one of which would match the indices l and m from (4.23a,j):

$$\begin{aligned} \langle F| &= \langle 0|c_N \dots c_l \dots c_1 \\ |F\rangle &= c^\dagger_1 \dots c^\dagger_m \dots c^\dagger_N |0\rangle. \end{aligned} \tag{4.28}$$

Since the operators in (4.28) anticommute we can move c_l and $c^\dagger_m$ to the right and left of their respective strings of operators, taking account of the sign changes to become

$$\langle F|F\rangle = \langle 0|c_N \dots c_1 c_l (-1)^{l-1}(-1)^{m-1} c^\dagger_m c^\dagger_1 \dots c^\dagger_N|0\rangle. \tag{4.29}$$

This means that the expectation value $\langle c_{k\alpha} c^\dagger_{l\gamma'} c_{m\gamma} c^\dagger_{p\alpha}\rangle$ in (4.23a) (and its symmetric in β counterpart (4.23j)) can be written:

$$\langle F_l| c_l c_{k\alpha} c^\dagger_{l\gamma'} c_{m\gamma} c^\dagger_{p\alpha} c^\dagger_m |F_m\rangle, \tag{4.30}$$

where the shorthand $\langle F_l|$ and $|F_m\rangle$ has been used to indicate that the respective operators c_l and $c^\dagger_m$ are missing from each. Now remember that in (4.23a) and (4.23j) the indices $k, p > k_F$ and $l, m \leq k_F$, meaning that we can use the anticommutation relations for their respective operators to write (4.30) as

$$\langle F_l| c_l c^\dagger_{l\gamma'} c_{k\alpha} c^\dagger_{p\alpha} c_{m\gamma} c^\dagger_m |F_m\rangle = \langle F_l|\delta_{ll}\delta_{kp}\delta_{mm}|F_m\rangle. \tag{4.31}$$

This is clearly zero unless $l = m$ (which importantly also requires that $\gamma' = \gamma$), so for (4.23a) and (4.23j) we can effectively write

$$\langle c_{k\alpha} c^{\dagger}_{l\gamma'} c_{m\gamma} c^{\dagger}_{p\alpha} \rangle = \delta_{kp}\delta_{lm}. \tag{4.32}$$

We have now deduced the full set of conditions for any terms of (4.23) to be non-zero, which provide the elements of the generalised density matrix for the system. We have argued that only six terms from (4.23) need to be considered, (4.23a,g,h,j,o,p), and we have shown that the expectation values in these remaining terms can each be written as products of four delta functions. These delta functions indicate how the matrix elements depend on the specific α, β subsystem of interest. Specifically, we can see that (4.23a) requires (4.26a) and (4.32) (and similarly (4.23j) requires the corresponding conditions for α instead of β). As such, these terms will appear in the matrix elements $\rho^{\rm red}_{\sigma\gamma,\sigma'\gamma'} = \rho^{\rm red}_{\beta\gamma,\beta\gamma}$ (and $\rho^{\rm red}_{\sigma\gamma,\sigma'\gamma'} = \rho^{\rm red}_{\alpha\gamma,\alpha\gamma}$) only. Similarly, (4.23g,h,o,p) require (4.26) and (4.27) (and their respective symmetric counterparts), and thus these terms appear only in the matrix elements $\rho^{\rm red}_{\beta\alpha,\beta\alpha}$, $\rho^{\rm red}_{\alpha\beta,\beta\alpha}$, $\rho^{\rm red}_{\beta\alpha,\alpha\beta}$ and $\rho^{\rm red}_{\alpha\beta,\alpha\beta}$, respectively. Together, these terms populate the general 9×9 reduced density matrix for the three-level system for all $\alpha \neq \beta$ as follows:

$$\rho^{\rm red} = \left(\begin{array}{ccc|ccc|ccc}
\rho^{\rm red}_{11,11} & & & \rho^{\rm red}_{12,21} & & & & & \\
& \rho^{\rm red}_{12,12} & & & & & \rho^{\rm red}_{13,31} & & \\
& & \rho^{\rm red}_{13,13} & & & & & & \\
\hline
& \rho^{\rm red}_{21,12} & & \rho^{\rm red}_{21,21} & & & & & \\
& & & & \rho^{\rm red}_{22,22} & & & & \\
& & & & & \rho^{\rm red}_{23,23} & & \rho^{\rm red}_{23,32} & \\
\hline
& & \rho^{\rm red}_{31,13} & & & & \rho^{\rm red}_{31,31} & & \\
& & & & & \rho^{\rm red}_{32,23} & & \rho^{\rm red}_{32,32} & \\
& & & & & & & & \rho^{\rm red}_{33,33}
\end{array}\right), \tag{4.33}$$

where precise expressions for the matrix elements are calculated from (4.23), as discussed further below.

It is clear that for any particular α, β subsystem only one of the three off-diagonal pairs will exist, and one of the 3×3 diagonal blocks will have all zero elements. As a simple guide to which elements are non-zero, we can further simplify each of the remaining terms in (4.23) by noting that the respective delta-functions imply that

$$\rho^{\rm red}_{\alpha\beta,\alpha\beta}(r) = \rho^{\rm red}_{\beta\alpha,\beta\alpha}(r) = -\rho^{\rm red}_{\alpha\beta,\beta\alpha}(r) = -\rho^{\rm red}_{\beta\alpha,\alpha\beta}(r) = f, \tag{4.34}$$

with

$$f = f(r) = \frac{1}{2MV} \sum_{k,p>k_F} \Gamma_k e^{i(k-p).r} \Gamma_p, \tag{4.35}$$

and density-like terms are found when the exponentials are unity from δ_{lm}:

$$\rho^{\text{red}}_{\alpha\gamma,\alpha\gamma}(r) = \rho^{\text{red}}_{\beta\gamma,\beta\gamma}(r) = d, \tag{4.36}$$

where

$$d = \frac{1}{2MV} \sum_{k>k_F} \Gamma_k^2 \sum_{l\leq k_F} 1 = \frac{k_F}{2MV} \sum_{k>k_F} \Gamma_k^2. \tag{4.37}$$

Expressions (4.34) and (4.36) thus provide a straightforward recipe for deducing the non-zero elements of the reduced density matrix for any particular α, β subsystem. For the three-level model in question, the subsystem density matrices are provided explicitly in Appendix C. The reduced density matrix can be used to deduce many physical properties of the system, but in particular we are here interested in the entropy measures with a view to finding entanglement criteria.

4.2.2 Entropy measures

As discussed in Section 4.1, the density matrix and reduced density matrices can be used to find the corresponding Rényi entropy (4.1):

$$S_R(\rho) := \frac{1}{1-\delta} \ln \text{Tr}(\rho^\delta), \quad \delta > 1.$$

This provides a generalised entropy expression for the system, and provides a strong condition for the presence of entanglement via the violation of (4.7). On inspection of (4.33) for the current generalised three-level system, it can be shown that for all possible α, β subsystems with $\alpha \neq \beta$ (see (C.2), (C.4), (C.6) in Appendix C), the trace of the reduced density matrix raised to the power δ can be found by the succinct closed expression:

$$\text{Tr}((\rho^{\text{red}})^\delta) = 6d^\delta + \sum_{i=1}^{\delta} \left(\frac{2^i}{i!}\right) \frac{\delta!}{(\delta-i)!} d^{\delta-i} f^i, \tag{4.38}$$

where f and d are given by (4.35) and (4.37) respectively.

For example, the Rényi entropy (4.1) with $\delta = 2$ for all α, β subsystems is found to be:

$$S_R(\rho^{\text{red}}) = -\ln(6d^2 + 4df + 4f^2). \tag{4.39}$$

As mentioned in the introduction, the popular von Neumann entropy measure $S_{vN}(\rho)$ is the $\delta = 1$ limit of the Rényi entropy, and is given by (4.2). For the current three-level system the von Neumann entropy for the possible α, β subsystems is

$$S_{vN}(\rho^{\text{red}}) = 5d\ln(d) + (d + 2f)\ln(d + 2f). \tag{4.40}$$

The expressions for subsystem entropy contributes to the criteria for entanglement in the system via (4.7). Notice that we started with the three-level singlet state analogue (4.11), and traced out all of the bath except for a single bath fermion. Using only this information to provide entropy measures, we find an expression for the entanglement between the original whole bath-impurity system and a single bath fermion plus the impurity. In this case, the criterion can be expressed using the Rényi entropy for the maximally entangled state (4.12), which will be zero since this is a pure state, and the entropy for the α, β subsystems, which is calculated by combining (4.1) and (4.38). The criterion for entanglement between the whole bath plus impurity and a single bath fermion plus impurity is thus the violation of the following inequality:

$$0 \geq \frac{1}{1-\delta}\ln\left(6d^\delta + \sum_{i=1}^{\delta}\left(\frac{2^i}{i!}\right)\frac{\delta!}{(\delta-i)!}d^{\delta-i}f^i\right), \tag{4.41}$$

valid for any $\delta > 1$, or alternatively for $\delta = 1$ we replace the right hand side of (4.41) with the von Neumann entropy limit (4.40).

Since we showed with (4.14) that the impurity is maximally entangled with the entire bath, it would seem reasonable to expect that the inequality (4.41) will be violated for most values of the parameters. Perhaps the more interesting criterion is therefore for the entanglement between the single bath fermion and the impurity. In this case we use the density matrices represented by (4.33) (see (C.2), (C.4), (C.6)) to represent the entire system, and note that the effect of tracing out the impurity from this joint system produces the same density matrices as was calculated for (4.13), which gave an entropy value of ln(2).

Thus the criterion for entanglement between the single bath fermion and the impurity in this model is found by the violation of the following inequality:

$$\frac{1}{1-\delta}\ln\left(6d^{\delta}+\sum_{i=1}^{\delta}\left(\frac{2^i}{i!}\right)\frac{\delta!}{(\delta-i)!}d^{\delta-i}f^i\right)\geq\ln(2), \tag{4.42}$$

which is again valid for any $\delta > 1$, or alternatively for $\delta = 1$ we replace the left hand side of (4.42) with the von Neumann entropy (4.40). This is a powerful criterion for entanglement, and allows numerical solutions for entropy measures and hence entanglement criteria in the model to be found given estimates of the variational parameters Γ_k, Γ_p. Although it was reported in [101] that there is no entanglement between the impurity and the single bath fermion in the two-level case, it is not immediately apparent that this will be the case for (4.42). We leave this important question open to consideration in further work.

4.3 Feynman-Hellmann method

In the introduction to this chapter we outlined the method of using entropy as a criterion for entanglement, and in Section 4.2 we applied this to an estimate of the ground state of the bosonised ACS model using the variational principle. This produced entropy measures in terms of quantities that were dependent on variational parameters. As discussed in Sections 3.1 and 4.1, exact values of the ground state, and indeed all the energy eigenstates of the model, may be found by means of the Bethe Ansatz. While the results of the Bethe Ansatz are not presented in this thesis, we show in the current section that, where an exact ground state is available, the method for finding the correspondingly exact values of the entropy can be extended to the case of the three-level dissipative system of Chapter 3. We shall refer to this method as the Feynman-Hellmann method, and the exposition follows the general argument outlined for the two-level system in [92, 88].

For two-level systems, the expectation values of spin operators can be combined to produce an expression for the density matrix of that system via

$$\rho=\frac{1}{2}\boldsymbol{I}+\sum_{i=x,y,z}\langle\sigma_i\rangle\sigma_i. \tag{4.43}$$

As discussed in the introduction to this chapter and in Section 4.2, the density matrix provides a wealth of information about the system, and can be used to find entropy measures which may in turn be used as entanglement criteria and also to indicate the degree of entanglement in the model. In the two-level case, the Feynman-Hellmann Theorem has been used to find expressions for the expectation values of the spin-$\frac{1}{2}$ operators for the Spin-Boson Hamiltonian (3.1b) [92, 88]. The Feynman-Hellmann Theorem states that the partial derivative of the energy $E(\tau)$ of a system, with respect to some variable τ, is equal to the expectation value of the partial derivative of the system Hamiltonian with respect to that same variable (see for example [32]):

$$\frac{\partial E(\tau)}{\partial \tau} = \left\langle \frac{\partial H(\tau)}{\partial \tau} \right\rangle . \tag{4.44}$$

When an exact eigenstate of a model is available, by solution of the Bethe Ansatz for example, the Feynman-Hellmann Theorem thus enables exact calculation of the expectation values derived from the system Hamiltonian. This was done for the ground state of the delocalised phase of the two-level case in [92], for example. Therein, entanglement measures for the Spin-Boson model (3.1b) were found using the von Neumann entropy (4.2), which is easily calculated in the two-level case, once the density matrix has been diagonalised, to be

$$S_{vN}(\rho) = -p_+ \ln p_+ - p_- \ln p_- . \tag{4.45}$$

Here $p_\pm = (1 \pm \sqrt{\langle\sigma_x\rangle^2 + \langle\sigma_y\rangle^2 + \langle\sigma_z\rangle^2})/2$ are the eigenvalues of the density matrix, and $\sigma_{x,y,z}$ are the usual Pauli matrices (2.1). Notice that the expectation value $\langle\sigma_y\rangle = 0$ because the SB Hamiltonian (3.1b) is invariant under the transformation $\sigma_y \to -\sigma_y$.

From the analogue expression for (4.43) in the three-level case we can find the density matrix corresponding to the exactly solvable three-level Hamiltonian (3.63) from Chapter 3. In the following subsection we will present the derivation of this three-level density matrix and in Subsection 4.3.2 we will discuss the nature of the roots and the entropy calculation.

4.3.1 Finding the three-level density matrix

For the three-level quantum dissipative system that was introduced in Chapter 3, the Feynman-Hellmann method of finding exact values for the entropy has the same overall structure as for the two-level case but increases in complexity. The 3×3 density matrix can be found by the analogue to (4.43) as the sum of the expectation values of the Gell-Mann matrices $\lambda_{\mathtt{A}}$ (see (B.7)) as follows:

$$\rho = s\boldsymbol{I} + \sum_{\mathtt{A}=1..8} \langle \lambda_{\mathtt{A}} \rangle \lambda_{\mathtt{A}}, \tag{4.46}$$

where s is a constant that normalises the trace of the density matrix to one, and $\boldsymbol{I}$ is the 3×3 identity matrix.

Recall the Hamiltonian for the three-level dissipative system (3.63):

$$\begin{aligned} H^B_{QDS} \;:=\; & \varepsilon_{\mathtt{3}}\lambda_{\mathtt{3}} + \varepsilon_{\mathtt{8}}\lambda_{\mathtt{8}} + \Delta(\lambda_{\mathtt{1}} + \lambda_{\mathtt{4}} + \cos\zeta\lambda_{\mathtt{6}} + \sin\zeta\lambda_{\mathtt{7}}) + \\ & \sum_p \hbar\omega_p(b^\dagger_{\mathtt{3}p}b_{\mathtt{3}p} + b^\dagger_{\mathtt{8}p}b_{\mathtt{8}p}) + \sum_p \hbar C_{\mathtt{3}p}\lambda_{\mathtt{3}}(b_{\mathtt{3}p} + b^\dagger_{\mathtt{3}p}) + \hbar C_{\mathtt{8}p}\lambda_{\mathtt{8}}(b_{\mathtt{8}p} + b^\dagger_{\mathtt{8}p}). \end{aligned}$$

It is immediately clear that by discrete parity symmetry the Hamiltonian is invariant under $\lambda_{\mathtt{2}} \to -\lambda_{\mathtt{2}}$ and $\lambda_{\mathtt{5}} \to -\lambda_{\mathtt{5}}$, meaning the expectation values $\langle\lambda_{\mathtt{2}}\rangle = \langle\lambda_{\mathtt{5}}\rangle = 0$. The main problem for finding the density matrix (4.46) for this system is thus that the matrices $\lambda_{\mathtt{6}}$ and $\lambda_{\mathtt{7}}$ come weighted by trigonometric factors. To deal with this, let us define another pair of matrices $\lambda'_{\mathtt{6}}$ and $\lambda'_{\mathtt{7}}$, which remain orthogonal to the standard Gell-Mann matrices:

$$\begin{aligned} \lambda'_{\mathtt{6}} &= \cos\zeta\lambda_{\mathtt{6}} + \sin\zeta\lambda_{\mathtt{7}} = \begin{pmatrix} 0 & 0 & 0 \\ 0 & 0 & e^{-i\zeta} \\ 0 & e^{i\zeta} & 0 \end{pmatrix}, \\ \lambda'_{\mathtt{7}} &= -\sin\zeta\lambda_{\mathtt{6}} + \cos\zeta\lambda_{\mathtt{7}} = \begin{pmatrix} 0 & 0 & 0 \\ 0 & 0 & -ie^{-i\zeta} \\ 0 & ie^{i\zeta} & 0 \end{pmatrix}. \end{aligned} \tag{4.47}$$

It is straightforward to show that the combination $\langle\lambda_{\mathtt{6}}\rangle\,\lambda_{\mathtt{6}} + \langle\lambda_{\mathtt{7}}\rangle\,\lambda_{\mathtt{7}}$ that is required as a component of the density matrix (4.46) is identical to the combination $\langle\lambda'_{\mathtt{6}}\rangle\,\lambda'_{\mathtt{6}} + \langle\lambda'_{\mathtt{7}}\rangle\,\lambda'_{\mathtt{7}}$. However, since the Hamiltonian (3.63) contains only $\lambda'_{\mathtt{6}}$ and not $\lambda'_{\mathtt{7}}$, we can argue by the same token as for $\lambda_{\mathtt{2}}$ and $\lambda_{\mathtt{5}}$ that the Hamiltonian is invariant under $\lambda'_{\mathtt{7}} \to -\lambda'_{\mathtt{7}}$, meaning we can set $\langle\lambda'_{\mathtt{7}}\rangle = 0$. This leaves the following terms in the density matrix:

$$\rho = s\boldsymbol{I} + \langle\lambda_{\mathtt{1}}\rangle\lambda_{\mathtt{1}} + \langle\lambda_{\mathtt{3}}\rangle\lambda_{\mathtt{3}} + \langle\lambda_{\mathtt{4}}\rangle\lambda_{\mathtt{4}} + \langle\lambda'_{\mathtt{6}}\rangle\lambda'_{\mathtt{6}} + \langle\lambda_{\mathtt{8}}\rangle\lambda_{\mathtt{8}}. \tag{4.48}$$

In order to find an explicit and exactly calculable expression for (4.48) we use the Feynman-Hellmann Theorem (4.44) to find the required component expectation values. By differentiating (3.63) with respect to Δ, ϵ_3 and ϵ_8 respectively we obtain the following expectation values immediately:

$$\begin{aligned}\frac{\partial E}{\partial \Delta} &= \langle(\lambda_1 + \lambda_4 + \cos\zeta\lambda_6 + \sin\zeta\lambda_7)\rangle \\ \frac{\partial E}{\partial \epsilon_3} &= \langle\lambda_3\rangle \\ \frac{\partial E}{\partial \epsilon_8} &= \langle\lambda_8\rangle\,. \end{aligned} \tag{4.49}$$

Observe that the expectation value of the sum of operators in the first term is linear and may therefore be separated to give:

$$\begin{aligned}\frac{\partial E}{\partial \Delta} &= \langle\lambda_1\rangle + \langle\lambda_4\rangle + \cos\zeta\,\langle\lambda_6\rangle + \sin\zeta\,\langle\lambda_7\rangle\,, &(4.50)\\ &= \langle\lambda_1\rangle + \langle\lambda_4\rangle + \langle\lambda_6'\rangle\,. &(4.51)\end{aligned}$$

We can further simplify the expression (4.48) for the density matrix of this system by noting that the Gell-Mann matrices λ_1, λ_4 and λ_6' satisfy the following symmetry. For the operator U and inverse

$$U = \begin{pmatrix} 0 & 0 & 1 \\ 1 & 0 & 0 \\ 0 & 1 & 0 \end{pmatrix}, \quad U^{-1} = \begin{pmatrix} 0 & 1 & 0 \\ 0 & 0 & 1 \\ 1 & 0 & 0 \end{pmatrix}, \tag{4.52}$$

we have

$$U\lambda_1 U^{-1} = \lambda_6, \quad U\lambda_6 U^{-1} = \lambda_4, \quad U\lambda_4 U^{-1} = \lambda_1. \tag{4.53}$$

Consider now the matrix $R(\zeta)$ and its inverse:

$$R(\zeta) = \begin{pmatrix} 1 & 0 & 0 \\ 0 & 1 & 0 \\ 0 & 0 & e^{i\zeta} \end{pmatrix}, \quad R^{-1}(\zeta) = \begin{pmatrix} 1 & 0 & 0 \\ 0 & 1 & 0 \\ 0 & 0 & e^{-i\zeta} \end{pmatrix}. \tag{4.54}$$

Using the operators U and $R(\zeta)$ in combination shows that we can transform matrices $\lambda_1 \to \lambda_6' \to \lambda_4 \to \lambda_1$:

$$R(\zeta)U\lambda_1 U^{-1}R^{-1}(\zeta){=}\lambda_6', \;\; R(\zeta)U\lambda_6' U^{-1}R^{-1}(\zeta){=}\lambda_4, \;\; R(\zeta)U\lambda_4 U^{-1}R^{-1}(\zeta){=}\lambda_1.$$

This means that we can effectively write (4.51) as

$$\frac{\partial E}{\partial \Delta} = 3\,\langle\lambda_1\rangle \equiv 3\,\langle\lambda_4\rangle \equiv 3\,\langle\lambda_6'\rangle\,. \tag{4.55}$$

With these simplifications the density matrix (4.48) can now be written in terms of precise values, which we know may be calculated exactly by the Bethe Ansatz:

$$\begin{aligned}\rho &= \frac{1}{3}\boldsymbol{I} + \langle\lambda_1\rangle\lambda_1 + \langle\lambda_3\rangle\lambda_3 + \langle\lambda_1\rangle\lambda_4 + \langle\lambda_1\rangle\lambda_6' + \langle\lambda_8\rangle\lambda_8 \\ &= \frac{1}{3}\boldsymbol{I} + \frac{1}{3}\frac{\partial E}{\partial\Delta}(\lambda_1 + \lambda_4 + \lambda_6') + \frac{\partial E}{\partial\epsilon_3}\lambda_3 + \frac{\partial E}{\partial\epsilon_8}\lambda_8 \\ &= \frac{1}{3}\boldsymbol{I} + \begin{pmatrix} b + \frac{c}{\sqrt{3}} & a & a \\ a & -b + \frac{c}{\sqrt{3}} & ae^{-i\zeta} \\ a & ae^{i\zeta} & \frac{-2c}{\sqrt{3}} \end{pmatrix} \\ &= \frac{1}{3}\boldsymbol{I} + \widetilde{\rho}, \end{aligned} \tag{4.56}$$

where we have used the shorthand notation

$$a = \frac{1}{3}\frac{\partial E}{\partial\Delta},\ \ b = \frac{\partial E}{\partial\epsilon_3}\ \text{ and }\ c = \frac{\partial E}{\partial\epsilon_8}. \tag{4.57}$$

Note also that for this 3×3 system we have $\mathrm{Tr}(\rho) = 3\mathrm{s}$ and so to normalise $\mathrm{Tr}(\rho) = 1$ we have set $s = \frac{1}{3}$.

In finding the exact values of the entropy using the derivatives that make up the components of the density matrix, it is important to remember that ζ is not a free parameter, but in fact sets the limit within which the model is exactly solvable via the relation (3.72):

$$\cot^2(\zeta) = \frac{\sin^2 J_\parallel}{\sin(J_\perp + J_\parallel)\sin(J_\perp - J_\parallel)}. \tag{4.58}$$

In Section 3.4 we found the relationship between the coupling parameters $J_\parallel, J_\perp$ and the calculable components Δ, C_{p3} and C_{p8} of the three-level dissipative system.

We have now found the density matrix for the three-level dissipative system Hamiltonian (3.63). In the following subsection we will find the nature of the roots of this matrix and outline the method for finding the corresponding entropy, which provides an in-principle exact upper bound on the inequality (4.7), the violation of which indicates entanglement. We will conclude the chapter with some observations and suggestions for further work.

4.3.2 Nature of the roots and entropy measure

In order to find the entropy measure for use in the entanglement criterion (4.7), we find the roots of the density matrix (4.56) of the three-level Hamiltonian (3.63). We may find the nature of the roots of this density matrix by considering the characteristic polynomial corresponding to $\widetilde{\rho}$ from (4.56), for ease of calculation. The characteristic equation for $\widetilde{\rho}$ with eigenvalues x is the following cubic function:

$$x^3 - (3a^2 + b^2 + c^2)x - \left(\frac{2b^2c}{\sqrt{3}} - \frac{2c^3}{3\sqrt{3}} + 2a^3\cos(\zeta)\right) = 0, \tag{4.59}$$

where a, b and c are given by (4.57). Notice in particular that the diagonal elements in $\widetilde{\rho}$ sum to zero, meaning there are no quadratic terms in x in (4.59). We can find the nature of the roots of (4.59) by differentiating, which gives

$$3x^2 - 3a^2 - b^2 - c^2 = 0, \tag{4.60}$$

and corresponding discriminant

$$36a^2 + 12b^2 + 12c^2. \tag{4.61}$$

Since the Hamiltonian (3.63) is hermitian, we must have real parameters a, b, c, and consequently we can see that the discriminant (4.61) of the derivative of the characteristic equation (4.59) must always be strictly positive. This confirms that $\widetilde{\rho}$ from (4.56) must always have three real roots. Moreover, since we know that the density matrix (4.56) must be positive we can say that the three roots must always be greater than or equal to zero.

The characteristic equation (4.59) has the generic form

$$x^3 - \mathfrak{a}x - \mathfrak{b} = 0. \tag{4.62}$$

Cardano's method [36, 37] provides a straightforward method for solving such cubic functions, yielding roots:

$$x = u + \frac{\mathfrak{a}}{3u}, \tag{4.63}$$

where

$$u = \sqrt[3]{-\frac{\mathfrak{b}}{2} \pm \sqrt{\frac{\mathfrak{b}^2}{4} + \frac{\mathfrak{a}^3}{27}}}. \tag{4.64}$$

In the current case there are three distinct real roots x_1, x_2, x_3, which can be found by considering the three cube roots in u, i.e. the primary root, and the primary root multiplied by the factors $(-\frac{1}{2} \pm \frac{\sqrt{3}i}{2}) = -e^{\pm\frac{i\pi}{3}}$.

Explicit calculation for zero bias

If we consider the case of zero bias ($\epsilon_3 = \epsilon_8 = 0$), the characteristic equation (4.59) becomes

$$x^3 - 3a^2x - 2a^3\cos(\zeta) = 0, \tag{4.65}$$

which we know from (4.63) and (4.64) will have roots

$$x = u + \frac{a^2}{u}, \tag{4.66}$$

with

$$\begin{aligned} u &= \sqrt[3]{a^3\cos(\zeta) \pm \sqrt{a^6\cos^2(\zeta) - a^6}} \\ &= ae^{\pm\frac{i\zeta}{3}}. \end{aligned} \tag{4.67}$$

Explicitly, the three distinct real roots x_1, x_2, x_3 are found by considering the three cube roots in u, from the primary root (4.67) and the primary root multiplied by the factors $-e^{\pm\frac{i\pi}{3}}$:

$$\begin{aligned} u_1 &= ae^{\pm\frac{i\zeta}{3}}, \\ u_2 &= -ae^{\pm\frac{i(\zeta+\pi)}{3}}, \\ u_3 &= -ae^{\pm\frac{i(\zeta-\pi)}{3}}. \end{aligned} \tag{4.68}$$

Combining (4.68) with (4.66) gives the final solutions for the eigenvalues x:

$$\begin{aligned} x_1 &= a\left(e^{\frac{i\zeta}{3}} + e^{-\frac{i\zeta}{3}}\right) &&= 2a\cos\left(\tfrac{\zeta}{3}\right), \\ x_2 &= -a\left(e^{\frac{i(\zeta+\pi)}{3}} + e^{-\frac{i(\zeta+\pi)}{3}}\right) &&= -2a\cos\left(\tfrac{(\zeta+\pi)}{3}\right), \\ x_3 &= -a\left(e^{\frac{i(\zeta-\pi)}{3}} + e^{-\frac{i(\zeta-\pi)}{3}}\right) &&= -2a\cos\left(\tfrac{(\zeta-\pi)}{3}\right). \end{aligned} \tag{4.69}$$

Since the matrix ρ in (4.56) differs from $\widetilde{\rho}$ by a third times the identity matrix, it is clear that the eigenvalues r_1, r_2, r_3 of ρ are given by the three real, positive eigenvalues x_1, x_2, x_3 of $\widetilde{\rho}$:

$$r_1 = \tfrac{1}{3} + 2a\cos\left(\tfrac{\zeta}{3}\right), \;\; r_2 = \tfrac{1}{3} - 2a\cos\left(\tfrac{(\zeta+\pi)}{3}\right), \;\; r_3 = \tfrac{1}{3} - 2a\cos\left(\tfrac{(\zeta-\pi)}{3}\right). \tag{4.70}$$

From this one can deduce the Rényi entropy from (4.1):

$$S_R(\rho) = \frac{1}{1-\delta}\ln\left(r_1^\delta + r_2^\delta + r_3^\delta\right), \tag{4.71a}$$

$$\begin{aligned} = \frac{1}{1-\delta}\ln\Bigg(&\left(\tfrac{1}{3} + 2a\cos\left(\tfrac{\zeta}{3}\right)\right)^\delta + \left(\tfrac{1}{3} - 2a\cos\left(\tfrac{(\zeta+\pi)}{3}\right)\right)^\delta \\ &+ \left(\tfrac{1}{3} - 2a\cos\left(\tfrac{(\zeta-\pi)}{3}\right)\right)^\delta\Bigg), \end{aligned} \tag{4.71b}$$

and the corresponding von Neumann entropy from (4.2):

$$\begin{aligned} S_{vN}(\rho) &= -\mathrm{Tr}(\rho \ln \rho) \\ &= -(r_1 \ln r_1 + r_2 \ln r_2 + r_3 \ln r_3) \qquad (4.72a) \\ &= \left(\tfrac{1}{3} + 2a\cos\left(\tfrac{\zeta}{3}\right)\right) \ln \left(\tfrac{1}{3} + 2a\cos\left(\tfrac{\zeta}{3}\right)\right) \\ &\quad + \left(\tfrac{1}{3} - 2a\cos\left(\tfrac{(\zeta+\pi)}{3}\right)\right) \ln \left(\tfrac{1}{3} - 2a\cos\left(\tfrac{(\zeta+\pi)}{3}\right)\right) \\ &\quad + \left(\tfrac{1}{3} - 2a\cos\left(\tfrac{(\zeta-\pi)}{3}\right)\right) \ln \left(\tfrac{1}{3} - 2a\cos\left(\tfrac{(\zeta-\pi)}{3}\right)\right). \qquad (4.72b) \end{aligned}$$

The Rényi entropy (4.71b) provides the upper bound for the criterion on entanglement by (4.7) in the case of zero bias, where a violation of the inequality for any $\delta > 1$ indicates entanglement, and similarly the von Neumann entropy (4.72b) provides the upper bound for the case $\delta = 1$. For the general case of characteristic equation (4.59), the expressions (4.71a) and (4.72a) give a direct, and in principle exactly calculable, upper bound for the criterion for entanglement in the three-level dissipative system from Chapter 3.

4.4 Discussion

In Chapter 3 we developed a new exactly solvable three-level dissipative system by bosonisation of an Anisotropic Coqblin-Schrieffer (ACS) model. The development followed the analogous case of the bosonisation of the spin-$\frac{1}{2}$ anisotropic Kondo model, and we were investigating this family of exactly solvable models to expose the details of the interaction between a quantum and a classical system. In the current chapter we have broadened the analysis of this quantum-classical interaction by extending two existing methods for calculating measures of entanglement in bipartite system-environment models to the three-level case. In the first instance we generalised a method relying on a variational approximation to the ground state of the model in Section 4.2, and in Section 4.3 we demonstrated the in-principle exact calculation of entanglement measures using the Feynman-Hellmann method. Both methods are experimentally accessible, and both have previously been used to study entanglement in the bipartite case.

The development of the variational approach in Section 4.2 found the 9×9 reduced density matrix of the system and found all of its non-zero elements

explicitly by utilising the anticommutation relations of the fermionic operators involved, and the possibility of pairing with operators from the Fermi sea. From the reduced density matrix we found a closed form for its trace to a general power for use in the Rényi entropy in Subsection 4.2.2. An expression for the von Neumann entropy was also calculated, as this is often quoted as an entanglement measure in the literature, and gives the entanglement criterion for the case $\delta = 1$. Using the pure state density matrix for the entire bath and impurity system to provide the upper bound for the entropic inequality (where a violation of the inequality demonstrates entanglement), the criterion for entanglement between this whole composite system and the system of a single bath fermion plus the impurity was presented. Furthermore, the criterion for entanglement between the single impurity and a single bath fermion was presented, where the entropy for the reduced density matrix of the impurity alone provides the upper bound of the inequality. Numerical results for these entropy criteria may be calculated experimentally with estimates for the variational parameters.

The variational approach to entanglement is by its nature a numerical approximation. It was shown in Chapter 3 that the ACS model was exactly solvable, and to make use of this we found analytic expressions in Section 4.3 from which the density matrix could be calculated exactly. The Feynman-Hellmann theorem was used to find the density matrix of the three-level dissipative system Hamiltonian in terms of derivatives of the ground state energy, which is in principle exactly calculable from the Bethe Ansatz. Clear expressions for the density matrix and its components were given, and we demonstrated the entropy calculations explicitly for the case of zero bias. These entropy measures can again serve as the upper bound on the entanglement criterion. As mentioned in the introduction to this chapter, entropy measures can be used to give a measure of the degree of entanglement, which is an exciting prospect for further work on this model, promising more insight into the relationship between the system and its environment.

We have argued that the Rényi entropy is adequate as a *criterion* for entanglement. In consideration of the above suggestion to extend the work of this chapter to discuss entanglement *measures*, it is of course important to establish conclusively the validity of the Rényi and von Neumann entropies

for this purpose. This would require a detailed examination of their handling of the structure of entangled states. The non-locality suggested by a violation of the CHSH inequalities might, for example, indicate that some non-additive entropic measure such as the Tsallis entropy [126] is a better choice of measure.

There are a number of other possible further extensions to the methods and models discussed in this chapter. In Section 4.2 we used an extension of the two-level singlet state with variational parameters as the approximation to the ground state of the three-level system. Alternative representations of low-lying states include the symmetric (sextet) analogue of the antisymmetric triplet which we have studied, and an anonymous reviewer has suggested that using a hole wavefunction

$$|\Psi\rangle = \sum_{\alpha,k} \Gamma_k c_{k,\alpha} \chi_\alpha^\dagger |F\rangle, \tag{4.73}$$

which is an $SU(3)$ singlet, might have lower energy and thus be a better approximation to the ground state. In further work it would thus be informative to find the entropy and entanglement measures relating to these alternative starting points. Furthermore, the careful exposition of the details of calculating the non-zero elements of the reduced density matrices can also be adapted easily to alternative system-environment Hamiltonians, and include multiple impurities, for example. Similarly, the Feynman-Hellmann method for deducing the exactly calculable elements of the density matrix as described in Section 4.3 can be extended to other exactly-solvable system-environment Hamiltonians.

Chapter 5

Conclusion

This thesis in theoretical physics has investigated quantum entanglement with specific examples of the relationship between quantum and classical systems in order to help clarify the transition from quantum to classical theory. We motivated this investigation in the Introduction by highlighting the lack of consistent fundamental theory as demonstrated by the EPR paradox. Experimental confirmation of the entanglement phenomenon confirms the tension between the uncertainty principle and special relativity, compounding the need to re-assess the approach to the quantum-classical boundary, which this thesis begins to address.

5.1 Chapter summary

We began, in Chapter 2, by outlining the construction of experimentally verifiable tests of the EPR paradox. We demonstrated how the exact, mathematical transcription of the paradox could be given a regularisation to facilitate comparison with current experimentally accessible states from quantum optics. We showed that current tests using bipartite NOPA-states approach the same EPR limit as the exact transcription, with the same maximum level of locality violation as measured by the CHSH inequalities through their Wigner function transcription. Furthermore, we proposed a regularised mathematical transcription of the EPR paradox extended to tripartite continuous variable states (η-states). We demonstrated carefully the structure of these states and again compared them with their GHZ NOPA-type quantum optics counterpart. In

this case, we showed that the GHZ NOPA-type and regularised η-states have significant differences in their structure, and their mathematical transcriptions do not approach equivalence. Whereas the GHZ NOPA-type states approach maximal inequality violation for a single value of the regularisation parameter (corresponding to infinite squeezing), the regularised η-states exhibit two regions of violation. This opens the question as to whether there are alternative experimental ways to approach CHSH and locality violation.

The locality violation demonstrated in Chapter 2 highlighted the curious classical interpretation of the effects of a quantum phenomenon. In contrast, we considered the effects of classical phenomena on quantum descriptions in Chapter 3. This included a discussion of the examples of the Spin-Boson and Kondo models in which a quantum impurity interacts with an environment or bath. The exposition followed the explicit mathematical development of the models in order to reveal the details of this interaction. We demonstrated the well-known equivalence of the Spin-Boson and spin-$\frac{1}{2}$ XXZ-type anisotropic Kondo model for the special case of ohmic coupling, and used this established method of relating a fermion gas-impurity model to its dissipative system counterpart to investigate an extension of the equivalence to other exactly solvable models. The careful re-examination of the link between these models used the methods of constructive bosonisation and unitary transformation, with emphasis on the role of the Klein factors and coupling coefficients in the interpretation of the structure of the model. The details revealed a previously unreported observation regarding the fully anisotropic XYZ-type Kondo model, which we showed corresponds to an exactly solvable, extended two-level system with the upper and lower levels having infinite degeneracy.

The analysis of fermion gas-impurity models continued in Chapter 3 by showing that an extension of the methods to exactly solvable three-level quantum dissipative systems (3LQDS) was possible. This was demonstrated in detail starting from an Anisotropic Coqblin-Schrieffer model, using the methods of bosonisation and unitary transformation. As in the XYZ-type case, particular attention was given to the role of the Klein factors, and the coupling parameters. The model was shown to be exactly solvable by demonstrating that the scattering matrix of the model could be reparametrised in terms of the trigonometric R-matrix for the A_2^1 series which obeys the Yang-Baxter

equation.

In Chapter 4 we found expressions for the criterion for entanglement in the three-level dissipative system discussed in Chapter 3. We demonstrated the construction of a reduced density matrix from a proposed ground state wavefunction, using a variational Ansatz as an example. Recognising that an exact solution to the 3LQDS model is in principle calculable by the Bethe Ansatz we found the exact joint system density matrix directly from the model Hamiltonian via the Feynman-Hellmann Theorem. In both instances we extended the explicit procedure for the methods involved from the known two-level case to the three-level model in a way that may be extended further easily to a range of other systems of interest. In each case we gave entropy measures for these density matrices to provide a criterion for entanglement in the model, and laid the foundations for developing entanglement measures in the three-level model.

5.2 Discussion and further work

This thesis has examined and extended in intricate detail some well-known models from theoretical physics, to help bring some further information to the debate regarding the quantum-classical transition. Throughout the developments we have been careful to include frequent indicators of the experimental accessibility of results, in recognition of the importance that such corroboration has for scientific advancement. The discussion sections of each chapter provide several suggestions for practical applications and further work, some of which we will summarise here and provide some further comment.

The emergence of differences between the tripartite EPR-type η-states and the GHZ NOPA-type states in Chapter 2 suggests the possibility that these may translate into experimental differences. The theory that led to the development of the tripartite η-states may be extended with relative ease to include a whole family of such potentially interesting states. Firstly, note that the presentation discussed the canonically conjugate pair of difference in position and total momentum. A parallel exposition may easily be presented for the alternative starting point of difference in momentum and total position, along with

the tripartite counterpart to this example. Moreover, the η-state regularisation parameters can be exchanged for any other regularisation parameter that preserves the state symmetry, and can include cases where the regularisation weighting of each mode is considered independently (i.e. three regularisation parameters for the tripartite state). In Subsection 2.3.2 we examined a few clear choices for phase space parameters to extremise the CHSH inequalities using the η-states, but a fuller investigation could document the behaviour of these inequalities for the entire parameter space. A similar analysis can also be conducted with the N-partite state generalisation.

We have chosen to present in this thesis the CHSH violation of the Gaussian limit $\eta = 0$ for the EPR-type states, as this is required for current experimental protocols. However, it may well be of theoretical interest to examine the full non-Gaussian expressions in more detail, and they may in the future provide some experimentally accessible information. To further develop the practical applicability of the current results it will be instructive to formalise the relationship between the Bell-operator notation for the CHSH inequalities and the variance calculations used in quantum optics, as well as the experimental interpretation of the new regularisation parameters and their limits.

In the thesis we used the EPR example with CHSH inequality violation to highlight the inconsistency in current fundamental theory. In terms of the interpretation of this inequality violation, we mentioned in the Introduction that it is regarded as a violation of locality, and that there is some controversy over what this means in practical terms, with the distinction between locality and causality. The EPR experiment, which gives rise to correlations repeatedly confirmed by experiment, is simply a mathematical consequence of entangled states, and in itself offers no explanation of its relationship to classical environments or special relativity. Nevertheless the example is clear in its confirmation of a paradox in fundamental physical theory by juxtaposing the clear understanding of the mathematical structure of entangled states and the strange consequences for classical interpretation – that locality can be violated.

Having seen the effect of quantum structures on classical interpretation, we continued the investigation into the quantum-classical relationship by studying the effects of a classical environment interacting with a quantum system in

Chapters 3 and 4. In the process we demonstrated the utility of the constructive bosonisation method for relating fermion gas-impurity models to their quantum dissipative system counterpart, and exposed the intricacies of the technique. It is worth noting that while we applied the bosonisation procedure to Hamiltonians in this thesis the method applies equally well to the bosonisation of states, and it may be informative to bosonise the fermionic bath from the Kondo model, for example.

The re-analysis of the well-known XYZ-type model in Subsection 3.3.2 using the detailed bosonisation procedure showed the model corresponds to an exactly solvable, extended two-level system with the upper and lower levels having infinite degeneracy. This may facilitate new developments for quantum random walks, where each step of the walk is interpreted as a jump to a neighbouring site on the lattice. Bethe Ansatz methods may provide new analytic insight into the walker behaviour, and further investigations may reveal the details of the influence of the oscillator bath on the walker performance.

The analysis of an Anisotropic Coqblin-Schrieffer model in Section 3.4 led to a new exactly solvable three-level dissipative system. It might be possible to map the bosonised ACS model to other dissipative systems through alternative standard R-matrices. Since the ACS Hamiltonian is only one of many possible Fermi-gas starting points for the bosonisation procedure, it could be expected that the same method might reveal more exactly solvable dissipative systems. The range of applications and importance of such models in condensed matter theory makes this an exciting prospect indeed. The theory for the three-level system discussed herein applies to any triatomic triple well potential, such as ammonia, the methyl $-CH_3$ and Bose-Einstein condensate atomic transistors, to mention only a few. Due to the many applications of models similar to the bosonised ACS model, there are a wealth of different approaches to their analysis in the literature. The ACS model deserves a rigorous contextualisation within this greater body of research, but this is beyond the scope of this thesis. A review of the models and the relationship between their mathematical descriptions would require a detailed analysis, but the yield in terms of interpretational clarity may well make the task worthwhile.

It was demonstrated in Subsection 3.4.1 that the ACS model is exactly solvable. The consequence is that one of the most important extensions to the

work on the ACS model is finding its exact solution by the Bethe Ansatz. Not only does this enable the calculation of a range of useful dynamical and thermodynamical quantities such as magnetic susceptibility and specific heat, but also the exact values of entropy calculations through the derivatives of the energy eigenvalues as indicated in Chapter 4. For the cases where an exact solution is not known, we showed in Section 4.2 that useful entropy measures may be found nevertheless, using a variational approach. We gave clear procedures for calculating these, and calculations of the reduced density matrices showed a more subtle dependency on the particular states of the impurity and bath than was apparent in the spin-$\frac{1}{2}$ Kondo case. Explicit numerical evaluation of the entropy measures can be done by finding the values of the variational parameters involved. Moreover, the investigation can be extended by considering alternative possible ground states for the model and finding the corresponding entropy measures. A most interesting extension for both the variational and Feynman-Hellmann approaches is the calculation of entanglement measures, rather than simply entanglement criteria from the entropy. However, as mentioned in Section 4.4, the validity of any particular entropy measure for dealing with the structure of entangled states should also be considered in more detail.

So far we have mentioned a range of generalisations and suggestions for further work for each of the investigations covered in this thesis. The overarching topic of this thesis – the quantum-classical transition – is of course so wide that we could never hope to touch on every facet in one thesis. We have only very lightly introduced the concept of decoherence, and discussed its relationship to dissipation, but it is clear that a fuller investigation of its relationship with all the parameters in the models is of crucial importance to the topic. In that regard, one might also want to consider the relationship between all four of the canonical system-environment models used to discuss dissipation and decoherence. The four include spin-boson and spin-spin models as discussed herein, as well as boson-boson models (quantum Brownian motion) and boson-spin models [111]. Much work has been done in formalising the relationship between the Spin-Boson and Kondo models, but the details of this fuller canonical set of models may contain further insights.

The emphasis of this thesis has been on exposing explicit details of simple mod-

els relating to the quantum-classical interface. The investigation has revealed new insights and the development of new models, and we have suggested several possibilities for practical applications. Particular focus has been on highlighting the tension between quantum and classical theory and establishing the structure of entangled states, using quantum system-environment models to reveal details of their interaction, and providing a means for investigating their entanglement relationship. The further work suggested in this chapter – in particular solving the Bethe Ansatz for the ACS model, finding explicit and exact values for the entanglement criteria, and extending the investigation to precise entanglement measures – shows great promise for further developing the examination of the quantum-classical transition. As such the work presented herein provides a firm foundation for the re-examination of this relationship more generally.

Appendix A

Additional notes and working to Chapter 2

A.1 Normalisation of bipartite $|\eta\rangle_s$

The regularised bipartite EPR-state transcription is given by (2.8):

$$|\eta\rangle_s \;:=\; N_2\, e^{-\frac{1}{2s^2}|\eta|^2+\frac{1}{s}\eta a^\dagger-\frac{1}{s}\eta^* b^\dagger+\frac{1}{s^2}a^\dagger b^\dagger}|00\rangle.$$

In order to normalise we first find

$${}_s\langle\eta'|\eta\rangle_s \;=\; \langle 00|N_2 e^{-\frac{1}{2s^2}|\eta'|^2+\frac{1}{s}\eta'^* a-\frac{1}{s}\eta' b+\frac{1}{s^2}ab}\cdot N_2 e^{-\frac{1}{2s^2}|\eta|^2+\frac{1}{s}\eta a^\dagger-\frac{1}{s}\eta^* b^\dagger+\frac{1}{s^2}a^\dagger b^\dagger}|00\rangle.$$

We inset a complete set of coherent states (2.42) to get:

$$\begin{aligned}
{}_s\langle\eta'|\eta\rangle_s \;&=\; \frac{N_2^2}{\pi}e^{-\frac{1}{2s^2}(|\eta'|^2-|\eta|^2)} \\
&\quad\cdot\iint\langle 00|e^{\frac{1}{s}\eta'^* a-\frac{1}{s}\eta' b+\frac{1}{s^2}ab}|w,z\rangle\langle w,z|e^{\frac{1}{s}\eta a^\dagger-\frac{1}{s}\eta^* b^\dagger+\frac{1}{s^2}a^\dagger b^\dagger}|00\rangle d^2w d^2z \\
&=\; \frac{N_2^2}{\pi}e^{-\frac{1}{2s^2}(|\eta'|^2-|\eta|^2)} \\
&\quad\cdot\iint e^{-(|w|^2+|z|^2)}e^{\frac{1}{s}\eta'^* w-\frac{1}{s}\eta' z+\frac{1}{s^2}wz}e^{\frac{1}{s}\eta w^*-\frac{1}{s}\eta^* z^*+\frac{1}{s^2}w^* z^*}d^2w d^2z.
\end{aligned}$$

We rearrange the exponentials in the integral to fit the form required for Berezin's formula (2.46) to get:

$$
\begin{aligned}
{}_s\langle\eta'|\eta\rangle_s = \frac{N_2^2}{\pi} e^{-\frac{1}{2s^2}(|\eta'|^2-|\eta|^2)} \iint \exp\Bigg[& -\frac{1}{2}(w,z,w^*,z^*) \begin{pmatrix} 0 & -\frac{1}{s^2} & 1 & 0 \\ -\frac{1}{s^2} & 0 & 0 & 1 \\ 1 & 0 & 0 & -\frac{1}{s^2} \\ 0 & 1 & -\frac{1}{s^2} & 0 \end{pmatrix} \begin{pmatrix} w \\ z \\ w^* \\ z^* \end{pmatrix} \\
& + \left(\frac{1}{s}\eta'^*, -\frac{1}{s}\eta', \frac{1}{s}\eta, -\frac{1}{s}\eta^* \right) \begin{pmatrix} w \\ z \\ w^* \\ z^* \end{pmatrix} \Bigg] d^2w d^2z.
\end{aligned}
$$

On using the formula (2.46) this becomes:

$$
\begin{aligned}
{}_s\langle\eta'|\eta\rangle_s &= N_2^2 e^{-\frac{1}{2s^2}(|\eta'|^2-|\eta|^2)} \left[\det \begin{pmatrix} 1 & 0 & 0 & -\frac{1}{s^2} \\ 0 & 1 & -\frac{1}{s^2} & 0 \\ 0 & -\frac{1}{s^2} & 1 & 0 \\ -\frac{1}{s^2} & 0 & 0 & 1 \end{pmatrix} \right]^{-1/2} \\
&\quad \times \exp\left[\frac{1}{2} \left(\frac{1}{s}\eta'^*, -\frac{1}{s}\eta', \frac{1}{s}\eta, -\frac{1}{s}\eta^* \right) \begin{pmatrix} 1 & 0 & 0 & -\frac{1}{s^2} \\ 0 & 1 & -\frac{1}{s^2} & 0 \\ 0 & -\frac{1}{s^2} & 1 & 0 \\ -\frac{1}{s^2} & 0 & 0 & 1 \end{pmatrix}^{-1} \begin{pmatrix} \frac{1}{s}\eta \\ -\frac{1}{s}\eta^* \\ \frac{1}{s}\eta'^* \\ -\frac{1}{s}\eta' \end{pmatrix} \right] \\
&= N_2^2 e^{-\frac{1}{2s^2}(|\eta'|^2-|\eta|^2)} \sqrt{\frac{s^8}{s^8-2s^4+1}} \\
&\quad \times \exp\left[\frac{s^2}{2(s^4-1)} \left(\frac{1}{s}\eta'^*, -\frac{1}{s}\eta', \frac{1}{s}\eta, -\frac{1}{s}\eta^* \right) \begin{pmatrix} s^2 & 0 & 0 & 1 \\ 0 & s^2 & 1 & 0 \\ 0 & 1 & s^2 & 0 \\ 1 & 0 & 0 & s^2 \end{pmatrix} \begin{pmatrix} \frac{1}{s}\eta \\ -\frac{1}{s}\eta^* \\ \frac{1}{s}\eta'^* \\ -\frac{1}{s}\eta' \end{pmatrix} \right] \\
&= \frac{N_2^2 s^4}{(s^4-1)} e^{-\frac{1}{2s^2}(|\eta'|^2-|\eta|^2)} \exp\left(\frac{s^2}{2(s^4-1)} \right. \\
&\quad \left. \times \left(\eta'^*\eta - \frac{1}{s^2}\eta'^*\eta' + \eta'\eta^* - \frac{1}{s^2}\eta'\eta'^* - \frac{1}{s^2}\eta\eta^* + \eta\eta'^* - \frac{1}{s^2}\eta^*\eta + \eta^*\eta' \right) \right).
\end{aligned}
$$

Setting $\eta' = \eta$ we find

$$
\begin{aligned}
{}_s\langle\eta|\eta\rangle_s &= \frac{N_2^2 s^4}{(s^4-1)} \exp\left(-\frac{1}{s^2}|\eta|^2 + \frac{s^2}{2(s^4-1)} \left(4|\eta|^2 \left(1 - \frac{1}{s^2} \right) \right) \right) \\
&= \frac{N_2^2 s^4}{(s^4-1)} \exp\left(|\eta|^2 \frac{(s^2-1)}{s^2(s^2+1)} \right),
\end{aligned}
$$

making the normalisation condition:

$$
\frac{N_2^2 s^4}{(s^4-1)} \exp\left(|\eta|^2 \frac{(s^2-1)}{s^2(s^2+1)} \right) = 1,
$$

with the result

$$|N_2| = \left| \frac{(s^4-1)^{1/2}}{s^2} \exp\left(-\frac{1}{2}|\eta|^2 \frac{(s^2-1)}{s^2(s^2+1)} \right) \right|. \tag{A.1}$$

A.2 Normalisation of tripartite $|\eta, \eta', \eta''\rangle_s$

The normalisation of the tripartite state (2.30) proceeds in the same way as the construction of (A.1), by inserting a complete set of coherent states (2.42) and integrating using Berezin's formula (2.46). In this case the relevant inverse matrix and determinant are the same as shown in-text for the tripartite Wigner function in (2.48) and (2.49) respectively. This leads to

$$\begin{aligned} {}_s\langle \eta, \eta'\eta'' | \eta, \eta', \eta'' \rangle_s &= \frac{N_3^2 s^6}{(s^4-1)\sqrt{s^4-4}} \exp\Bigg(\Bigg(s^4 - \frac{1}{2s^2} - 3 \Bigg) \left(|\eta|^2 + |\eta'|^2 + |\eta''|^2 \right) \\ &\quad + \left(\frac{s^4-2}{s^2} \right) \left(\eta^*\eta'^* + \eta^*\eta''^* + \eta''^*\eta'^* + \eta'\eta + \eta''\eta + \eta''\eta' \right) \\ &\quad + \eta'\eta^* + \eta''\eta^* + \eta\eta'^* + \eta''\eta'^* + \eta\eta''^* + \eta'\eta''^* \\ &\quad + \frac{1}{s^2} \left(\eta^2 + \eta'^2 + \eta''^2 + \eta^{*2} + \eta'^{*2} + \eta''^{*2} \right) \Bigg) \\ &= \frac{N_3^2 s^6}{(s^4-1)\sqrt{s^4-4}} \exp(F(\eta, \eta', \eta'')), \end{aligned} \tag{A.2}$$

from which we deduce

$$|N_3|^2 = \left| \frac{(s^4-1)\sqrt{s^4-4}}{s^6} e^{-F(\eta,\eta',\eta'')} \right|. \tag{A.3}$$

Appendix B

Additional notes and working to Chapter 3

B.1 Charge sector projection

This section of the appendix is a reproduction of the original appendix which appeared in J.Phys.A 43(25):255305 [78].

It was pointed out in the text that the bosonisation transcription was carried out to the neglect of various terms accumulating fermion-number (charge) dependent factors. For example the longitudinal couplings in the three-level model (3.57) certainly amount to a sum over not only the bosonic modes, which is of course one source of the dissipative coupling, but also contain an explicit number operator term. Similarly the standard expression for the bilinear fermion kinetic energy term (involving as it does a derivative of the fermion field, albeit evaluated at zero) is known to contain a term quadratic in the respective charge operators (in fact the coefficients can also differ for different fermionic boundary conditions, but we do not need this option for our basic derivation). Overall we assume that the residual fermion number terms amount to an additional contribution from these sources of

$$\mathtt{C}\sum_{\alpha}\widehat{N}_{\alpha}^{2}+\sum_{\alpha}\mathtt{C}_{\alpha}\widehat{N}_{\alpha}\equiv\mathtt{C}\big(\widehat{N}_{3}^{2}+\widehat{N}_{8}^{2}\big)+\big(\mathtt{C}_{3}\widehat{N}_{3}+\mathtt{C}_{8}\widehat{N}_{8}\big)+\big(\mathtt{C}\widehat{N}_{0}^{2}+\mathtt{C}_{0}\widehat{N}_{0}\big).$$

As mentioned already, total fermion charge is conserved, so for $\widehat{N}_0$ taken fixed at eigenvalue N_0 say, the last term is an additive constant. For the remaining

terms we turn to the relative conserved quantities $\widehat{N}_3 + S_3$, $\widehat{N}_8 + S_8$ and to the projections onto fixed eigenspaces with eigenvalues M_3, M_8, respectively. Introduce weight labels $|m, y\rangle$ for the basis of the three-dimensional representation of $SU(3)$ corresponding to the the impurity system states, where m, y are the eigenvalues of λ_3, λ_8 (so that $\frac{1}{2}m$, $\frac{1}{2}y$ are the correctly normalised eigenvalues of $\frac{1}{2}\lambda_3 = S_3$ and $\frac{1}{2}\lambda_8 = S_8$, or isospin and hypercharge, respectively). Imposing the projections, we see that for the total states $|m, y; \psi\rangle$, the fermionic part $|\psi\rangle$ must have charges $N_3 = M_3 - \frac{1}{2}m$, $N_8 = M_8 - \frac{1}{2}y$ and the charge dependent piece becomes on these states

$$\begin{aligned} \mathtt{C}\big(M_3^2 + M_8^2\big) + \tfrac{1}{4}(m^2 + y^2) + \big(\mathtt{C}_3 M_3 + \mathtt{C}_8 M_8\big) \\ - \big(\mathtt{C}M_3 + \tfrac{1}{2}\mathtt{C}_3\big)m - \big(\mathtt{C}M_8 + \tfrac{1}{2}\mathtt{C}_8\big)y. \end{aligned} \tag{B.1}$$

Finally note that the weight basis of the three-dimensional fundamental representation is $|\pm 1, 1/\sqrt{3}\rangle$ and $|0, -2/\sqrt{3}\rangle$, so that by construction $(m^2 + y^2) \equiv \frac{4}{3}$ for all states. Thus the first line of the transcription is a further additive constant, while the second line amounts to an external 'magnetic' coupling and hence an adjustment to the detuning parameters ε_3, ε_8, by a shift of $-\big(\mathtt{C}M_3 + \frac{1}{2}\mathtt{C}_3\big)$, $-\big(\mathtt{C}M_8 + \frac{1}{2}\mathtt{C}_8\big)$, respectively.

B.2 Equivalence of SB Model and XXZ-type spin-$\frac{1}{2}$ Kondo model

B.2.1 Constructive bosonisation

Here we demonstrate the equivalence of equations (3.35) and (3.36), setting $\hbar = v_F = 1$ for convenience in this intermediate working. The emergent exponential damping term dependent on the regularisation parameter a is commonly ignored in the literature, as Leggett et al discuss in [95] that the free Hamiltonian may be left unrestricted when the cutoff is imposed on the

coupling terms. Starting with (3.36) we find:

$$\begin{aligned}
H_0^B &= \int_{-L/2}^{L/2} \frac{dx}{2\pi}\frac{1}{2} : (\partial_x \varphi_\alpha(x))^2 : \\
&= \int_{-L/2}^{L/2} \frac{dx}{2\pi}\frac{1}{2} : \left(\partial_x \left(-\sum_{p>0} \frac{1}{\sqrt{n_p}}(e^{ipx} b_{p\mu}^\dagger + e^{-ipx} b_{p\alpha}) e^{-ap/2}\right)\right)^2 : \\
&= \int_{-L/2}^{L/2} \frac{dx}{2\pi}\frac{1}{2} : \left(-\sum_{p>0} \frac{ip}{\sqrt{n_p}}(e^{ipx} b_{p\alpha}^\dagger - e^{-ipx} b_{p\alpha}) e^{-ap/2}\right)^2 : \\
&= \int_{-L/2}^{L/2} \frac{dx}{2\pi}\frac{1}{2} : \left(\sum_{n>0} \frac{2\pi i\sqrt{n}}{L}(e^{2\pi inx/2} b_{n\alpha}^\dagger - e^{-2\pi inx/2} b_{n\alpha}) e^{-a\pi n/L}\right) \\
&\quad \times \left(\sum_{n>0} \frac{2\pi i\sqrt{n}}{L}(e^{2\pi inx/2} b_{n\alpha}^\dagger - e^{-2\pi inx/2} b_{n\alpha}) e^{-a\pi n/L}\right) : \\
&= \frac{1}{4\pi}\left(\frac{2\pi i}{L}\right)^2 \sum_{m>0}\sum_{n>0} \sqrt{mn} \int_{-L/2}^{L/2} e^{-a\pi(m+n)/L} \\
&\quad \times : \left[e^{2\pi ix(m+n)/L} b_{n\alpha}^\dagger b_{m\alpha}^\dagger - e^{2\pi ix(m-n)/L} b_{n\alpha} b_{m\alpha}^\dagger \right. \\
&\qquad \left. - e^{2\pi ix(m-n)/L} b_{n\alpha}^\dagger b_{m\alpha} + e^{2\pi ix(m+n)/L} b_{n\alpha} b_{m\alpha}\right] : dx.
\end{aligned}$$

Note we dropped the q subscript on the n since it was superfluous in the calculation. Looking at the individual parts of the integral we see that:

$$\begin{aligned}
\int_{-L/2}^{L/2} e^{\frac{i2\pi x(m+n)}{L}} dx &= \frac{L}{2\pi i(m+n)}\left[e^{i\pi(m+n)} - e^{-i\pi(m+n)}\right] = 0, \quad m, n > 0. \\
\int_{-L/2}^{L/2} e^{\frac{i2\pi x(m-n)}{L}} dx &= 0, \quad \forall\ m \neq n \\
&= L, \quad if\ \ m = n.
\end{aligned}$$

Thus we have remaining terms for the case $m = n$ only, giving:

$$\begin{aligned}
H_0^B &= -\frac{\pi}{L^2}\sum_{n>0} n e^{\frac{2\pi an}{L}} : \left[-L b_{n\alpha} b_{n\alpha}^\dagger - L b_{n\alpha}^\dagger b_{n\alpha}\right] : \\
&= \frac{\pi}{L}\sum_{n>0} n e^{\frac{-2\pi an}{L}} : \left[2 b_{n\alpha}^\dagger b_{n\alpha}\right] : \\
&= \sum_{p>0} p b_{p\alpha}^\dagger b_{p\alpha} e^{-ap}. \qquad \text{(B.2)}
\end{aligned}$$

Here we used the fact that $bb^\dagger$ is $b^\dagger b$ in normal ordered form.

B.2.2 Unitary mapping

Here we provide further calculational details for the derivation of equations (3.41) and (3.42) in the main text. See also Appendix B.1 for comment on the fermion number dependent terms which are omitted here.

Unitary operation with operator $U = e^{i\sqrt{2}S^z\varphi_S(0)}$ on the free Hamiltonian H_0 from (3.37) produces

$$\begin{aligned}
UH_0U^\dagger &= H_0 + \left[i\sqrt{2}S_z\varphi_S(0), H_0\right] \\
&= H_0 + \frac{\sqrt{2}iv_F\hbar S_z}{4\pi}\left(\int_{-L/2}^{L/2}\left[\varphi_S(0), (\partial_x\varphi_S(x))^2\right]dx\right) \\
&= H_0 + \frac{\sqrt{2}iv_F\hbar S_z}{4\pi}\left(\int_{-L/2}^{L/2}(2\pi i\delta(0-x)\partial_x\varphi_S(x) + \partial_x\varphi_S(x)2\pi i\delta(0-x))\,dx\right) \\
&= H_0 + \frac{\sqrt{2}iv_F\hbar S_z}{4\pi}\left(4\pi i\partial_x\varphi_S(0)\right) \\
&= H_0 - \sqrt{2}v_F\hbar S_z\partial_x\varphi_S(0) \\
&= H_0 - 2iv_F\hbar S_z\sum_{p>0}\sqrt{\frac{\pi p}{L}}e^{-ap/2}\left(b_{pS} - b_{pS}^\dagger\right), \qquad \text{(B.3)}
\end{aligned}$$

where we have used the fact that charge/spin combinations commute and

$$\begin{aligned}
\left.\frac{\partial\varphi_S}{\partial x}\right|_{x=0} &= \frac{\partial}{\partial x}\frac{1}{\sqrt{2}}\left(\varphi_\uparrow(0) - \varphi_\downarrow(0)\right) \\
&= \frac{1}{\sqrt{2}}\sum_p n_p^{-1/2}ipe^{-ap/2}\left(b_{p\uparrow} - b_{p\uparrow}^\dagger - b_{p\downarrow} + b_{p\downarrow}^\dagger\right) \\
&= \sum_p\sqrt{\frac{2\pi p}{L}}ie^{-ap/2}(b_{pS} - b_{pS}^\dagger). \qquad \text{(B.4)}
\end{aligned}$$

The perpendicular term (3.38) requires the BCH rule and exponential expansion to remove the exponential factors. We have made use of the commutation relations

$$\begin{aligned}
[S_z, S_-] &= -S_- \\
[S_z, [S_z, S_-]] &= [S_z, -S_-] = S_-, \qquad \text{(B.5)}
\end{aligned}$$

in the exponential expansion showing unitary transformation of the spin op-

erators results in

$$\begin{aligned} US_{-}U^{\dagger} &= S_{-}\left(1 - i\sqrt{2}\varphi_S + \frac{1}{2}(i\sqrt{2}\varphi_S)^2 - \frac{1}{3}(i\sqrt{2}\varphi_S)^3 + \dots\right) = e^{-i\sqrt{2}\varphi_S(0)}S_{-} \\ US_{+}U^{\dagger} &= e^{i\sqrt{2}\varphi_S(0)}S_{+}. \end{aligned} \tag{B.6}$$

B.3 Gell-Mann matrix notation for Section 3.4

Gell-Mann matrices $\lambda_{\mathtt{A}}$ are one of the many possible representations of the special unitary group $SU(3)$, and are the 3×3 equivalent of the Pauli matrices (2.1) as used in the two-level cases outlined in Subsections 3.3.1 and 3.3.2 because they are traceless, hermitian and $Tr(\lambda_i\lambda_j) = 2\delta_{ij}$. The group has dimension 8 and the standard representation is:

$$\begin{aligned} \lambda_{\mathtt{1}} &= \begin{pmatrix} 0 & 1 & 0 \\ 1 & 0 & 0 \\ 0 & 0 & 0 \end{pmatrix}, \quad \lambda_{\mathtt{2}} = \begin{pmatrix} 0 & -i & 0 \\ i & 0 & 0 \\ 0 & 0 & 0 \end{pmatrix}, \quad \lambda_{\mathtt{2}} = \begin{pmatrix} 1 & 0 & 0 \\ 0 & -1 & 0 \\ 0 & 0 & 0 \end{pmatrix}, \\ \lambda_{\mathtt{4}} &= \begin{pmatrix} 0 & 0 & 1 \\ 0 & 0 & 0 \\ 1 & 0 & 0 \end{pmatrix}, \quad \lambda_{\mathtt{5}} = \begin{pmatrix} 0 & 0 & -i \\ 0 & 0 & 0 \\ i & 0 & 0 \end{pmatrix}, \quad \lambda_{\mathtt{6}} = \begin{pmatrix} 0 & 0 & 0 \\ 0 & 0 & 1 \\ 0 & 1 & 0 \end{pmatrix}, \\ \lambda_{\mathtt{7}} &= \begin{pmatrix} 0 & 0 & 0 \\ 0 & 0 & -i \\ 0 & i & 0 \end{pmatrix}, \ \lambda_{\mathtt{8}} = \frac{1}{\sqrt{3}}\begin{pmatrix} 1 & 0 & 0 \\ 0 & 1 & 0 \\ 0 & 0 & -2 \end{pmatrix}. \end{aligned} \tag{B.7}$$

Any 3×3 traceless matrix x, with elements $x_{\alpha\beta}$, can then be expressed in terms of orthogonal coordinates $x_{\mathtt{A}}$ via

$$x_{\alpha\beta} = \tfrac{1}{2}\sum_{\mathtt{A}=\mathtt{1}}^{\mathtt{8}} x_{\mathtt{A}}\big(\lambda_{\mathtt{A}}\big)_{\alpha\beta}, \qquad x_{\mathtt{A}} = \tfrac{1}{2}Tr(x\lambda_{\mathtt{A}}), \tag{B.8}$$

including of course the elementary matrices themselves. Quantities may also be manipulated using the completeness relation

$$\delta_{\alpha\beta}\delta_{\gamma\delta} = \tfrac{1}{3}\delta_{\gamma\beta}\delta_{\alpha\delta} + \tfrac{1}{2}\sum_{\mathtt{A}=\mathtt{1}}^{\mathtt{8}}\big(\lambda_{\mathtt{A}}\big)_{\gamma\beta}\big(\lambda_{\mathtt{A}}\big)_{\alpha\delta}. \tag{B.9}$$

The right hand side may be written uniformly over an extended set of λ-matrices $\lambda_{\mathtt{A}}$, $\mathtt{A} = \mathtt{0}, \mathtt{1}, \mathtt{2}, \cdots, \mathtt{8}$ by introducing $\lambda_{\mathtt{0}} = \sqrt{\frac{2}{3}}\,1_{3\times3}$ to stand in for the identity matrix.

Note now that an alternative form of (3.33) is

$$\begin{aligned} H_{AKM} \equiv & \sum_{p,\alpha} \hbar v_F p {:}c^\dagger_{p\alpha} c_{p\alpha}{:} + J_\parallel \sum_{p,\alpha,p',\alpha'} {:}c^\dagger_{p\alpha}(\sigma_z)_{\alpha\alpha'} c_{p'\alpha'}{:} S_z \\ & + \tfrac{1}{2} J_\perp \sum_{p,\alpha,p',\alpha'} \big(c^\dagger_{p\alpha}(\sigma_-)_{\alpha\alpha'} c_{p'\alpha'} S_+ + c^\dagger_{p\alpha}(\sigma_+)_{\alpha\alpha'} c_{p'\alpha'} S_- \big). \end{aligned} \quad \text{(B.10)}$$

In interpreting one-particle operators in second-quantised form, when considering 3 states $|\alpha\rangle := c^\dagger_\alpha |0\rangle$ associated with a fixed fermionic creation mode it is clear that

$$\langle \gamma | c^\dagger_\alpha c_\beta | \delta \rangle = \delta_{\delta\alpha}\delta_{\beta\gamma} \equiv (e_{\alpha\beta})_{\delta\gamma}, \quad \text{(B.11)}$$

– that is, that the combination $c^\dagger_\alpha c_\beta$ plays the role of elementary matrices on such labelled states. By extension, the Gell-Mann matrices play the role of the Pauli matrices in (B.10) for the three-level model in Section 3.4. A term in the particle-impurity interaction such as $\lambda_{\mathtt{A}} \otimes \lambda_{\mathtt{A}}$ may be written (omitting the $\otimes$):

$$\lambda_{\mathtt{A}} \otimes \lambda_{\mathtt{A}} \to \sum_{\alpha,\beta} \frac{1}{2} Tr(\lambda_{\mathtt{A}} e_{\alpha\beta}) c^\dagger_\alpha c_\beta \cdot \lambda_{\mathtt{A}} \equiv \frac{1}{2} \sum_{\alpha\beta} c^\dagger_\alpha (\lambda_{\mathtt{A}})_{\alpha\beta} c_\beta \cdot \lambda_{\mathtt{A}}. \quad \text{(B.12)}$$

B.3.1 Algebra of $S'_{\alpha\alpha}$, $S'_{\alpha\beta}$ operators

This appendix will confirm the algebraic structure of the operators defined in (3.62):

$$S'_{\alpha\beta} := -\mathcal{F}^\dagger_\beta \mathcal{F}_\alpha S_{\alpha\beta}, \quad S'_{\alpha\alpha} := \mathcal{F}^\dagger_\alpha \mathcal{F}_\alpha S_{\alpha\alpha} = S_{\alpha\alpha}.$$

In order to satisfy the usual closed $SU(N)$ algebraic structure, operators must obey the commutation relation:

$$[O_{ij}, O_{kl}] = \delta_{jk} O_{il} - \delta_{il} O_{kj}.$$

Since these are composite operators, we note the useful commutator identities for combinations of operators:

$$\begin{aligned} [AB, A'B'] &= AA'[B,B'] + [A,A']B'B \\ [A, BC] &= [A,B]C + B[A,C]. \end{aligned}$$

Explicit calculation of the following commutators will thus check whether the operators satisfy the $SU(3)$ algebra. Due to the symmetries of the commutation relations, these are the only combinations that require explicit calculation. It becomes clear immediately that the operators $S_{\alpha\beta}$ must be elementary matrices, so that we can also apply the condition $e_{ij}e_{kl} = \delta_{jk}e_{il}$.

$$\begin{aligned}
\left[S'_{\alpha\alpha}, S'_{\alpha\beta}\right] &= [S_{\alpha\alpha}, -\mathcal{F}^\dagger_\beta\mathcal{F}_\alpha]S_{\alpha\beta} - \mathcal{F}^\dagger_\beta\mathcal{F}_\alpha[S_{\alpha\alpha}, S_{\alpha\beta}], \\
&= -\mathcal{F}^\dagger_\beta\mathcal{F}_\alpha S_{\alpha\beta} = S'_{\alpha\beta}. \\
\left[S'_{\alpha\beta}, S'_{\beta\alpha}\right] &= \mathcal{F}^\dagger_\beta\mathcal{F}_\alpha\mathcal{F}^\dagger_\alpha\mathcal{F}_\beta[S_{\alpha\beta}, S_{\beta\alpha}] + [\mathcal{F}^\dagger_\beta\mathcal{F}_\alpha, \mathcal{F}^\dagger_\alpha\mathcal{F}_\beta]S_{\beta\alpha}S_{\alpha\beta}, \\
&= S_{\alpha\alpha} - S_{\beta\beta}. \\
\left[S'_{\alpha\beta}, S'_{\gamma\alpha}\right] &= \mathcal{F}^\dagger_\beta\mathcal{F}_\alpha\mathcal{F}^\dagger_\alpha\mathcal{F}_\gamma[S_{\alpha\beta}, S_{\gamma\alpha}] + [\mathcal{F}^\dagger_\beta\mathcal{F}_\alpha, \mathcal{F}^\dagger_\alpha\mathcal{F}_\gamma]S_{\gamma\alpha}S_{\alpha\beta}, \\
&= -\mathcal{F}^\dagger_\alpha\mathcal{F}_\gamma S_{\gamma\beta} = -S'_{\gamma\beta} \\
\left[S'_{\alpha\beta}, S'_{\gamma\beta}\right] &= \mathcal{F}^\dagger_\beta\mathcal{F}_\alpha\mathcal{F}^\dagger_\beta\mathcal{F}_\gamma[S_{\alpha\beta}, S_{\gamma\beta}] + [\mathcal{F}^\dagger_\beta\mathcal{F}_\alpha, \mathcal{F}^\dagger_\beta\mathcal{F}_\gamma]S_{\gamma\beta}S_{\alpha\beta} \\
&= 0. \qquad \text{(B.13)}
\end{aligned}$$

It is thus clear that, provided the $S_{\alpha\beta}$ are elementary matrices, the operators $S'_{\alpha\alpha}$ and $S'_{\alpha\beta}$ satisfy the $SU(3)$ algebra.

Appendix C

Appendix to Chapter 4

C.1 Explicit 9×9 subsystem density matrices for three-level dissipative system

This appendix provides the explicit form of the three possible subsystem density matrices for Subsection 4.2.1. For each particular subsystem, the elements are calculated using (4.33), (4.34) and (4.36). Note that we consider only the cases $\alpha < \beta$ since the cases $\alpha > \beta$ are equivalent to their symmetric counterpart, and $\alpha = \beta$ is precluded by the definition (4.11).

Reduced density matrix for $\alpha = 1, \beta = 2$

Using the recipe for finding the non-zero elements of (4.33) we find that for $\alpha = 1, \beta = 2$, (4.34) and (4.36) become

$$\begin{aligned} \rho^{\mathrm{red}}_{12,12}(r) &= \rho^{\mathrm{red}}_{21,21}(r) = -\rho^{\mathrm{red}}_{12,21}(r) = -\rho^{\mathrm{red}}_{21,12}(r) = f, \\ \rho^{\mathrm{red}}_{1\gamma,1\gamma}(r) &= \rho^{\mathrm{red}}_{2\gamma,2\gamma}(r) = d, \end{aligned} \tag{C.1}$$

to give

$$\rho^{\mathrm{red}} = \left(\begin{array}{ccc|ccc|ccc} d & & & & & & & & \\ & d+f & & -f & & & & & \\ & & d & & & & & & \\ \hline & -f & & d+f & & & & & \\ & & & & d & & & & \\ & & & & & d & & & \\ \hline & & & & & & 0 & & \\ & & & & & & & 0 & \\ & & & & & & & & 0 \end{array}\right). \tag{C.2}$$

Note that this is equivalent to the case $\alpha = 2, \beta = 1$.

Reduced density matrix for $\alpha = 1, \beta = 3$

The non-zero elements for the subsystem with $\alpha = 1, \beta = 3$ are found from (4.34) and (4.36), which become

$$\begin{aligned} \rho^{\rm red}_{13,13}(r) &= \rho^{\rm red}_{31,31}(r) = -\rho^{\rm red}_{13,31}(r) = -\rho^{\rm red}_{31,13}(r) = f, \\ \rho^{\rm red}_{1\gamma,1\gamma}(r) &= \rho^{\rm red}_{3\gamma,3\gamma}(r) = d, \end{aligned} \tag{C.3}$$

to give

$$\rho^{\rm red} = \left(\begin{array}{ccc|ccc|ccc} d & & & & & & & & \\ & d & & & & & & & \\ & & d+f & & & & -f & & \\ \hline & & & 0 & & & & & \\ & & & & 0 & & & & \\ & & & & & 0 & & & \\ \hline & & -f & & & & d+f & & \\ & & & & & & & d & \\ & & & & & & & & d \end{array}\right). \tag{C.4}$$

Note that this is equivalent to the case $\alpha = 3, \beta = 1$.

Reduced density matrix for $\alpha = 2, \beta = 3$

The non-zero elements for the subsystem with $\alpha = 2, \beta = 3$ are found from (4.34) and (4.36), which become

$$\begin{aligned} \rho^{\rm red}_{23,23}(r) &= \rho^{\rm red}_{32,32}(r) = -\rho^{\rm red}_{23,32}(r) = -\rho^{\rm red}_{32,23}(r) = f, \\ \rho^{\rm red}_{2\gamma,2\gamma}(r) &= \rho^{\rm red}_{3\gamma,3\gamma}(r) = d, \end{aligned} \tag{C.5}$$

to give

$$\rho^{\rm red} = \left(\begin{array}{ccc|ccc|ccc} 0 & & & & & & & & \\ & 0 & & & & & & & \\ & & 0 & & & & & & \\ \hline & & & d & & & & & \\ & & & & d & & & & \\ & & & & & d+f & & -f & \\ \hline & & & & & & d & & \\ & & & & & -f & & d+f & \\ & & & & & & & & d \end{array}\right). \tag{C.6}$$

Note that this is equivalent to the case $\alpha = 3, \beta = 2$.

BIBLIOGRAPHY

[1] G. Adesso and F. Illuminati. Equivalence between entanglement and optimal fidelity of CV teleportation. *Physical Review Letters*, 95(150503), 2005.

[2] G. Adesso and F. Illuminati. Entanglement in continuous variable systems: Recent advances and current perspectives. *Journal of Physics A: Mathematical and Theoretical*, 40:7821–7880, 2007.

[3] I Affleck, M Oshikawa, and H Saleur. Quantum Brownian Motion on a Triangular Lattice and $c = 2$ Boundary Conformal Field Theory. *Nuclear Physics B*, 594(3):535–606, 2001.

[4] Y. Aharonov, L. Davidovich, and N. Zagury. Quantum random walks. *Physical Review A*, 48(1687), 1993.

[5] Luigi Amico, Rosario Fazio, Andreas Osterloh, and Vlatko Vedral. Entanglement in many-body systems. *Reviews of Modern Physics*, 80(2):517–576, 2008.

[6] P. W. Anderson. Localized magnetic states in metals. *Phys. Rev.*, 124(1):41–53, Oct 1961.

[7] P.W. Anderson. A poor man's derivation of scaling laws for the Kondo problem. *Journal of Physics C: Solid State Physics*, 3:2436–2441, 1970.

[8] P.W. Anderson and G. Yuval. Exact results in the Kondo Problem: equivalence to a classical one-dimensional Coulomb gas. *Physical Review Letters*, 23(2):89–92, 1969.

[9] N. Andrei. Diagonalization of the Kondo Hamiltonian. *Physical Review Letters*, 45(5):379–382, Aug 1980.

[10] N. Andrei, K. Furuya, and J.H. Lowenstein. Solution of the Kondo problem. *Reviews of Modern Physics*, 55(2):331–402, 1983.

[11] D. Arnaudon, N. Crampe, L. Frappat, and E.. Ragoucy. Spectrum and Bethe ansatz equations for the $U_q(gl(n))$ closed and open spin chains in any representation. *Ann. H. Poincaré*, 7:1217, 2006.

[12] Alain Aspect, Jean Dalibard, and Gérard Roger. Experimental Test of Bell's Inequalities Using Time- Varying Analyzers. *Phys. Rev. Lett.*, 49(25):1804–1807, Dec 1982.

[13] Alain Aspect, Philippe Grangier, and Gérard Roger. Experimental Realization of Einstein-Podolsky-Rosen-Bohm Gedankenexperiment: A New Violation of Bell's Inequalities. *Phys. Rev. Lett.*, 49(2):91–94, Jul 1982.

[14] Hans-A. Bachor and Timothy C. Ralph. *A Guide to Experiments in Quantum Optics*. Wiley-VCH, Weinheim, 2004.

[15] K. Banaszek and K. Wodkiewicz. Nonlocality of the Einstein-Podolsky-Rosen state in the Wigner representation. *Phys. Rev. A*, 58:4345–4347, 1998.

[16] K. Banaszek and K. Wodkiewicz. Nonlocality of the Einstein-Podolsky-Rosen state in the phase space. *Acta Physica Slovaca*, 49:491, 1999.

[17] R.J. Baxter. One-Dimensional Anisotropic Heisenberg Chain. *Annals of Physics*, 70:323–337, 1972.

[18] R.J. Baxter. 8-Vertex model in lattice statistics and one-dimensional anisotropic Heisenberg chain. I. Some fundamental eigenvectors. *Annals of Physics*, 76(1):1–24, 1973.

[19] R.J. Baxter. 8-Vertex model in lattice statistics and one-dimensional anisotropic Heisenberg chain. II. Equivalence to a generalized ice-type lattice model. *Annals of Physics*, 76(1):25–47, 1973.

[20] R.J. Baxter. 8-Vertex model in lattice statistics and one-dimensional anisotropic Heisenberg chain. III. Eigenvectors of transfer matrix and Hamiltonian. *Annals of Physics*, 76(1):48–71, 1973.

[21] R.J. Baxter. *Exactly solved models in statistical mechanics*. Academic Press Inc., London, 1982.

[22] V.V. Bazhanov. Trigonometric solutions of triangle equations and classical Lie algebras. *Physics Letters B*, 159(4–6):321–324, 1985.

[23] J.S. Bell. On the Einstein Podolsky Rosen paradox. *Physics (NY)*, 1:195, 1965.

[24] J.S. Bell. *Speakable and unspeakable in quantum mechanics*. Cambridge University Press, 1987.

[25] F.A. Berezin. *The Method of Second Quantisation*. Academic, New York, 1966.

[26] H. Bethe. Zur Theorie der Metalle. Eigenwerte und Eigenfunktionen der linearen Atomkette. *Zeitschrift für Physik*, 71:205, 1931.

[27] M. Blume, V.J. Emery, and A. Luther. Spin-boson systems: One-dimensional equivalents and the Kondo problem. *Physical Review Letters*, 25(7):450–453, 1970.

[28] D. Bohm. *Quantum Theory*. Constable, London, 1951.

[29] N. Bohr. Can Quantum-Mechanical Description of Physical Reality be Considered Complete? *Physical Review*, 48:696–702, 1935.

[30] N. Bohr. Quantum Mechanics and Physical Reality. *Nature*, 136:65, 1935.

[31] L. Borda. Kondo screening cloud in a one-dimensional wire: Numerical renormalization group study. *Physical Review B*, 75(4):041307(R), 2007.

[32] B.H. Bransden and C.J. Joachain. *Quantum Mechanics*. Prentice Hall, 2nd edition, 2000.

[33] A.J. Bray and M.A. Moore. Influence of dissipation on quantum coherence. *Phys. Rev. Lett.*, 49(21):1545–1549, Nov 1982.

[34] A.O. Caldeira and A.J. Leggett. Quantum tunnelling in a dissipative system. *Annals of Physics*, 149(2):374, 1983.

[35] A.O. Caldeira and A.J. Leggett. Quantum tunnelling in a dissipative system. *Annals of Physics*, 153:445, 1984.

[36] G. Cardano. *Ars Magna*. Nurmberg, 1545.

[37] G. Cardano (translated by T.R. Witmer). *Ars Magna (or The Rules of Algebra)*. Dover, New York, NY, 1993.

[38] Sudip Chakravarty. Quantum fluctuations in the tunneling between superconductors. *Phys. Rev. Lett.*, 49(9):681–684, Aug 1982.

[39] C. Chamon, M. Oshikawa, and I. Affleck. Junctions of three quantum wires and the dissipative Hofstadter model. *Physical Review Letters*, 91(20):206403, 2003.

[40] Z-B. Chen and Y-D. Zhang. Greenberger-Horne-Zeilinger nonlocality for continuous-variable systems. *Phys. Rev. A*, 65(4):044102, Apr 2002.

[41] S.Y. Cho and R.H. McKenzie. Quantum entanglement in the two-impurity Kondo model. *Physical Review A*, 73(1):012109, Jan 2006.

[42] J.F. Clauser, M.A. Horne, A. Shimony, and R.A. Holt. Proposed experiment to test local hidden-variable theories. *Phys. Rev. Lett.*, 23(15):880, 1969.

[43] B. Coqblin and J.R. Schrieffer. Exchange interaction in alloys with Cerium impurities. *Physical Review*, 185(2):847–853, 1969.

[44] T. A. Costi and G. Zaránd. Thermodynamics of the dissipative two-state system: A Bethe-Ansatz study. *Phys. Rev. B*, 59(19):12398–12418, May 1999.

[45] T.A. Costi and Ross H. McKenzie. Entanglement between a qubit and the environment in the spin-boson model. *Phys. Rev. A*, 68(3):034301, Sep 2003.

[46] P. Coveney and R. Highfield. *The Arrow of Time*. Flamingo, 1991.

[47] J. Dunningham and V. Vedral. Nonlocality of a single particle. *Physical Review Letters*, 99:180404, 2007.

[48] A. Einstein. Zur Elektrodynamik bewegter Körper. *Annalen der Physik*, 17:891, 1905.

[49] A. Einstein, B. Podolsky, and N. Rosen. Can Quantum-Mechanical Description of Physical Reality Be Considered Complete. *Phys. Rev.*, 47:777–780, 1935.

[50] V. J. Emery and A. Luther. Low- temperature properties of the Kondo Hamiltonian. *Phys. Rev. B*, 9(1):215–226, Jan 1974.

[51] H. Everett. Relative State Formulation of Quantum Mechanics. *Reviews of Modern Physics*, 29:454–462, 1957.

[52] H. Everett. The theory of the universal wavefunction. In B.S. DeWitt and R.N. Graham, editors, *The Many-Worlds Interpretation of Quantum Mechanics, Princeton Series in Physics,*, pages 3–140. Princeton University Press, 1972.

[53] H-Y. Fan. Normally ordering some multimode exponential operators by virtue of the IWOP technique. *Journal of Physics A*, 23:1833–1839, 1990.

[54] H-Y. Fan and J.R. Klauder. Eigenstates of two particles' relative position and total momentum. *Physical Review A*, 49(2):704–707, 1994.

[55] H-Y. Fan and S-G. Liu. New approach for finding multipartite entangled state representations via the IWOP technique. *International Journal of Modern Physics A*, 22(24):4481–4494, 2007.

[56] H-Y. Fan and W-Q. Wang. Coherent-Entangled State in Three-Mode and Its Applications. *Communications in Theoretical Physics*, 46(6):975–982, 2006.

[57] H-Y. Fan and Y. Zhang. Common eigenkets of three-particle compatible observables. *Physical Review A*, 57(5):3225–3228, 1998.

[58] V.A. Fateev and P.B. Wiegmann. The exact solution of the $s-d$ exchange model with arbitrary impurity spin S (Kondo problem). *Physics Letters*, 81A:179, 1981.

[59] A. Ferraro and M.G.A. Paris. Nonlocality of two-and three-mode continuous variable systems. *Journal of Optics B: Quantum and Semiclassical Optics*, 7:174–182, 2005.

[60] V.M. Filyov, A.M. Tsvelick, and P.B. Wiegmann. Thermodynamics of the $s-d$ exhange model (Kondo problem). *Physics Letters A*, 81:175–178, 1981.

[61] R.A. Fisher, M.M. Nieto, and V.D. Sandberg. Impossibility of naively generalizing squeezed coherent states. *Physical Review D*, 29(6):1107–1110, 1984.

[62] N. Gisin. Hidden quantum nonlocality revealed by local filters. *Physics Letters A*, 210(3):151 – 156, 1996.

[63] D. Giulini, E. Joos, C. Kiefer, J. Kupsch, I.-O. Stamatescu, and H.D. Zeh. *Decoherence and the Appearance of a Classical World in Quantum Theory*. Springer, Berlin; New York, 1996.

[64] J.R. Gott. *Time Travel in Einstein's Universe*. Phoenix, 2001.

[65] D.M. Greenberger, M.A. Horne, and A. Zeilinger. Nonlocality of a Single Photon? *Physical Review Letters*, 75:2064, 1995.

[66] M. Gulácsi. The one dimensional Kondo lattice model at partial band filling. *Advances in Physics*, 53(7):769–937, 2004.

[67] F.D.M Haldane. 'Luttinger liquid theory' of one-dimensional fluids: I. Properties of the Luttinger model and their extension to the general 1D interacting spinless fermi gas. *Journal of Physics C: Solid State Physics*, 14:2585–2609, 1981.

[68] M.W. Hamilton. Phase shifts in multilayer dielectric beam splitters. *American Journal of Physics*, 68(2):186–191, 2000.

[69] S. Hawking. Chronology Protection Conjecture. *Physical Review D*, 46(2), 1992.

[70] W. Heisenberg. Über den anschaulichen Inhalt der quantentheoretischen Kinematik und Mechanik. *Zeitschrift für Physik*, 43:172–198, 1927.

[71] W. Heisenberg. Zur Theorie des Ferromagnetismus. *Zeitschrift für Physik*, 49:619–636, 1928.

[72] A. Hewson. *The Kondo Problem to Heavy Fermions*. Cambridge University Press, Cambridge, England, 1997.

[73] M. Hillery, R.F. O'Connell, M.O. Scully, and E.P. Wigner. Distribution functions in physics: Fundamentals. *Physics Reports (Review Section of Physics Letters)*, 106(3):121–167, 1984.

[74] R. Horodecki and M. Horodecki. Information-theoretic aspects of inseparability of mixed states. *Physical Review A*, 54(3):1838–1843, 1996.

[75] P. Horwich. *Asymmetries in Time*. Bradford Books, 2nd edition, 1988.

[76] S.H. Jacobsen. *The Topology of Time: An investigation linking entropy, decoherence and the structure of spacetime*. B.Sc. Honours Thesis, Unpublished, University of York, U.K., 2005.

[77] S.H. Jacobsen and P.D. Jarvis. Regularized tripartite continuous variable EPR-type states with Wigner functions and CHSH violations. *Journal of Physics A: Mathematical and Theoretical*, 41(3):365301, 2008.

[78] S.H. Jacobsen and P.D. Jarvis. Exactly solvable three-level quantum dissipative systems via bosonisation of fermion gas-impurity models. *Journal of Physics A*, 43(25):255305, 2010.

[79] M. Jimbo. Quantum r-matrix for the Generalized Toda System. *Communications in Mathematical Physics*, 102(4):537–547, 1986.

[80] E. Joos and H.D. Zeh. The emergence of classical properties through interaction with the environment. *Zeitschrift Für Physik B*, 59(2):223–243, 1985.

[81] E. Joos, H.D. Zeh, C. Kiefer, D. Giulini, J. Kupsch, and I.-O. Stamatescu. *Decoherence and the Appearance of a Classical World in Quantum Theory*. Springer, New York, 2nd edition, 2003.

[82] B.S. Kay. Decoherence of macroscopic closed systems within Newtonian quantum gravity. *Classical and Quantum Gravity*, 15(12):L89–L98, 1998.

[83] J. Kempe. Quantum random walks - an introductory overview. *Contemporary Physics*, 44(4):307–327, 2003.

[84] C. Kiefer and E. Joos. Decoherence: Concepts and Examples. In P. Blanchard and A. Jadczyk, editors, *Quantum Future*, pages 105–128, Berlin, 1998. Springer.

[85] J.R. Klauder and B-S. Skagerstam. *Coherent States: applications in physics and mathematical physics*. World Scientific, Singapore, 1985.

[86] S. Kochen and E.P. Specker. The problem of hidden variables in quantum mechanics. *Journal of Mathematics and Mechanics*, 17:59–87, 1967.

[87] J. Kondo. Resistance minimum in dilute magnetic alloys. *Progress of theoretical physics*, 32(1):37–49, 1964.

[88] A. Kopp and K. Le Hur. Universal and Measurable Entanglement Entropy in the Spin-Boson Model. *Physical Review Letters*, 98:220401, 2007.

[89] L. Kouwenhoven and L. Glazman. Revival of the Kondo effect. *Physics World*, 14:33–38, 2001.

[90] A. Kuzmich, I. A. Walmsley, and L. Mandel. Violation of Bell's inequality by a generalized Einstein-Podolsky-Rosen state using homodyne detection. *Phys. Rev. Lett.*, 85(7):1349–1353, Aug 2000.

[91] N. Laflorencie, E.S. Sørensen, and I. Affleck. The Kondo effect in spin chains. *Journal of Statistical Mechanics: Theory and Experiment*, 2008(2):PO2007, 2008.

[92] K. Le Hur. Entanglement entropy, decoherence, and quantum phase transitions of a dissipative two-level system. *Annals of Physics*, 323:2208–2240, 2008.

[93] R. Le Poidevin. *Travels in Four Dimensions*. Oxford University Press, 2003.

[94] R. Le Poidevin and M. MacBeath. *The Philosophy of Time*. Oxford University Press, England, 1993.

[95] A.J. Leggett, S. Chakravarty, A.T. Dorsey, Matthew P.A. Fisher, Anupam Garg, and W. Zwerger. Dynamics of the dissipative two-state system. *Reviews of Modern Physics*, 59(1):1–85, 1987.

[96] A.J. Leggett, S. Chakravarty, A.T. Dorsey, Matthew P.A. Fisher, Anupam Garg, and W. Zwerger. Erratum: Dynamics of the dissipative two-state system. *Reviews of Modern Physics*, 67(3):725–726, 1995.

[97] D.H. Mellor. *Real Time II*. Routledge, 1998.

[98] N.D. Mermin. Extreme quantum entanglement in a superposition of macroscopically distinct states. *Phys. Rev. Lett.*, 65(15):1838–1840, Oct 1990.

[99] J.E. Moyal. Quantum mechanics as a statistical theory. *Proceedings of the Cambridge Philosophical Society*, 45(1):99.

[100] K.M. O'Connor and W.K. Wootters. Entangled Rings. *Physical Review A*, 63(5):052302, 2001.

[101] S. Oh and J. Kim. Entanglement of an impurity and conduction spins in the Kondo model. *Physical Review B*, 73(5):052407, 2006.

[102] Omar Osenda, Zhen Huang, and Sabre Kais. Tuning the entanglement for a one-dimensional magnetic system with anisotropic coupling and impurities. *Phys. Rev. A*, 67(6):062321, Jun 2003.

[103] Z.Y. Ou and L. Mandel. Violation of Bell's inequality and classical probability in a two-photon correlation experiment. *Phys. Rev. Lett.*, 61(1):50–53, Jul 1988.

[104] Z.Y. Ou, S.F. Pereira, H.J. Kimble, and K.C. Peng. Realization of the Einstein-Podolsky-Rosen paradox for continuous variables. *Phys. Rev. Lett.*, 68(25):3663–3666, Jun 1992.

[105] R. Penrose. *The Emperor's New Mind*. Oxford University Press, New York, 1989.

[106] R. Penrose, with A. Shimony, N. Cartwright, and S. Hawking. *The Large, the Small and the Human Mind*. Cambridge University Press, Cambridge, England, Canto edition, 2000.

[107] M.B. Plenio and S. Virmani. An introduction to entanglement measures. *Quantum Information and Computation*, 7(1):1–51, 2007.

[108] M.D. Reid. Demonstration of the Einstein-Podolsky-Rosen paradox using Nondegenerate Parametric Amplification. *Physical Review A*, 40(2):913–923, 1989.

[109] A. Royer. Wigner function as the expectation value of a parity operator. *Phys. Rev. A*, 15:449–450, February 1977.

[110] M. Schlosshauer. Decoherence, the measurement problem and quantum mechanics. *Reviews of Modern Physics*, 76:1267–1305, 2004.

[111] M. Schlosshauer, A.P. Hines, and G.J. Milburn. Decoherence and dissipation of a quantum harmonic oscillator coupled to two-level system. *Physical Review A*, 77:022111, 2008.

[112] E. Schrödinger. Die gegenwärtige Situation in der Quantenmechanik. *Naturwissenschaften*, 23:807–812; 823–828; 844–849, 1935.

[113] E. Schrödinger. Discussion of probability relations between separated systems. *Proceedings of the Cambridge Philosophical Society*, 31:555–563, 1935.

[114] E. Schrödinger. Discussion of probability relations between separated systems. *Proceedings of the Cambridge Philosophical Society*, 32:446–451, 1936.

[115] J.A. Stickney, D.Z. Anderson, and A.A. Zozulya. Transistorlike behaviour of a Bose-Einstein condensate in a triple-well potential. *Physical Review A*, 75:013608, 2007.

[116] A. Stotland, A.A. Pomeransky, E. Bachmat, and D. Cohen. The information entropy of quantum-mechanical states. *Europhysics Letters*, 67(5):700, 2004.

[117] B. Sutherland. Two-Dimensional Hydrogen Bonded Crystals without the Ice Rule. *Journal of Mathematical Physics*, 11:3183–6, 1970.

[118] M. Takahashi. *Thermodynamics of one-dimensional solvable models*. Cambridge University Press, Cambridge, UK, 1999.

[119] L.A. Takhtadzhan and L.D. Faddeev. The Quantum Method of the Inverse Problem and the Heisenberg XYZ model. *Russian Mathematical Surveys*, 34(5):11–68, 1979.

[120] Max Tegmark. Importance of quantum decoherence in brain processes. *Phys. Rev. E*, 61(4):4194–4206, Apr 2000.

[121] W. Thirring. Vorlesungen über mathematische Physik. *University of Vienna*, 1975.

[122] S. Tomonaga. Remarks on Blochs method of sound waves applied to many-fermion problems. *Progress of Theoretical Physics*, 5(4):544–569, 1950.

[123] D.A. Trifonov. On the squeezed states for n observables. *Physica Scripta*, 58(3):246–255, 1998.

[124] J.D. Trimmer. The present situation in quantum mechanics - a translation of Schrödinger's cat paradox paper. *Proceedings of the American Philosophical Society*, 124(5):323–338, 1980.

[125] D.R. Truax. Baker-Campbell-Hausdorf relations and unitarity of $SU(2)$ and $SU(1,1)$ squeeze operators. *Physical Review D*, 31(8):1988–1991, 1985.

[126] Constantino Tsallis. Possible generalization of Boltzmann-Gibbs statistics. *Journal of Statistical Physics*, 52(1–2):479–487, 1988.

[127] A.M. Tsvelick and P.B Wiegmann. Exact results in the theory of magnetic alloys. *Advances in Physics*, 32(4):453–713, 1983.

[128] P. van Loock and S.L. Braunstein. Multipartite entanglement for continuous variables: A quantum teleportation network. *Phys. Rev. Lett.*, 84:3482–3485, 2000.

[129] P. van Loock and S.L. Braunstein. Greenberger-Horne-Zeilinger nonlocality in phase space. *Phys. Rev. A*, 63(2), 2001.

[130] V. Vedral. Entanglement in the second quantization formalism. *Central European Journal of Physics*, 1:289, 2003.

[131] Frank Verstraete and Michael M. Wolf. Entanglement versus Bell Violations and Their Behavior under Local Filtering Operations. *Phys. Rev. Lett.*, 89(17):170401, Oct 2002.

[132] Jan von Delft and H. Schoeller. Bosonization for beginners - refermionization for experts. *Annalen der Physik (Leipzig)*, 7(4):225–306, 1998.

[133] J. von Neumann. *Mathematische Grundlagen der Quantenmechanik (Mathematical Foundations of Quantum Mechanics)*. Springer (Princeton University Press), Berlin, 1932 (1955).

[134] D.F. Walls and G.J. Milburn. *Quantum Optics*. Springer-Verlag, Berlin, 1994.

[135] A. Wehrl. Three theorems about entropy and convergence of density matrices. *Reports on Mathematical Physics*, 10(2):159–163, 1976.

[136] Ulrich Weiss. *Quantum Dissipative Systems*. World Scientific Publishing, 3 edition, 2008.

[137] R.F. Werner. Quantum states with Einstein-Podolsky-Rosen correlations admitting a hidden-variable model. *Phys. Rev. A*, 40(8):42774281, 1989.

[138] R.F. Werner and M.M. Wolf. Bell inequalities and entanglement. *Quantum Information and Computation*, 1(3):1–25, 2001.

[139] G.J. Whitrow. *The Natural Philosophy of Time*. Tomas Nelson and Sons Ltd., 1961.

[140] G.C. Wick. The evaluation of the collision matrix. *Phys. Rev.*, 80(2):268–272, Oct 1950.

[141] P.B. Wiegmann. Exact solution of $s-d$ exchange model at $t=0$. *Soviet Physics JETP Letters*, 31(7):364–370 (392–398), 1980.

[142] P.B. Wiegmann. Exact solution of the $s-d$ exchange model (Kondo problem). *Journal of Physics C: Solid State Physics*, 14:1462–1478, 1981.

[143] E.P. Wigner. On the quantum correction for thermodynamic equilibrium. *Phys. Rev.*, 40:749, 1932.

[144] Kenneth G. Wilson. The renormalization group: Critical phenomena and the Kondo problem. *Rev. Mod. Phys.*, 47(4):773–840, Oct 1975.

[145] C.N. Yang and C.P. Yang. One-dimensional chain of anisotropic spin-spin interactions. I. Proof of Bethe's hypothesis for ground state in a finite system. *Physical Review*, 150(1):321–327, 1966.

[146] Kei Yosida. Bound state due to the $s-d$ exchange interaction. *Phys. Rev.*, 147(1):223–227, Jul 1966.

[147] H-C. Yuan, H-M. Li, and H-Y. Fan. Generalized multi-mode bosonic realization of the $su(1,1)$ algebra and its corresponding squeezing operator. *Journal of Physics A: Mathematical and Theoretical*, 43:075304, 2010.

[148] B. Yurke, S.L. McCall, and J.R. Klauder. $SU(2)$ and $SU(1,1)$ interferometers. *Physical Review A*, 33(6):4033–4054, 1986.

[149] G. Yuval and P. W. Anderson. Exact results for the Kondo problem: One-body theory and extension to finite temperature. *Phys. Rev. B*, 1(4):1522–1528, Feb 1970.

[150] A.B. Zamolodchikov and A.B. Zamolodchikov. Factorized S-matrices in two dimensions as the exact solutions of certain relativistic quantum field theory models. *Annals of Physics*, 120(2), 1979.

[151] G. Zaránd and J. von Delft. Simple bosonization solution of the 2-channel Kondo model: I. analytical calculation of finite-size crossover spectrum. *ArXiv Condensed Matter e-prints cond-mat/9812182*.

[152] G. Zaránd and J. von Delft. Analytical calculation of the finite-size crossover spectrum of the anisotropic two-channel Kondo model. *Physical Review B*, 61(10):6918–6933, 2000.

[153] C. Zener. Interaction between the d shells in the transition metals. *Phys. Rev.*, 81(3):440–444, Feb 1951.

[154] W.H. Zurek. Collapse of the wavepacket: how long does it take? In G.T. Moore and M.O. Scully, editors, *Frontiers of Nonequilibrium Quantum Statistical Mechanics*, pages 145–150. Plenum, 1986.

[155] W.H. Zurek. Decoherence and the Transition from the Quantum to the Classical. *Physics Today*, 44(10):36–44, 1991.

INDEX